UNIVERSITY OF TWENTE.

Deltares
Enabling Delta Life

# Optimization of offshore wind farm power cable routing

**Tom Roetert 2014**

Deltares

# OPTIMIZATION OF OFFSHORE WIND FARM POWER CABLE ROUTING

DEVELOPMENT OF A TOOL THAT OPTIMIZES THE POWER CABLE ROUTE DESIGN FOR OFFSHORE WIND FARMS

*MASTER THESIS*
*IN CIVIL ENGINEERING AND MANAGEMENT*
*FACULTY OF ENGINEERING TECHNOLOGY*
*UNIVERSITY OF TWENTE*


| | |
|---|---|
| **Student:** | Thomas Jonathan Roetert BSc. |
| **Date:** | 12-12-2014 |
| **Graduation supervisor:** | Prof.dr. S.J.M.H. Hulscher |
| **Daily supervisor:** | Dr.ir. B.W. Borsje |
| **External supervisor:** | ir. R.W. Hasselaar (Deltares) |



UNIVERSITY OF TWENTE.

Deltares
Enabling Delta Life

# Summary

Offshore wind farms are of great interest as renewable energy source. However, offshore wind farms are still very expensive. Therefore, aimed at the innovation of offshore wind farms, a consortium of companies and knowledge institutions started the FLOW (Far and Large Offshore Wind) program. The main aim of the program is cost reduction in design, development and offshore wind farm operation of the offshore wind farms (FLOW, 2014). Part of this program is that Deltares investigates the optimization of power cable layout.

Up to now methods to optimize cable route layout are only based on a flat seabed and do not take the seabed dynamics into account (Jenkins et al., 2013; Morelissen et al., 2003). The result of this approach is that power cable coverage is not guaranteed over the wind farm design lifetime. The cable optimization is mainly executed based on shortest routes instead of cost reduction over the entire design lifespan. Therefore the aim of this research is:

> *"The development of a Matlab based tool to optimize the power cable route design based on expected morphological behaviour in the design lifetime of an offshore wind farm"*

To find the optimized cable layout a tool is developed including the optimization under a flat, static and dynamic seabed. These three steps help to identify the impact of bedforms on cable positions. First, the cable layout is determined based on a flat and static seabed. Found layouts show large similarities with the original layout in terms of total length. Thereby, the original layout is used during the optimization under a dynamic seabed.

All connections in the original layout are optimized in vertical and horizontal direction. The aim for this step is to minimize weights of all connections. Cable weights are determined based on the cost function incorporating risk of failure and costs of failure, cables and monitoring.

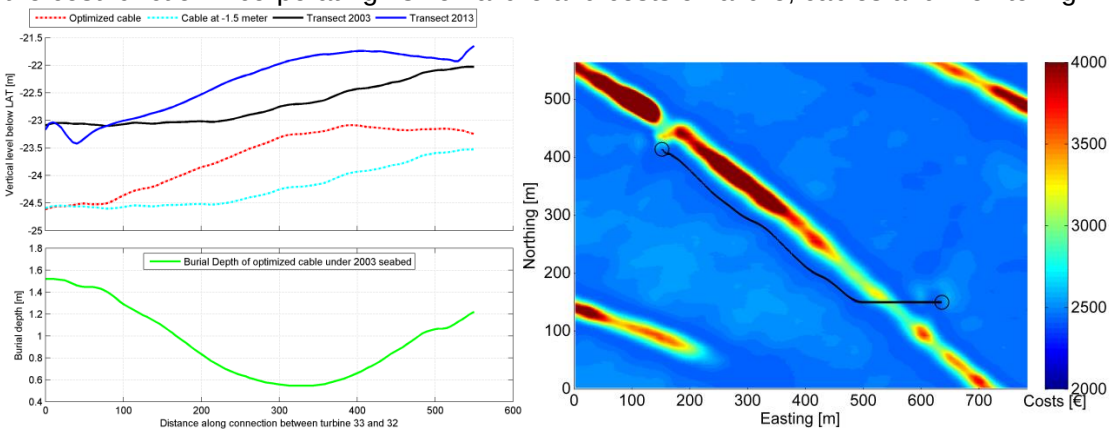


*Figure 0.1: Vertical (l) and horizontal (r) optimization of connection between turbine 33 and 32*

The red dotted line in Figure 0.1 (l) shows the optimized vertical cable position and the right figure displays the optimized horizontal cable position. Combining all optimized connections shows that all vertical optimizations lead to a decrease in costs. Results of the horizontal optimization depend on the fixed burial depth and bed level change. Combined with an option to include case-specific information, it can be assumed that the tool is general applicable.

The parameters used in the vertical and horizontal optimization were all fixed. To show the influence of the different parameters, a rough sensitivity analysis is executed. A parameter from all four cost function parts, risks, power loss, costs of repair and initial cable costs, is

analysed. Main conclusions are that the magnitude of the parameter and the dynamics of the crossed area form the greatest influence on total costs. Since the tool is designed to find the optimized cable layout over the wind farm design lifetime, also sensitivity of survey prediction is analysed. Parameter sensitivity after optimization based on predicted surveys, did not show large differences. Results for the vertical optimization stayed equal, while horizontal optimization results were only influenced of the connection interfered with sand waves.

The results of this research make a contribution towards renewable energy targets. With the aid of this tool, cable coverage can be guaranteed, reliability increases and project costs and risk of cable failure decreases.

# Preface

This report is the result of my master thesis project at Deltares in Delft. It is the last step in finishing my master Water Engineering and Management at the University of Twente. In this research, I constructed a tool which can optimize the wind farm power cable layout. The combination of research and a current subject proved to be very interesting and educational.

First, I would like to thank my daily supervisor Robert Hasselaar for the time he invested in me and the discussions and input during the process, which were very useful. Also a word of thanks for the other members of my graduation committee, Suzanne Hulscher and Bas Borsje, for the involvement and valuable feedback during the process.

Next, I would like to thank Deltares for making this research possible by offering their facilities. Further, a special thanks goes out to my fellow students at Deltares, who were of great help when struggling on various kind of problems and for making the master thesis period a lot of fun as well.

Last but not least, I would like to thank my parents, my brothers and Leonie for their encouragements and unconditional support during my entire study.

Tom Roetert

Delft, December 2014

# Contents

# 1 Introduction

Offshore wind farms are of great interest as renewable energy source. First of all is that offshore wind farms have the potential to meet a large share of European's future energy demand (Schillings et al., 2012). A second big advantage is that they are less confined in available space. Finally, offshore wind farms give the opportunity to produce more energy per unit due to stronger and steadier airflows above a flat sea surface (Petersen & Malm, 2006). However, while they are still very expensive, ongoing innovation is required.

Aimed at the innovation of offshore wind farms, a consortium of companies and knowledge institutions started the FLOW (Far and Large Offshore Wind) program. The main aim of the program is cost reduction in design, development and operation of offshore wind farms (FLOW, 2014). The FLOW program contains five main themes. Inside one of these themes, Deltares, TU Delft and IHC started the project: *'Optimizing cable installation and operation; a life cycle perspective'.* The main goal of the project is: *'Development of techniques and related equipment to optimize cable installation, protection, monitoring and IRM'*. Part of this project is that Deltares investigates optimization of the infield power cable layout.

This chapter describes the outline of the research project in which the problem definition, based on the literature review is provided in the first section. The sections thereafter describe the research objective and the research questions.

## 1.1 Problem definition

For offshore wind farms, sediment transport in the form of sand waves is of great importance. These sand wave patterns can reach several meters in height, hundreds of meters in wavelength and migration rates up to ten meter per year. Since large portions of the North Seabed are covered with these dynamic bedforms, significant amounts of sand are transported (Bijker et al., 1998; Borsje et al., 2013; Huntley et al., 1993).

The dynamic character of sand waves is very important in the wind farm power cable construction (Besio et al., 2004; Morelissen et al., 2003; Németh et al., 2002). Especially cable burial depth is imposed by the sand wave migration. When a cable is buried too deep, a thermal bottleneck may result. This increases the chance of fatigue of the power cable. On the contrary, if the cable is buried too close to the surface, the sand wave movement can cause a free span, which can lead to vortex-induced vibrations (Németh, 2003).

Because the cables still need to connect the wind turbines, the problem is also valid in the horizontal plane. A certain cable connection between two wind turbines may cross a sand wave field. The increased risk of failure can be overcome by diverting the cables around the sand wave field. However, the increased cable length implies extra costs. Therefore, in addition to the cable bending radius and the burial depth, the diversion is only accepted within a certain range (Németh, 2003).

Unfortunately, the current methods to optimize cable route design are not based on a dynamic seabed (Morelissen et al., 2003). Instead, route optimization is mainly based on algorithms describing a fixed wind farm layout (Jenkins et al., 2013). In addition, possible innovations in the cables are not investigated thoroughly. The result is that the design lifetime of power cables is not guaranteed. Up to now, cable optimization is mainly executed based on shortest routes instead of cost reduction.

## 1.2 Research objective

The problem definition indicates that knowledge of sand wave migration and cable limitations are missing in the cable route design. In order to understand the difficulties for the optimal cable layout in a wind farm, the question arises in what way the morphological seabed changes can be combined with an optimization routine. In this research, the expected morphological changes during the wind farm lifespan are analysed and calculated. The results are combined with a mathematical optimization routine in Matlab to provide a cable route design tool. The optimization of this tool is based on the cost reduction of the cable layout. Therefore the objective of this research is:

> *"The development of a Matlab based tool to optimize the power cable route design based on expected morphological behaviour in the design lifetime of an offshore wind farm"*

## 1.3 Research questions

To achieve the objective of this research several research questions are formulated:

### 1. Tool building

- What are the site-specific conditions of the Prinses Amaliawindpark and how can these be combined with an optimization routine in a Matlab based tool?
- How can the cable route layout be optimized based on a wind farm with a flat and static seabed?
- How can the cable routes be optimized in the horizontal and vertical plane based on cable limitations and what are the implications for the route optimization?
- How can the route weight of the routes be identified based on the risks, cable length and excavation costs?

*Figure 1.1: The Prinses Amaliawindpark. Case study for route optimization tool development*

### 2. Tool application

- What are the cost savings of the route optimization tool compared to the existing layout throughout the entire life span of the wind farm?
- What is the sensitivity of parameters in the cost function and the survey prediction?

3. **Tool evaluation**
   - Can the route optimization tool be adjusted, making it applicable to other offshore wind farm cable layout studies?
   - Can innovations in materials and routines lead towards an even higher cost reduction?
   - What are the contributions towards renewable energy targets?

## 1.4 Methodology

In order to answer the research questions and to achieve to research objective the following methodology is adopted. Figure 1.2 denotes the steps taken during the research.

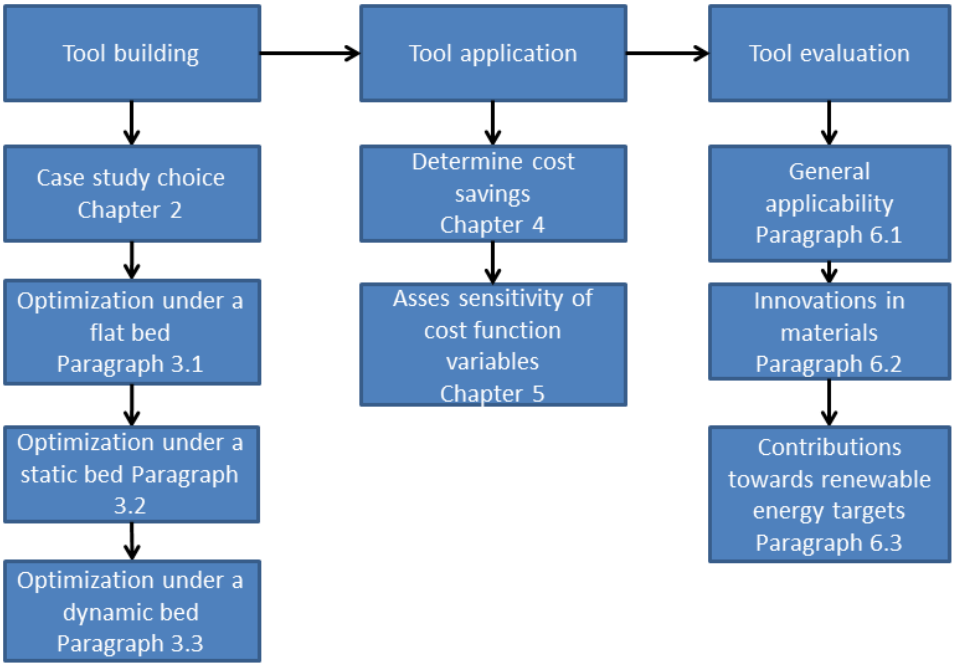


*Figure 1.2: Methodology used in the research*

- The basis for the development of the route optimization tool is formed by the Prinses Amaliawindpark case study. All relevant information of the wind farm is described and analysed for the route optimization
- The Prinses Amaliawindpark cable layout is determined in three ways: under a flat static and dynamic seabed. The static seabed is chosen to be represented by the first bathymetrical survey and the dynamic seabed with a start and an end survey.
- The aim for both the flat and static bed optimization is to find a near optimal layout for the Prinses Amaliawindpark, in where cable parts are not optimized yet.
- To find the near optimal layout an optimization algorithm is chosen. This algorithm optimizes a set of initial solutions until a stopping criterion is met. When the algorithm has met set requirements, the found solution is the near optimal solution.
- The found layout is then used in the optimization under a dynamic seabed. This step is divided in two parts, optimization under a vertical and horizontal plane. The route weights are determined with a cost function, which incorporates risks, cable costs and cost of failure based on the bed level change.

- When the three optimization steps are defined, the results are gathered. To compare the effectiveness of the tool, all results are compared with the original layout.
- Next step is the assessment of the sensitivity of parameters in the cost function. Here, the influences of changes in input are described.
- The research is concluded with the tool evaluation. Here, the general applicability, possible innovations in materials and routines and the contribution towards renewable energy are assessed. The effectiveness of the tool is shown by combining the evaluation with the results.

## 1.5 Report outline

The overall structure of the report is as follows:

**Chapter 2: Case study Prinses Amaliawindpark** – This chapter describes the choice for the case study on which the tool is developed. The site-specific conditions of the wind farm are discussed and all information relevant for this research is worked out.

**Chapter 3: Development of the route optimization tool –** This chapter contains the description of the route optimization tool, algorithm choice, optimization steps and Fourier extension. The chapter ends with an overview of the tool. With this chapter, combined with chapter 2, the research questions belonging to the tool are answered.

**Chapter 4: Result of the route optimization tool –** The application of the route optimization tool on the case study is described in this chapter. The research questions belonging to the tool application are answered with the results disclosed in this chapter.

**Chapter 5: Sensitivity analysis –** This chapter contains the assessment of sensitivity of the parameters in the cost function. With this chapter, the research question regarding the sensitivity analysis is answered.

**Chapter 6: Applicability of the route optimization tool –** The sixth chapter contains the effects of the route optimization tool. It describes the general applicability, possible innovations and the contribution towards renewable energy. The research question belonging to the tool development are answered with this chapter.

**Chapter 7: Discussion –** The seventh chapter contains the discussion of uncertainties and assumptions made during this research.

**Chapter 8: Conclusions and recommendations –** The final chapter contains the conclusions and recommendations for this research. The answers to the research questions are summarized and possible improvements are given.

# 2 Case study Prinses Amaliawindpark

This chapter introduces the Prinses Amaliawindpark case study, which is chosen to develop the route optimization tool. First, an overview of the wind farm is given containing the current layout and general information. In the second section, the available bathymetrical surveys are analysed. Finally, the chapter is concluded with the change in bathymetrical evolution and sand wave characteristics.

## 2.1 Required input

Development of the route optimization tool requires a case study with input of good quality. Main components that should be included are:

- Exact locations of  wind turbines
- Exact location of the offshore high voltage system (OHVS)
- Current power cable layout in offshore wind farm
- Multiple bathymetrical surveys, ranging from prior to wind farm construction to a significant amount of years in operation
- Information about cable constrains such as bending radius and capacity
- Information about production capacity of the wind turbines
- Information about the costs of cable installation and potential replacement

Given the requirement of multiple surveys, the case study should be focused on an existing offshore wind farm. Therefore, the Prinses Amaliawindpark is chosen. With information provided by Deltares and IHC, all required data can be covered.

## 2.2 Prinses Amaliawindpark characteristics

The Prinses Amaliawindpark, from here on called the PAWP, is an offshore wind farm located on the Dutch continental shelf 23 kilometres off the coast of IJmuiden (Figure 2.1).

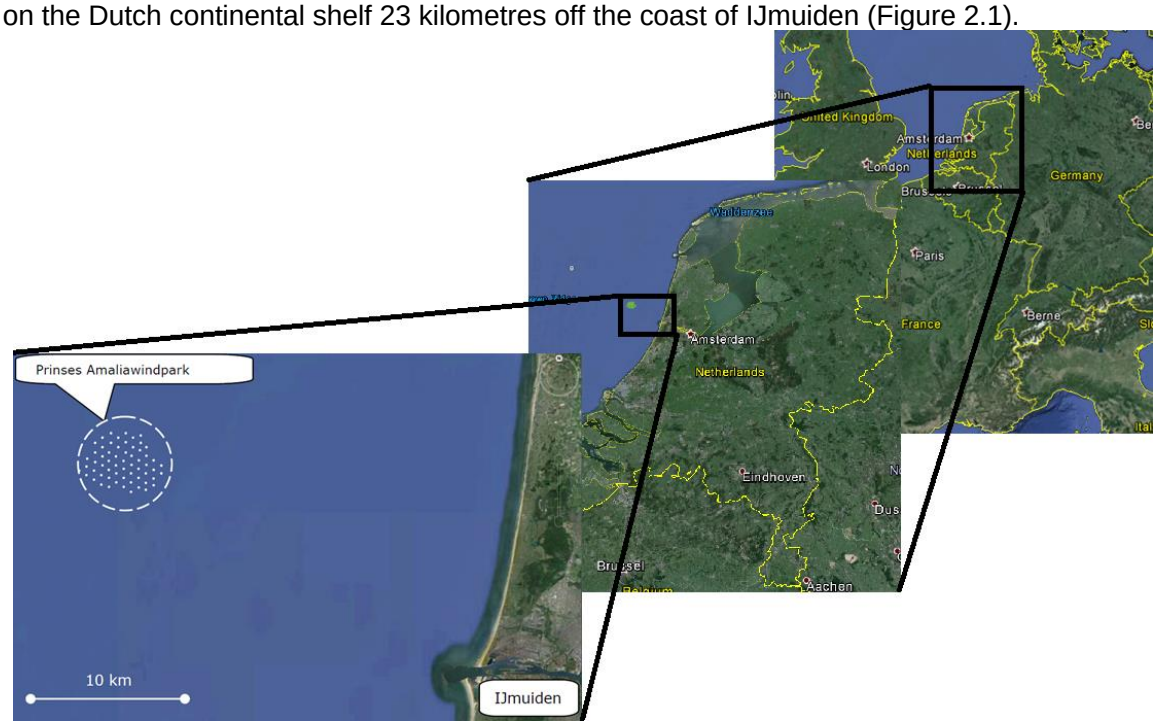


*Figure 2.1: Location of the Prinses Amaliawindpark in the North Sea (Bijker, 2013)*

Since July 1st 2008, the wind farm is operational and is designed to supply power to approximately 125.000 households. Other characteristics of the PAWP are:

- 60 wind turbines, each with a capacity of 2 Mega Watt
- Bed level in the wind farm is between 19 and 24 meter beneath lowest astronomical tide (LAT)
- Offshore wind farm survey stretches over 20 square kilometres
- Power production of 422.000 mega Watt hour
- $CO_2$ reduction of 225.000 tons per year
- One offshore high voltage system, from here on called the OHVS, transforming the voltage to 150.000 volt to minimize energy loss
- 28 kilometre of infield power cables
- A 25 kilometre long export power cable

### 2.2.1 Wind farm layout

A more detailed wind farm overview is presented in Figure 2.2. The figure shows the bed levels from a survey executed in 2003, turbine locations and original cable layout. The two blue arrows in the survey denote the locations of the transects for sand wave analysis.

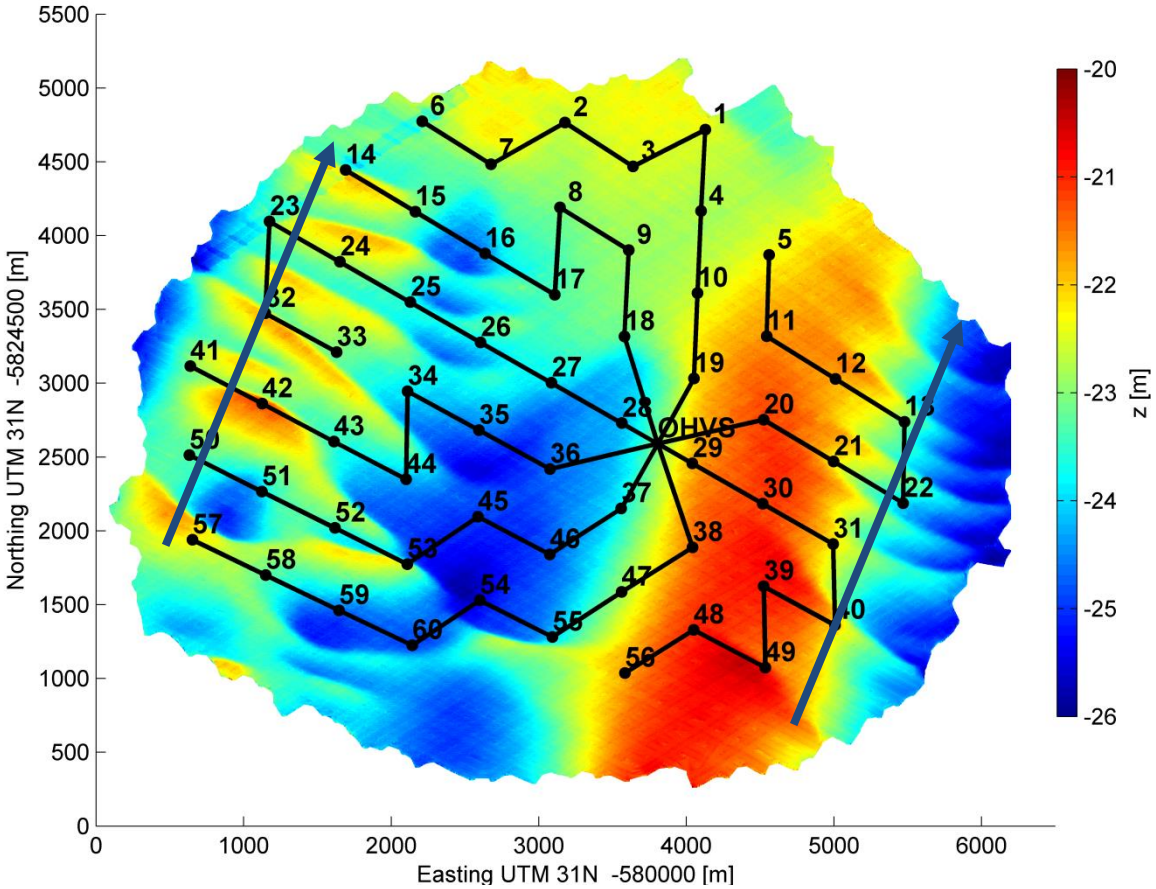


*Figure 2.2: Layout of the Prinses Amaliawindpark*

The turbines are placed in a structured grid with mutual distances of about 550-590 meters. Originally, turbine locations were presented in longitude and latitude. Transformation to a projected representation gives a better indication of dimensions.

The generated wind energy is transported from the wind turbines towards the OHVS via various strings. Each string has multiple turbines attached and together connect all turbines to the OHVS. The number of strings in a wind farm is variable. However, it is often chosen to minimize the number of strings based on string capacity.

In the Prinses Amaliawindpark, strings have a maximum capacity of eight wind turbines**.** Minimizing the number of strings, gives a total of eight strings. Except for every first connection, all connections are made up of two neighbouring wind turbines. Up to now, bedforms and their evolution are not taken into account in the determination of the cable layout. To get a better understanding of the bedforms and their behaviour, the bathymetry in the wind farm needs to be analysed.

## 2.3 Bathymetry

The seabed of the North Sea, as well as many other shallow seas, is not flat (Hulscher & van den Brink, 2001). Bed levels are of great importance in the development of offshore wind farms. Therefore, the PAWP bathymetry needs to be known prior to construction.

Figure 2.2 shows the PAWP bathymetry in 2003. The survey resolution is in two by two meter over an area of about twenty square kilometres. The bathymetry shows clear differences in bed height. Depths in the wind farm with respect to the lowest astronomical tide range from 26 meter to around 20 meter.

In the survey, two bedforms can be distinguished. The large bank east of the OHVS and stretching throughout the entire survey area, forms the crest of the largest visible bedform. The trough is located on the west side of the OHVS. This bedform has a wavelength of about 4 kilometres and amplitude of about 6 meters. Dimensions and the orientation with respect to the mean tidal current indicate that the large bedform can be recognised as a sand bank (Hulscher & van den Brink, 2001).

A different bedform type is located on top of the sand bank. The orientation is perpendicular to the sand bank. The bedforms have wave heights of several meters and wavelengths of hundreds of meters. These dimensions indicate that the bedforms can be recognised as sand waves (McCave, 1971; Sterlini et al., 2009). A description of sand waves can be found in the literature study Roetert (2014).

## 2.4 Bathymetrical evolution

The bathymetrical evolution is very important in offshore wind farm construction. Especially sand waves influence power cable burial depth (Besio et al., 2004; Morelissen et al., 2003; Németh et al., 2002). Sand waves can be large enough and migrate fast enough to cause changes in the bed level, significant compared to the diameter of pipelines and cables (Staub & Bijker, 1990). To get a better overview of the impact, the seabed evolution needs to be analysed.

Up to now, three bathymetrical surveys of the PAWP are performed. The 2003 survey is visible in Figure 2.2; the surveys of 2006 and 2013 are presented in Appendix A.1. Figure 2.2 already showed that the PAWP seabed consists of multiple bedforms. By comparing several surveys, seabed evolution and dynamics can be shown.

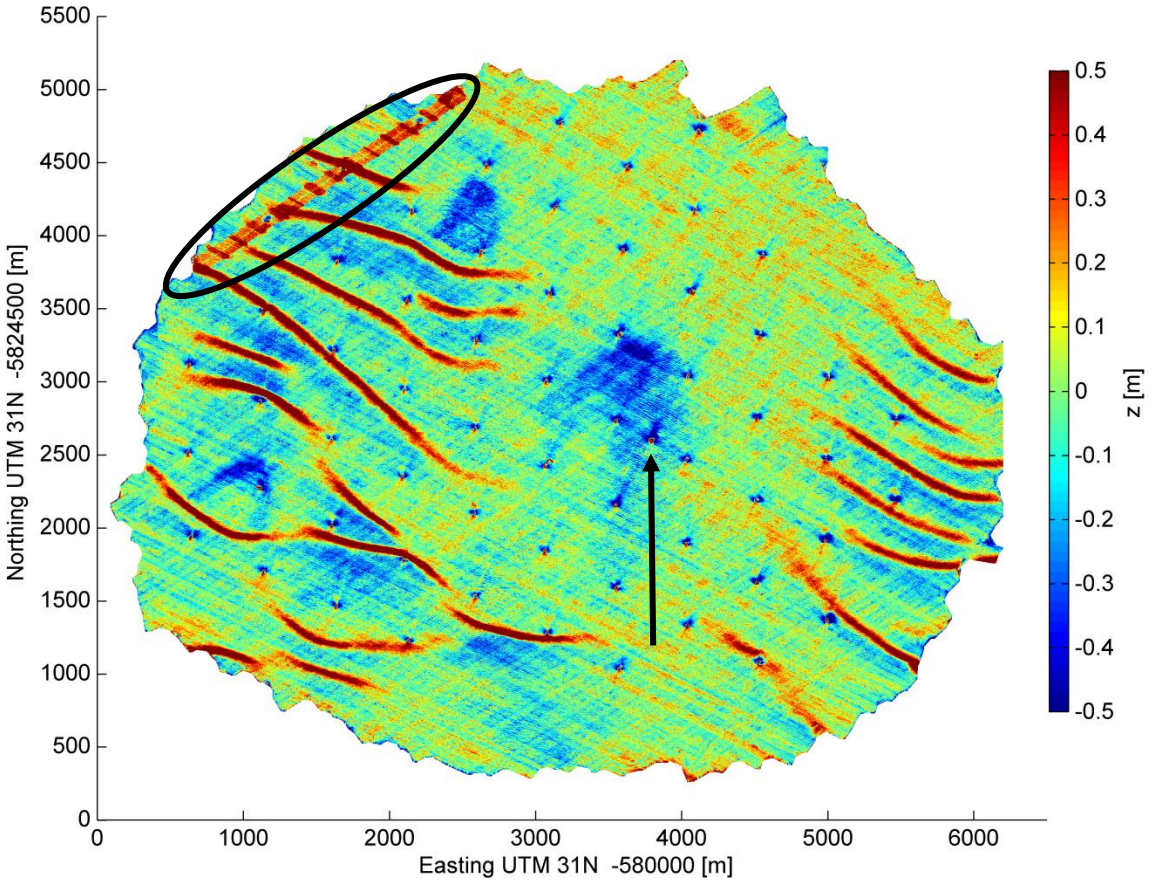


*Figure 2.3: Change in bed level over the period 2003-2013*

Figure 2.3 shows the bathymetrical evolution over the period 2003 to 2013. The evolution over the period 2003-2006 and 2006-2013 is found in Appendix A.2.The shown seabed evolution ranges from a 0.5-meter subsidence to a 0.5-meter increase in bed level. From the figure, some changes can be distinguished:

- The red lines represent the migration of sand wave crests, the direction of the red lines show a migration in the Northern/north-eastern direction
- In the area around the OHVS (indicated with the black arrow), a large subsiding area is found. At the time of the survey analyses it was not known whether the subsidence is caused by the presence of the wind farm (Bijker, 2013)
- The small blue points throughout the wind farm are the erosion pits around the wind turbines
- The red line in the left top corner, visible in the black circle, is caused by a deviation in the 2003 measurements (Bijker, 2013). The 2006 and 2013 survey, presented in Appendix A.1, do not show this deviation, therefore it is assumed that the aberration is not caused by human interactions with the seabed

The evolution visible in Figure 2.3 is taken over a period of 10 years, which is about half the lifetime of an offshore wind farm (Sirnevas & Musial, 2014). Therefore, it is assumed that present morphological evolution will continue during the rest of the wind farm lifetime.

## 2.5 Sand wave characteristics of the PAWP area

This section describes the characteristics of the sand wave fields in the PAWP. Figure 2.3 shows that sand wave migration is responsible for the largest evolution in the wind farm survey area. Compared with the wind farm design lifetime it can be assumed that these bedforms have the largest influence on cable burial depth. Previous research by Németh et al. (2002) confirms this assumption.

### 2.5.1 Wave height and wavelength

The PAWP includes two sand wave fields located in the western and eastern part of the survey area. The sand wave migration visible in Figure 2.3 denotes both fields. Since the sand waves are present throughout the entire length of the survey area, it is assumed that the fields extend outside the wind farm area.

To assess the sand wave characteristics, both are analysed in terms of wave height and length. Characteristics of both sand wave fields are analysed by means of two transects. The two arrows in Figure 2.2 represent the transect and direction along which the sand waves are analysed. The location of the transect is taken in the mean sand wave migration direction and along the route with the largest sand wave growth. Taking this transects gives the largest wave heights and migration rates.

The western and eastern sand wave field transects are shown respectively in Figure 2.4 and Figure 2.5. For comparison both transects have an equal length and are projected on the same scale.

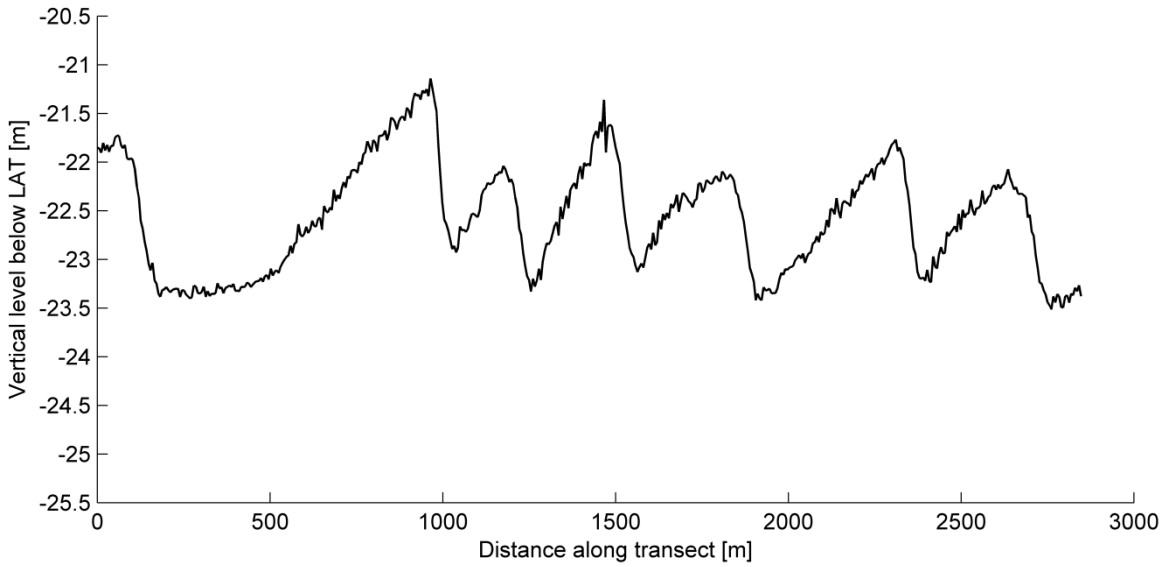


*Figure 2.4: 2003 transect of sand wave field in the western part of the survey area*

The transect shows three types of bedforms, larger sand waves with ripples and megaripples on top. These megaripples, have wavelengths of about 10 - 15 meter and heights of 8 – 12 cm. The inaccuracy in dimensions is caused by the survey cell size of two by two meter. The cell size also made it difficult to determine ripple characteristics.

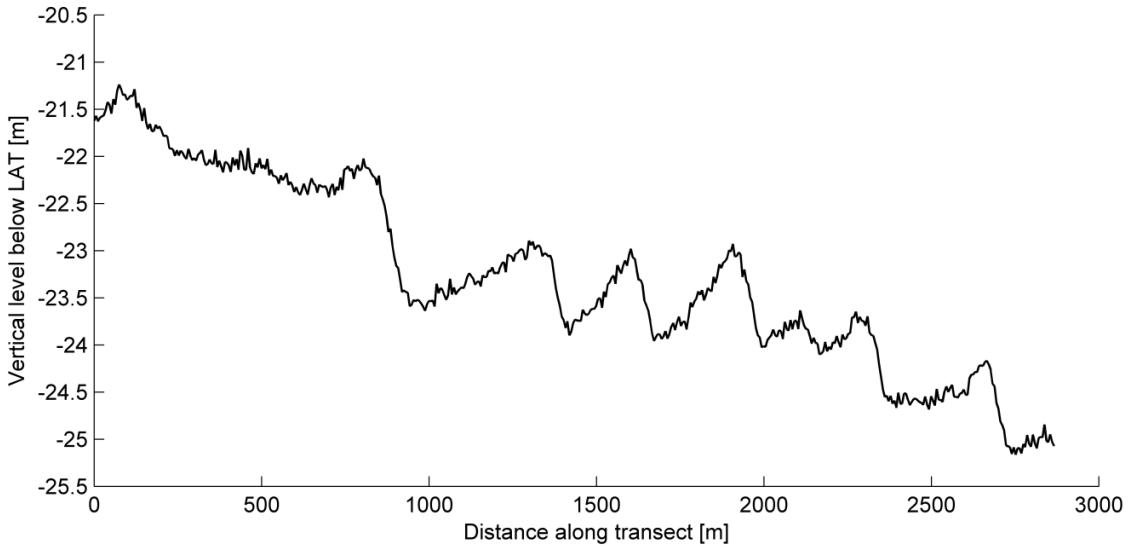


*Figure 2.5: 2003 transect of sand wave field in the eastern part of the survey area*

For the eastern sand wave field a decrease in bed level along the transect is visible (Figure 2.5). Following the right arrow in Figure 2.2, it can be seen that this decrease is caused due to the location on the sand bank.

From both transects, the mean wavelength and wave height are calculated by taking the distance between sand wave crest and compare them to the distance between sand wave troughs. Wave heights are found by measuring the difference in height between a crest and its adjacent trough. Results are presented respectively in Table 2.1 and Table 2.2. Outcomes show that the sand waves in the western field have longer wavelengths and heights.

*Table 2.1: Lengths of sand waves in PAWP area*

| Sand wave field | No. of waves | Mean $L_0^*$ [m] | Min-Max $L_0^*$ [m] |
|---|---|---|---|
| Western | 7 | 435 | 220 - 900 |
| Eastern | 8 | 381 | 180 - 700 |

*Table 2.2: Height of sand waves in PAWP area*

| Sand wave field | Mean wave height [m] | Min-Max wave height [m] |
|---|---|---|
| Western | 1.40 | 1.20 – 1.65 |
| Eastern | 0.92 | 0.28 – 1.50 |

Table 2.1 and Table 2.2 show that the sand waves in the western field are longer and higher. Both transects show large differences in minimum and maximum wave height and length. This is mainly caused by the first sand wave in both transects, which is longer and higher. However, sand wave characteristics found are comparable to literature

### 2.5.2 Sand wave migration

Sand wave migration has the greatest influence on power cable coverage. To assess the migration of both fields, the 2003 and 2013 transects are compared. Comparisons for the western and eastern sand wave field are shown respectively in Figure 2.6 and Figure 2.7. The migration speed is determined by comparing the middle of the sand waves lee side from the 2003 and 2013 transects. It is assumed that the only sand wave movement occurs in horizontal direction. Results for the migration speed are shown in Table 2.3.

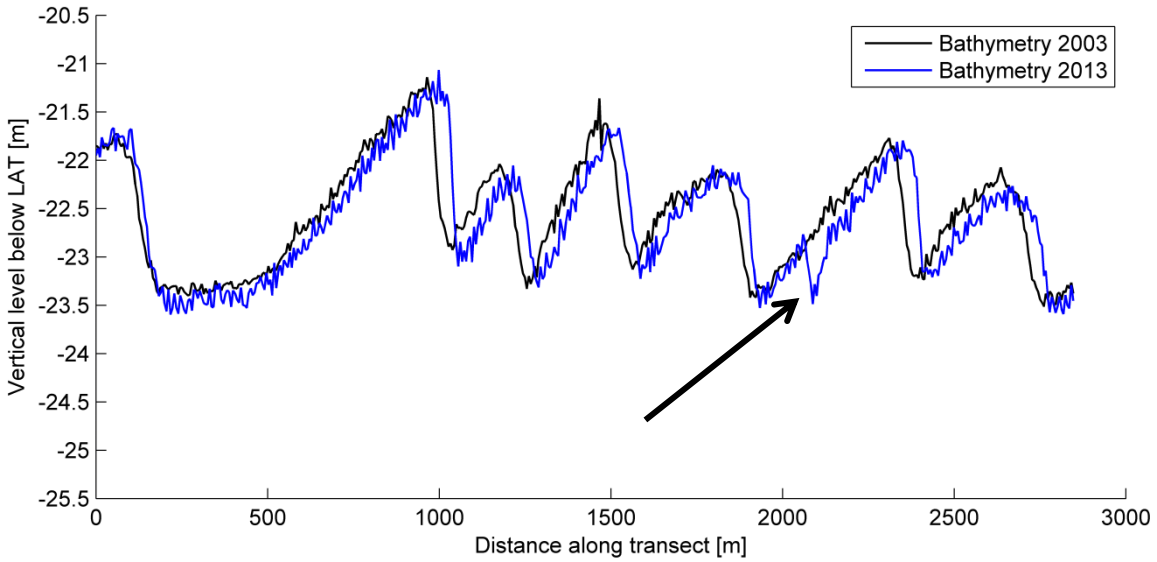


*Figure 2.6: Comparison of 2003 and 2013 transect in the western sand wave field*

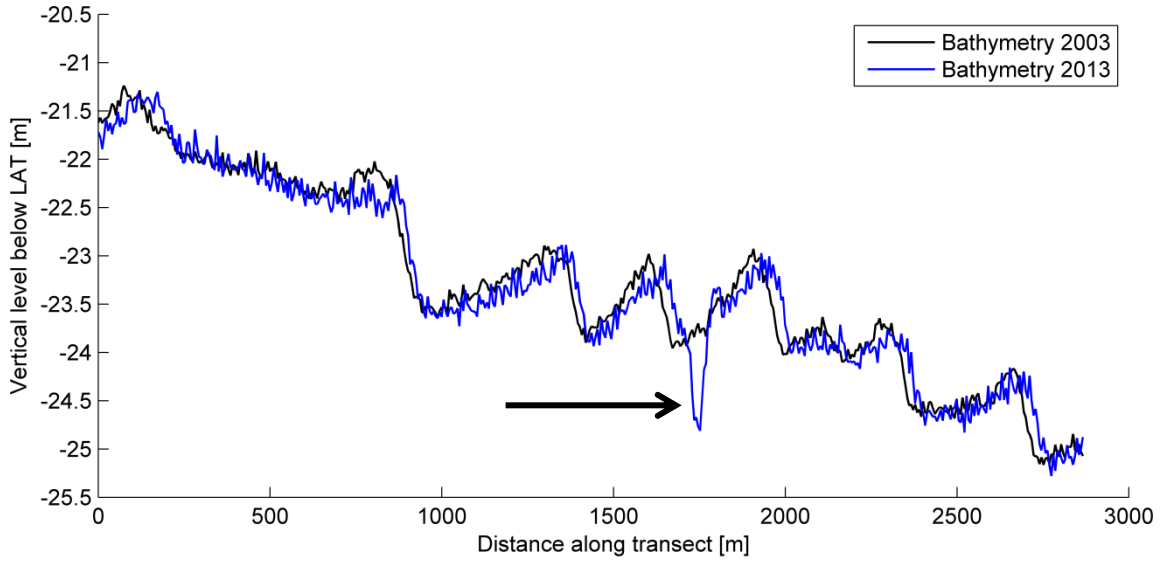


*Figure 2.7: Comparison of 2003 and 2013 transect in the eastern sand wave field*

Both transects show sand wave migration over the period 2003-2013. The wave height and length stayed roughly the same over this period. The sand waves in both transects migrate to the right. Given the location and direction of the arrows in Figure 2.2, it can be said that sand wave migration in the PAWP area occurs in Northern/north-eastern direction. Migration speeds for both transects are found in Table 2.3.

The transects of 2013 both show a strange jump. These jumps are indicated with arrows in Figure 2.6 and Figure 2.7. Since the jump locations coincide with turbine locations and Figure 2.3 shows that erosion pits are formed around wind turbines, it can be said that the jumps indicate erosion pits.

*Table 2.3: Migration speeds of transects in PAWP area*

| Sand wave field | Mean migration [m/y] | Min-Max migration [m/y] |
|---|---|---|
| Western | 3.4 | 1.9 – 4.5 |
| Eastern | 2.6 | 1.5 – 4.3 |

Results show differences in minimum and maximum migration speed. These differences are caused by a deviating migration speed of the first sand wave. However, migration speeds found are comparable to Besio et al. (2004) and Borsje et al. (2013).

### 2.5.3 Sand wave sensitivity analysis

The use of two bathymetrical surveys only provides information about the initial and end situation. Sand wave migration is therefore determined over this period. The dynamic character of sand waves however makes it difficult to assume that the migration speed remains constant over time. This gives rise to a possible sensitivity analysis. Since three surveys are available for the PAWP, the migration can be analysed in three periods: 2003 – 2013, 2003 – 2006 and 2006 – 2013.

To compare the differences, Figure 2.8 presents the transects of the western sand wave field in 2003, 2006 and 2013. From this transect the migration speeds are taken and compared in table 2.4. The migration speeds of the eastern transect are presented in table 2.5.

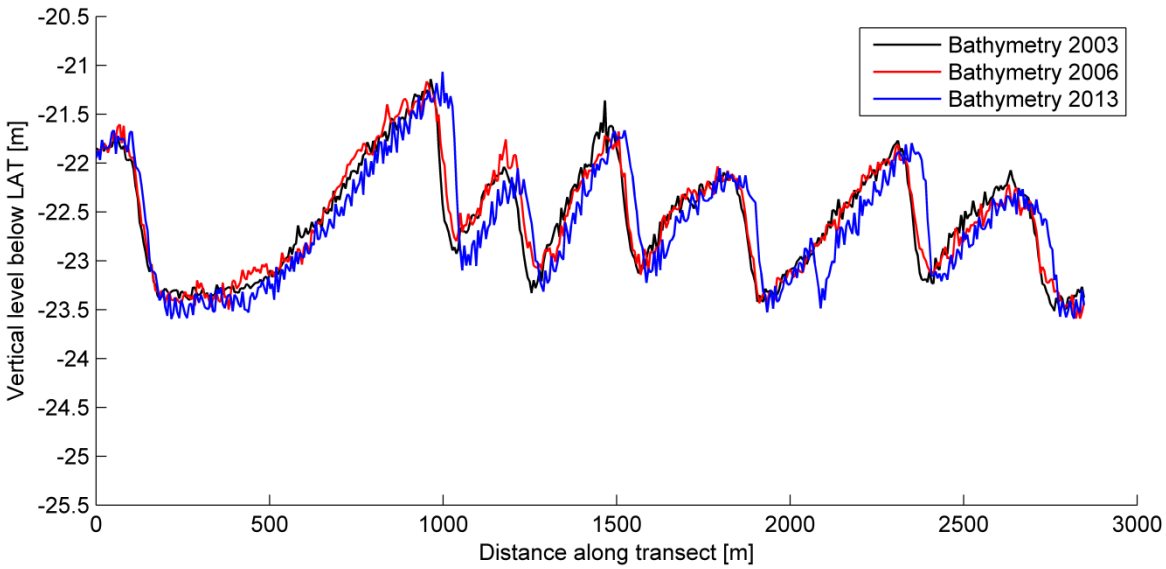


*Figure 2.8: Comparison of the 2003, 2006 and 2013 transects in the western sand wave field*

*Table 2.4: Migration speeds of transect in western part PAWP area*

| Period | Mean migration [m/y] | Min/max migration [m/y] |
|---|---|---|
| 2003-2013 | 3.4 | 1.9 – 4.5 |
| 2003-2006 | 2.3 | 1.5 – 4.7 |
| 2006-2013 | 3.7 | 2.1 – 4.9 |

*Table 2.5: Migration speeds of transect in eastern part PAWP area*

| Period | Mean migration [m/y] | Min/max migration [m/y] |
|---|---|---|
| 2003-2013 | 2.6 | 1.5 – 4.3 |
| 2003-2006 | 2.2 | 1.0 – 4.0 |
| 2006-2013 | 2.7 | 1.4 – 4.4 |

The results state that migration speeds are higher in the period 2006-2013. Results are however questionable. Based on expert review it is said that the quality of the 2006 survey is insufficient. Second, the size of the grid cells can influence results by 0 m/y to 0.4 m/y.

## 2.6 Summary

To develop the route optimization tool an extended case study is required. The quality of the case study is determined whether the requirements are met. Most important demands are the availability of good surveys and presence of a highly dynamic bed.

Figure 2.2 and Appendix A.1 provide an overview of the different bathymetrical surveys taken in the wind farm. Differences between the three surveys are shown in Figure 2.3 and Appendix A.2. Especially the 2003 and 2013 survey represent a very detailed seabed.

The second demand for a good case study is the dynamic behaviour of the seabed. An almost completely static seabed causes development of the dynamic bed optimization to be difficult. The PAWP exists roughly of two sand wave fields located on a sand bank. In the difference plots, it is visible that the sand waves migrate in Northern/North-eastern direction. The sandbank migration is hardly visible over a period of ten years, but is assumed perpendicular to the sand waves.

The availability of the wind turbine locations, bathymetrical surveys with high quality, dynamic seabed and present cable layout makes the PAWP very applicable as a case study for the optimization tool development.

# 3 Development of the route optimization tool

This chapter describes the development of the route optimization tool. The tool consist of three optimization steps: The optimization under a flat, static and dynamic seabed. For each step, some optimization algorithms are used. Figure 3.1 gives an overview of the different steps and their algorithms. With this chapter, the research questions belonging to the tool building are answered.

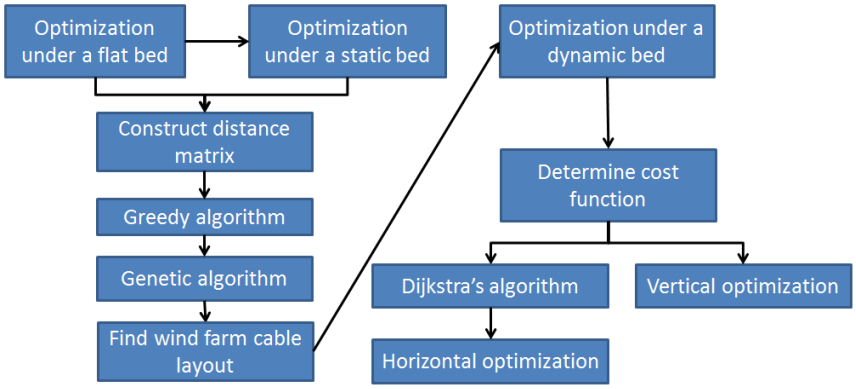


*Figure 3.1: Flow chart of different optimization steps*

## 3.1 Description of algorithms for optimization under a flat bed

The first optimization step is to find a cable layout under a flat seabed. In this step, the PAWP seabed is assumed completely flat a certain point in time. The first part of this step is to calculate a distance matrix containing the weights of the routes between two wind turbines. Since the seabed is flat and static, this weight is equal to the straight distance between two turbines. The aim for this optimization step is to find the shortest possible layout based on the distance matrix.

### 3.1.1 Wind farm layout problem outline

In a wind farm, all turbines need to be connected to one of more OHVS via some strings. For costs savings, the aim is to minimize total cable length. This problem can be seen as a combinatorial problem in were the costs of the total solution (cable layout) of a finite set of objects (turbine connections) needs to be minimized.

To solve the problem, a solution method is needed. This method has to find a set of cable routes based on given turbine and transformer positions, minimizing total cable costs, connecting every turbine to a transformer, not exceeding cable capacity and the planar constrain that cables do not cross each other (Bauer & Lysgaard, 2013).

Since the combinatorial problem has a finite set of solutions, a most optimal solution can be found. However, Jenkins et al. (2013) showed that the number of solutions increase drastically with the amount of wind turbines (Table 3.1). Jenkins et al. (2013) derived the total number of possible solutions by:

$$S = \tau!^{\sigma} * \frac{(\tau\sigma)!}{\tau!^{\sigma} * \sigma!}$$

In the formula, S is the number of total solutions, $\tau$ the number of turbines per string and $\sigma$ the number of strings. Table 3.1 shows the total amount of solutions for some cases. The number of wind turbines per string (TPS) and amount of strings is assumed equal.

*Table 3.1: Amount of possible solutions for the wind farm cable layout problem*

| Number of strings and TPS | Total number of turbines | Amount of possible solutions (Jenkins et al., 2013) | Amount of possible solutions (n!) |
|---|---|---|---|
| 1 | 1 | 1 | 1 |
| 3 | 9 | $6{,}05 * 10^{4}$ | $3{,}63 * 10^{5}$ |
| 5 | 25 | $1{,}29 * 10^{23}$ | $1{,}55 * 10^{25}$ |
| 8 | 64 | $3{,}15 * 10^{84}$ | $1{,}27 * 10^{81}$ |
| 10 | 100 | $2{,}60 * 10^{151}$ | $9{,}33 * 10^{160}$ |

Table 3.1 shows that an increase in number of turbines causes an exponential growth in the amount of possible solutions. Even for a simple wind farm containing 25 wind turbines, there are over $10^{23}$ solutions. To find the most optimal solution, every single solution has to be analysed. This way, the possibility of another solution being better than the existing solution is eliminated. As this is clearly not practical based on present computational power, a better method is required (Kumar & Panneerselvam, 2012). As long as not all possibilities are analysed, the found optimum is called the near optimal solution.

### 3.1.2 Genetic algorithm

For solving the combinatorial problem, many solutions are proposed. These solutions vary from the exact methods (Table 3.1) to the classic heuristics and the meta-heuristics (Kumar & Panneerselvam, 2012). The description of various meta-heuristics can be found in Appendix B. For the size and amount of solutions present in offshore wind farms, the genetic algorithm is found to be the most applicable. The genetic algorithm consists of six steps and can be found in Appendix B.1 and Figure 3.2.

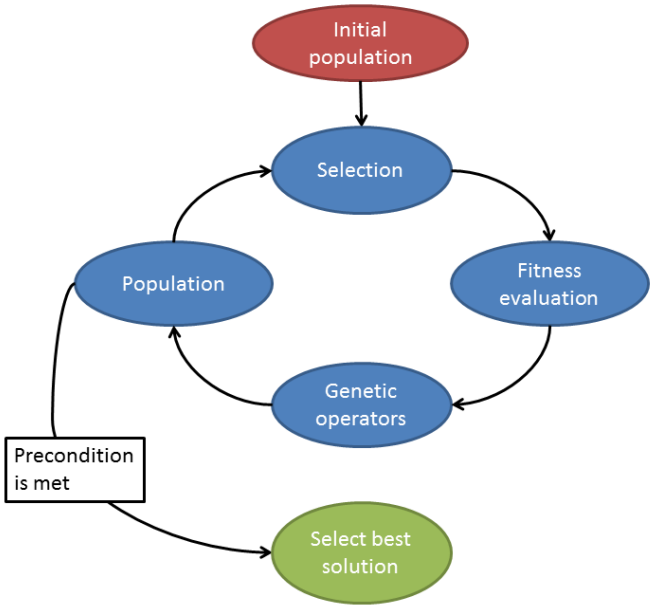


*Figure 3.2: Genetic algorithm used in route optimization tool*

The genetic algorithm starts with the creation of an initial population. This population consists of multiple solutions for the layout problem. For each solution, the total weight is calculated by means of the distance matrix.

From this population a set of eight solutions is taken. The solution with the lowest total weight is then chosen as best solution in this set. The fourth step consists of applying independently eight operations to the best solution. These new solutions are then placed back as set in the

population. This process iterates until a set precondition is met. Possible preconditions are a certain amount of computational time, a number of iterations or no significant improve in the total solution. Eventually, the best solution in terms of total weight is chosen as the near optimal.

### 3.1.3 Greedy algorithm

Outcomes and computational time of the genetic algorithm are influenced by size and quality of the initial population. Choosing random initial solutions both need a large population and a lot of computational time to get a layout comparable to or better than the original. Therefore, the greedy algorithm is chosen to construct initial solutions.

The operation of the greedy algorithm can be seen in Figure 3.3 A. Starting from the substation, the algorithm always connect the nearest turbine. Figure 3.3 B however shows a more optimal solution in terms of total length. Since the algorithm is only introduced to construct more directed initial solutions, this is accepted. A further description of the greedy algorithm can be found in Appendix B.2 .

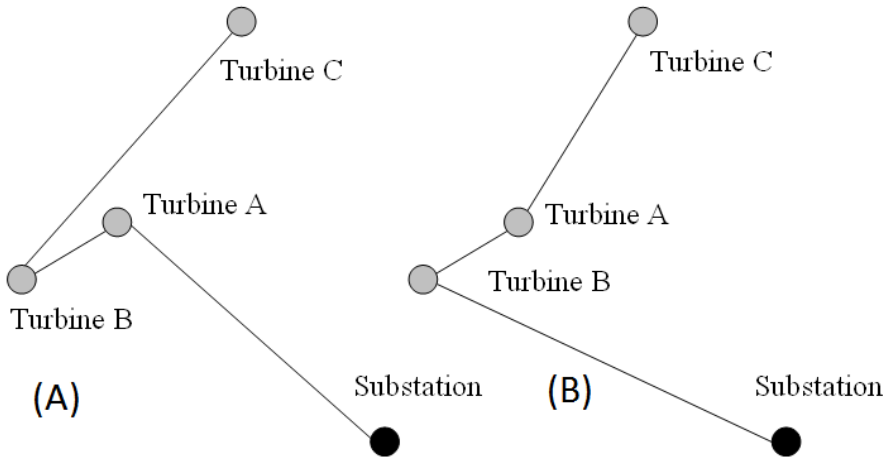


*Figure 3.3: Solution found by the greedy algorithm (A) and the optimal solution (B)*

## 3.2 Description of optimization under a static seabed

The first optimization step is extended towards a static seabed. The static seabed represents the seabed present at a certain moment in time. For offshore wind farms, this is prior to construction. The route weight is now determined based on the length of a cable placed one meter under the seabed. However, as changes in bed level are not taken into account, route weight is solely based on cable length. Aim of this step is also to find a near optimal cable layout by means of the route weights and the greedy and genetic algorithm.

An important remark is that ripples and megaripples are present on top of the sand waves, visible in Figure 2.4. Assuming a cable placed at a fixed burial depth, the final configuration follows the irregular (mega)ripple pattern. Since power cables cannot follow the (mega)ripple pattern due to their maximum bending radius, it is suggested that the cables should follow the sand wave pattern.

### 3.2.1 Filtering of bathymetry

Since the influence of the ripples and megaripples is unwanted, they should be excluded from the survey. This is executed in two steps, starting by averaging each cell in the survey with its surrounding cells. The size of the averaging square is chosen to be around the wavelength of the megaripples. Filtering gives a new survey with bed level heights following the average

mega ripple height. The filtered seabed is then lowered by half the mega ripple wave height, completely excluding smaller bedforms. Figure 3.4 includes a filtered part of the transect given in Figure 2.4.

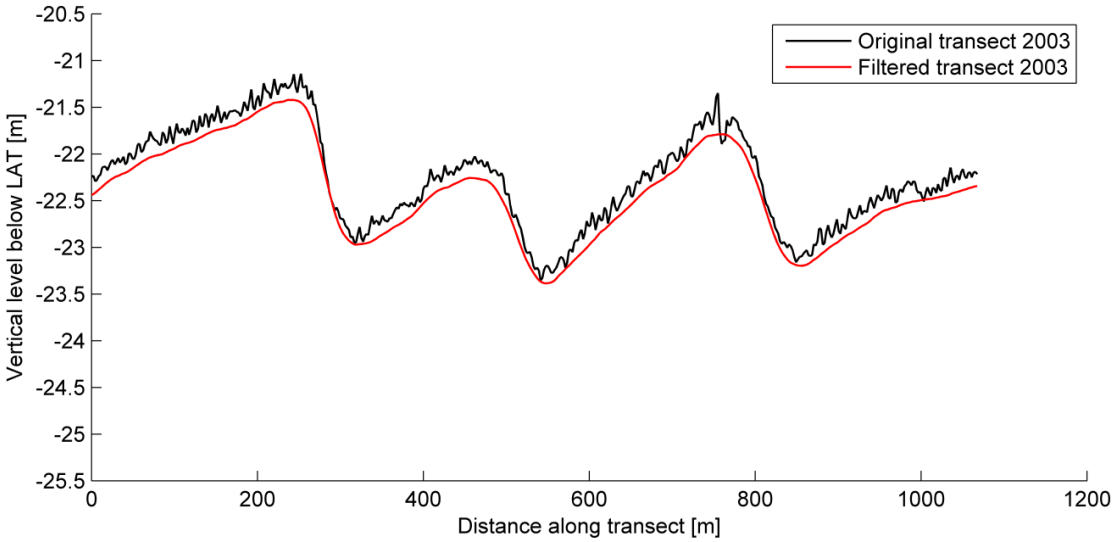


*Figure 3.4: Comparison of original transect (black) and filtered transect (red)*

The red line representing the filtered seabed gives a sand wave pattern almost directly underneath under the ripples and megaripples (Figure 3.4). The pattern found can be followed by power cables and is therefore assumed as static bed. With the exclusion it is assumed that the influence of ripple and megaripple influence is minimized.

The sand wave migration showed some small irregular patterns due to ripples and megaripples (Figure 2.6). Figure 3.5 presents the comparison of a filtered part from the 2003 and 2013 transects for the western sand wave field. Migration speeds found are between 3.2 and 3.6 meter per year, which are around the mean migration speed presented in Table 2.3.

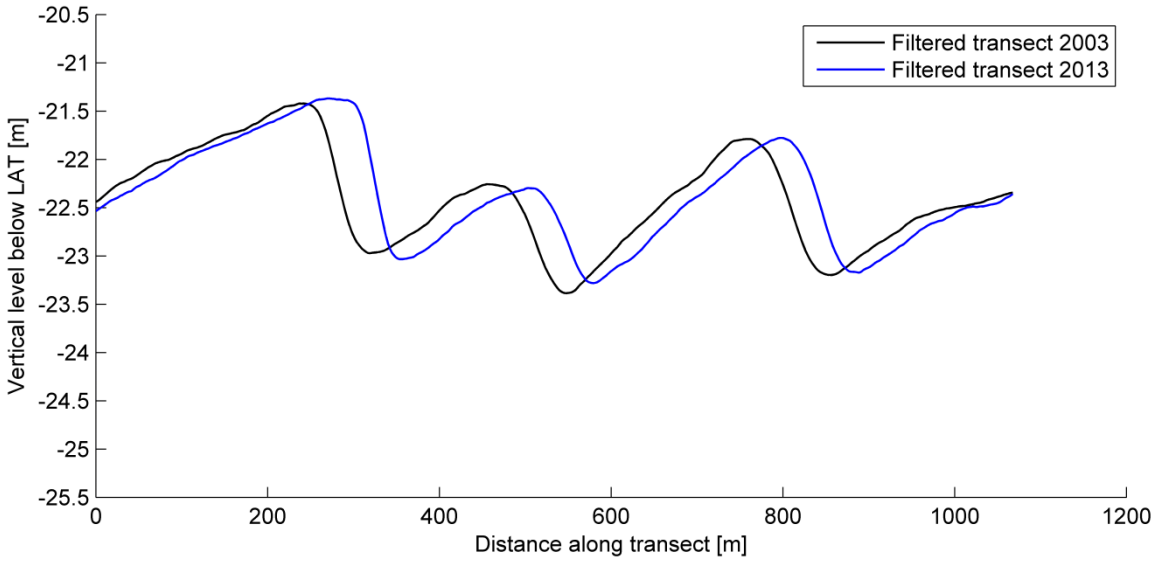


*Figure 3.5: Comparison of filtered 2003 and 2013 transect*

## 3.3 Description of algorithms for optimization under a dynamic seabed

The third optimization step is an extension of the previous two steps. In this section, the dynamic character of the seabed is taken into account. This step consists of three parts:

- Definition of a cost function
- Optimization in the vertical plane
- Optimization in the horizontal plane

The cost function forms together with a cable layout found in previous steps the input for both optimization parts. The optimizations in the vertical and horizontal plane are executed independent from each other.

### 3.3.1 Definition of cost function

To determine the optimal cable routes in the horizontal and vertical plane, the route weight needs to be determined. Since the seabed is dynamic, route weight cannot be solely based on cable lengths. To define the weight of each cable, a cost function is determined. This function consists of three parts:

- CAPEX – Capital expenditures, here initial cable costs
- OPEX – Operational expenditures, here monitoring costs
- Costs of cable failure – Costs of an event to happen multiplied with the internal and external risks

Since bed level change is different for every cell in the PAWP survey, a connection between two turbines is divided in sections. The length and type of each section is different for the vertical and horizontal optimization. Based on the three parts the cost function is defined as:

$$Costs(turbine\ x - turbine\ y) = \sum_{s=1}^{s=total\ of\ s} min\Big(CAPEX\big(C_i(s)\big) + OPEX\big(C_i + Ch_{bed}(s)\big) + \big(R_{int}(s) + R_{ext}(s)\big) * \Big(Power\ loss + CAPEX\big(C_r(s)\big)\Big)\Big)$$

The function describes that the sum of all sections in a connection between turbine x and y need to be minimized. $C_i$ describes the initial coverage, $Ch_{bed}$ change in bed level in a given period and $C_r$ defines required burial depth at time of failure. The internal and external risks are defined by $R_{int}$ and $R_{ext}$ respectively.

In the cost function, two variables are of influence, the initial burial depth and the change in bed level. Table 3.2 gives and overview of the influence of the variables on CAPEX, OPEX, internal risks and external risks. An arrow upward suggests a cost increase and an arrow downward suggest a decrease in costs.

*Table 3.2: Increase and decrease of costs per function*

| Initial burial depth | Bed evolution | CAPEX | OPEX | Costs of failure due to internal risks | Costs of failure due to external risks |
|---|---|---|---|---|---|
| Deeper ↓ | | ↑ | ↑ | ↑ | ↓ |
| Shallower ↑ | | ↓ | ↓ | ↓ | ↑ |
| | Subsidence ↓ | | ↑ | ↑ | ↓ |
| | Rise ↑ | | ↓ | ↓ | ↑ |

Table 3.2 shows that the CAPEX, OPEX and internal risks have the same direction in costs. When minimizing the cost function, these three are weighted out against external risks. As CAPEX states the initial costs, these do not change as the seabed evolves.

#### 3.3.1.1 *Risk of cable failure*

The risk of cable failure can be divided in three categories: morphological, internal and external risks. Extreme events such as storms are not taken into account in risk determination.

Most important morphological risks are vortex-induced-vibrations (VIV). When a piece of cable becomes exposed on the seafloor, the flow around it can induce cable vibrations. This can lead to further un-burial and cable fatigue (Raaijmakers et al., 2014). However, as cable exposure is considered a no go, the risk of failure becomes a factor ten higher when becoming exposed. Assigning a very high risk assures that possible exposure is prevented.

Internal risks can be seen as change of failure caused by faults in the cable. Faults can originate from the cable manufacturing, cable laying/ trenching, covering process and overheating. Only the risk of overheating changes for different burial depths. The internal risk is defined based on expert input and Holmstrøm (2007) and can be described by:

$$Risk(internal)\ [1 * y^{-1}] = 0.015 + 0.030 * (C_i + Ch_{bed})$$

External risks can be seen as human induced hazards endangering the power cable from the outside. The hazards are always associated with a physical impact in the form of penetration or drag (Raaijmakers et al., 2014). The chance of an event to happen is based on the return period and probability of actual damage. The indications of chances are presented in Table C.1 and Table C.2. Risks for penetrating and dragged objects are found respectively in Table C.3 and Table C.4.

Figure 3.6 (l) shows the internal, external and combined risks at burial depths from 0 to 3.0 meter. Since risks rise exponentially between 0 and 1.0 meter, Figure 3.6 (r) only displays risks to a maximum value of 0.3.

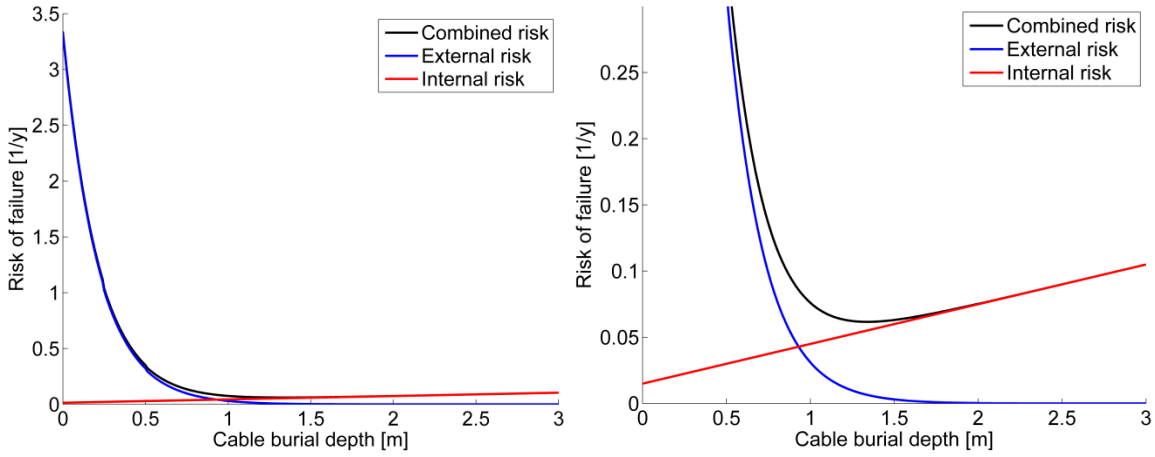


*Figure 3.6: Risks of failure for burial depths of 0 to 3.0 meter (l) and zoomed towards a maximum risk of 0.3 (r)*

For burial depths between 0 and 1.0 meter a sharp increase in total risk is visible. The combined lowest risk is to be found at a burial depth of 1.3 meter. However, since the figure is valid for a static seabed, optimal burial depth will vary for a dynamic seabed.

### 3.3.2 Vertical optimization

The second part of the optimization under a dynamic bed is to find the optimal cable position in the vertical plane. This position is up to now mainly based on the bathymetry prior to
During this step, the position in the horizontal plane is not changed. The steps taken in the vertical optimization are:

1. Choose a filtered start and end survey and determine the wind farm cable layout
2. Choose connection between two turbines to optimize and calculate transects for both surveys
3. Divide the connection between turbines in a number of sections with equal length
4. Work out the cost function for every section
    a. Vary initial burial depth from 0.0 to 3.0 meter with steps of 10 centimetre
    b. Determine for all burial depths the total costs
    c. Select the burial depth with lowest total costs
5. Combine all sections and give cable position in the vertical plane

The optimal position in the vertical plane can vary. It is assumed that sections with bed subsidence need a larger initial burial depth than sections with a rising seabed.

### 3.3.3 Horizontal optimization

The last part of the optimization under a dynamic seabed is to find the most optimal position in the horizontal plane. During this step, the position in the vertical plane is not changed and all sections have an equal initial burial depth. Up to now, the horizontal position of a cable does not deviate from a straight line between two turbines. To assess the position in the horizontal plane a few steps are taken:

1. Choose a filtered start and end survey and determine the wind farm cable layout
2. Choose connection between two turbines to optimize
3. Take survey area around the two turbines as a grid
4. Assign all cells in the grid with a fixed burial depth minus the bed level change over a certain period.
5. Apply cost function on all cells in the grid
6. Execute Dijkstra's algorithm (Appendix B.4) and find route with lowest total costs
7. Smoothen line to meet maximal bending radius constrain and calculate new costs

Since dynamic bedforms are present in the wind farm area the optimal position in the horizontal plane may vary. It is assumed that the most optimal route avoids subsiding areas and cross rising areas, given a fixed initial burial depth.

## 3.4 Route optimization tool outline

The optimizations steps described in previous sections are combined in a route optimization tool. The tool will be a user-friendly way to optimize wind farm cable layout. The variety of options available in the tool are:

- Select input for wind turbine locations and bathymetry
- Possibility to select a section of the entire wind farm to optimize with a polygon
- Define user input :
    - Population size
    - Number of iterations in the genetic algorithm
    - Maximal capacity per string

- Execute optimization under a flat and static seabed
    - Construct distance matrix between turbines
    - Construction of initial population (with or without greedy algorithm)
    - Execute optimization based on user input
- Use the found near optimal layout to further optimize under a dynamic seabed
- User input for cost function
    - Power loss (downtime, revenues and average power produced)
    - Capital expenditures (cable costs, excavation costs and monitoring costs)
- Vertical optimization
    - Selection of route part to optimize
    - Optimize all sections and give total minimized costs
    - Show optimized position in the horizontal plane per connection
- Horizontal optimization
    - Selection of route part to optimize
    - Optimize all sections and give total minimized costs
    - Show optimized position in horizontal plane per connection

To use the tool for optimization of a specific offshore wind farm cable layout, the following user input is required:

- Locations of wind turbines and OHVS
- In an existing wind farm  a survey prior to construction and a survey with the wind farm in operation
- For a new wind farm one survey, plus the migration speed and directions of sand waves
- Maximum amount of turbines per string
- Costs of power loss (downtime, revenues and average power produced)
- Capital expenditures (cable material per meter, excavation costs and monitoring costs)
- Costs of cable repair
- Internal and external risks based on location and materials used

The general layout of the tool is presented in Figure 3.7

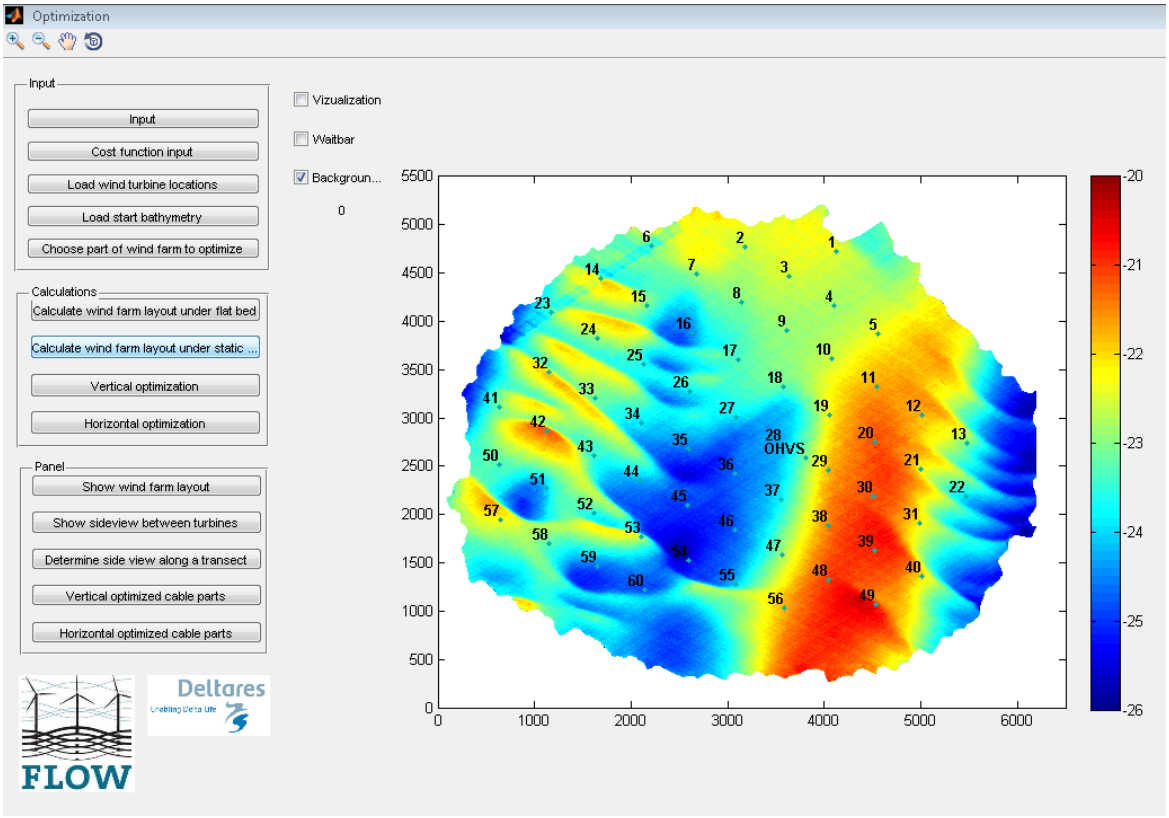


*Figure 3.7: Outline of the route optimization tool*

## 3.5 Summary

The genetic algorithm proves to be the best choice for the wind farm layout problem. To get more directed initial solutions, and decrease population size and computational time, the greedy algorithm was added. Both algorithms are combined to find a near optimal layout under a flat and static seabed.

The found cable layout is used for the optimization under a dynamic seabed. To start, a cost function is defined. This function weighs out the CAPEX, OPEX and the cost of failure due to internal and external risk against each other.

During the vertical optimization, ideal vertical cable positions are determined. This is done by dividing the connections between two turbines in sections. For every section, the cost function is applied to a range of initial burial depths. Next, for all sections the lowest costs and their associated burial depths are selected. Combing all sections gives the optimal cable position in the vertical plane.

Next, the horizontal cable position in the field is optimized per connection. An area around two turbines is taken from the survey and used as working grid. All cells in the grid are assigned with the bed level change over a certain period. The cost grid is then created by applying the cost function on every grid cell. Dijkstra's algorithm tries to find the shortest path, in terms of costs, through this grid.

The layout found, is a result of the minimization of the cost function. All steps together form the route optimization tool developed as graphical user interface (GUI) in Matlab.

# 4 Results of the route optimization tool

This chapter presents the results of the research. The chapter starts with results of the optimization under a flat and static seabed. In these steps, the near optimal PAWP cable layout is determined. All connections between two turbines in the layout are optimized during the third step. Based on a dynamic seabed, the cables are optimized in the vertical and horizontal plane. The ideal position is found by applying the cost function onto the possible cable routes. To discuss the effectiveness of the optimizations, both are executed separately. Finally, this chapter is concluded with the comparison of the original layout with the optimized layout. With this chapter, the research questions belonging to the tool application are answered.

## 4.1 Wind farm layout under a flat seabed

The optimization is started with the assumption of a flat seabed at a certain point in time. Because of this flat seabed, cable position is assumed 1.0 meter below bed level. Cable lengths can easily be calculated with the aid of Pythagoras. The lengths of all possible connections are stored in a distance matrix. Since there is no bed level change over time, the lengths are regarded as route weights. The genetic algorithm, initiated by the greedy algorithm, uses the route weights to determine the near optimal wind farm layout.

### 4.1.1 Initial population of genetic algorithm

The genetic algorithm, shown in Figure 3.2, starts with creating an initial population, containing multiple initial solutions. Originally, the genetic algorithm uses complete random initial solutions. The greedy algorithm develops quick and more directed solutions. With this method, the size of the population can be decreased resulting in lower computational times.

This paragraph introduces two variations of the greedy algorithm, which are discussed in Appendix B.2. The first method is the string-by-string solution. Here all strings are constructed one after the other. Figure 4.1 shows an initial string-by-string solution.

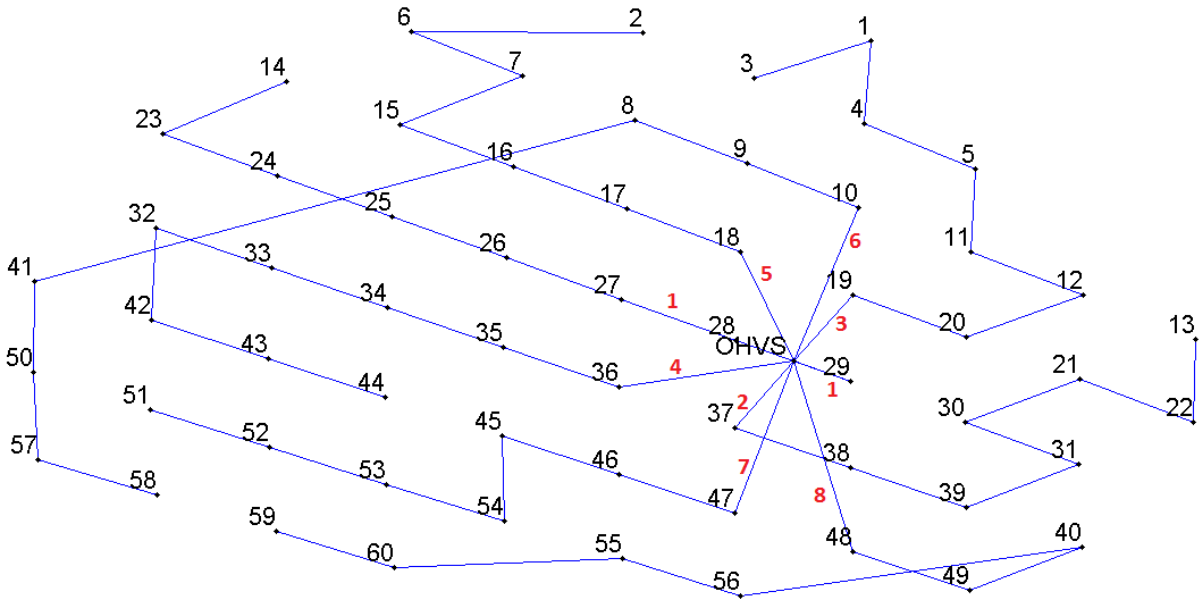


*Figure 4.1: String-by-string initial solution*

The initial solution displays a more directed solution, however, cables still cross and some large connections are visible (Figure 4.1). In addition, the connections around the OHVS are far from preferable.

Therefore, a second variation is introduced. To start, all strings are connected to the nearest turbine from the OHVS. In addition, the second turbine in the strings is selected turn by turn. This variation helps to give all strings a direction in the layout and assigns the eight turbines nearest to the OHVS each to a different string. The turn-by-turn start solution is presented in Figure 4.2.

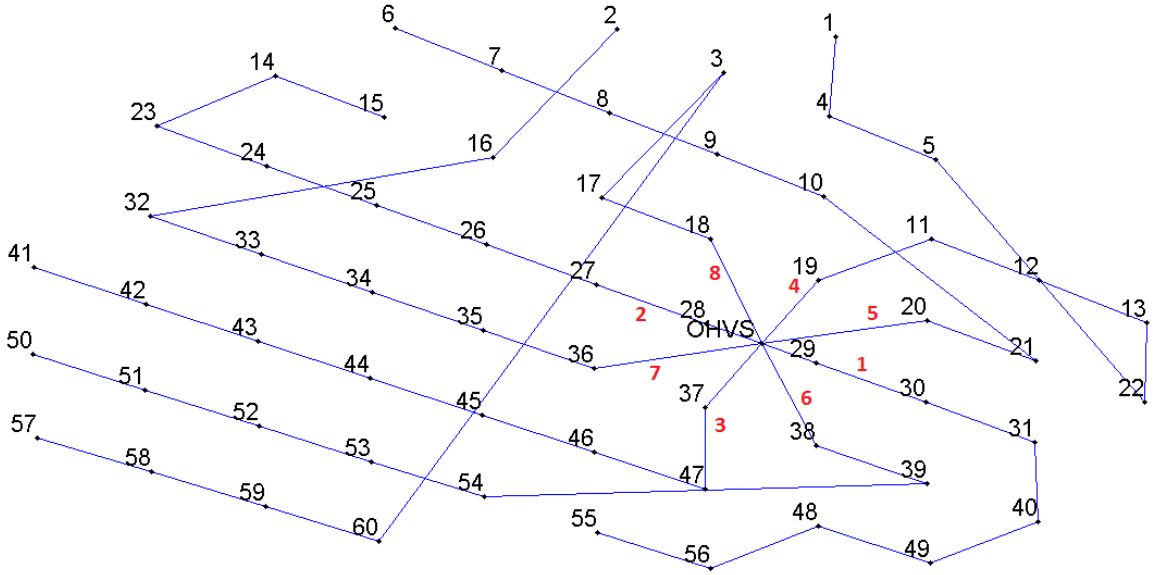


*Figure 4.2: String-by-string initial solution with turn-by-turn start*

The extended initial solution shows a layout comparable with the original PAWP layout (Figure 4.2). However, large connections and cable crossing still occurs. The large connections are made as the algorithm always chooses the nearest node. Since the algorithms single purpose is to form a qualitative input for the genetic algorithm, solutions found are accepted.

### 4.1.2 Optimization of initial solutions

Next step is to optimize all solutions in the population and find a near optimal cable layout. The genetic algorithm, described in Figure 3.2, is executed multiple times to find a cable layout for the PAWP. The stopping criterion is chosen based on the change in total solution. When during the last 500 iterations the final solution does not change with more than one percent, the genetic algorithm is stopped. Since not all possible solutions are assessed, the solution found is assumed a near optimal solution.

Figure 4.3 shows a layout for the PAWP found by means of the genetic algorithm. Results in terms of total weight, number of iterations and percentage difference with the original layout are presented in Table 4.1. Four other solutions found are shown in Appendix D.1.

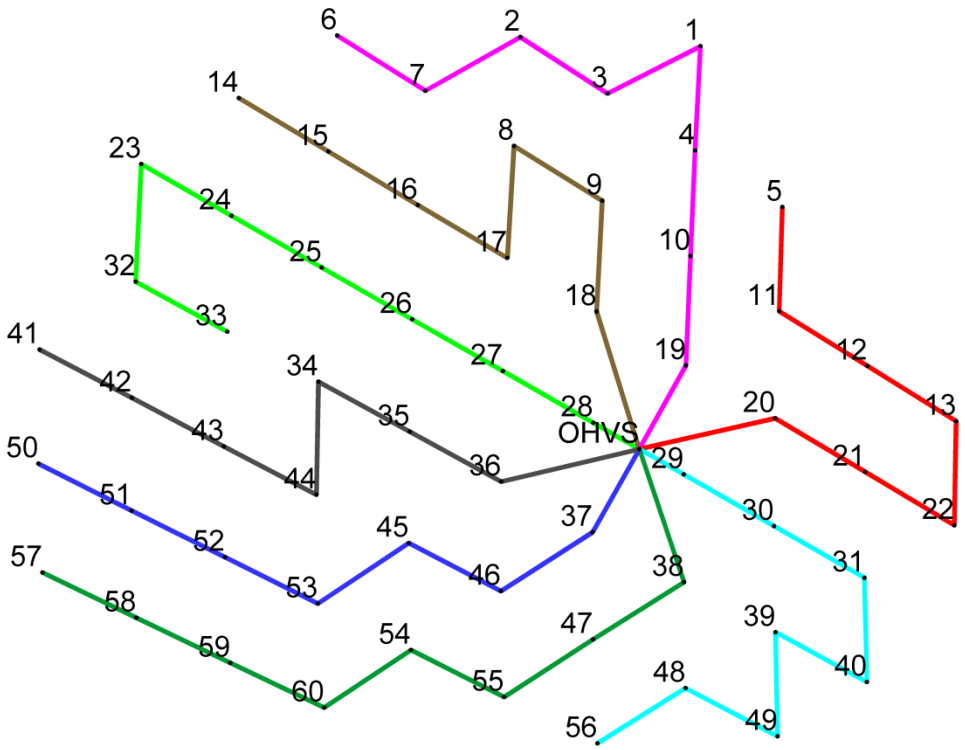


*Figure 4.3: PAWP layout found with optimization under static seabed*

*Table 4.1: Comparison of solutions for flat seabed optimization*

| ***Solution number*** | ***Total cable length [m]*** | ***Number of iterations*** | ***Difference with original cable length*** | ***Figure number*** |
|---|---|---|---|---|
| *Original* | $3.3487*10^4$ | | | *Figure 2.2* |
| *1* | $3.3679*10^4$ | 35505 | 0.57 % | *Figure 4.3* |
| *2* | $3.3776*10^4$ | 41087 | 0.86 % | *Figure D.3* |
| *3* | $3.3581*10^4$ | 31025 | 0.28 % | *Figure D.4* |
| *4* | $3.3468*10^4$ | 43025 | -0.06 % | *Figure D.5* |
| *5* | $3.3667*10^4$ | 29035 | 0.54 % | *Figure D.6* |

The found layout shown in Figure 4.3 has quite some similarities with the original PAWP layout. The total weight of the layout only differs 0.57% from the original layout. Table 4.1 shows results for five found solutions. Results show that despite visual differences in layouts, the total weights are quite comparable. The differences in visual layout are caused by small variations in mutual distances between turbines. Based on criteria of connecting all turbines, not exceeding string capacity and no cables cross, all layouts found can be regarded near optimal solutions.

### 4.1.3 Division of wind farm area

Although total cable lengths shown in Table 4.1 are similar to the original cable length, the number of iterations still proves to be quite long. Table 3.1 shows that for a linear increase in turbines, the amount of solutions increases exponentially. Division of the PAWP area in a few subareas decreases the amount of turbines and number of iterations per area. Combining the subareas gives a total near optimal solution. A division of the area in three parts is showed in Figure 4.4. Subdivisions in two and four parts are presented in Appendix D.2. Results from all three divisions are stated in Table 4.2.

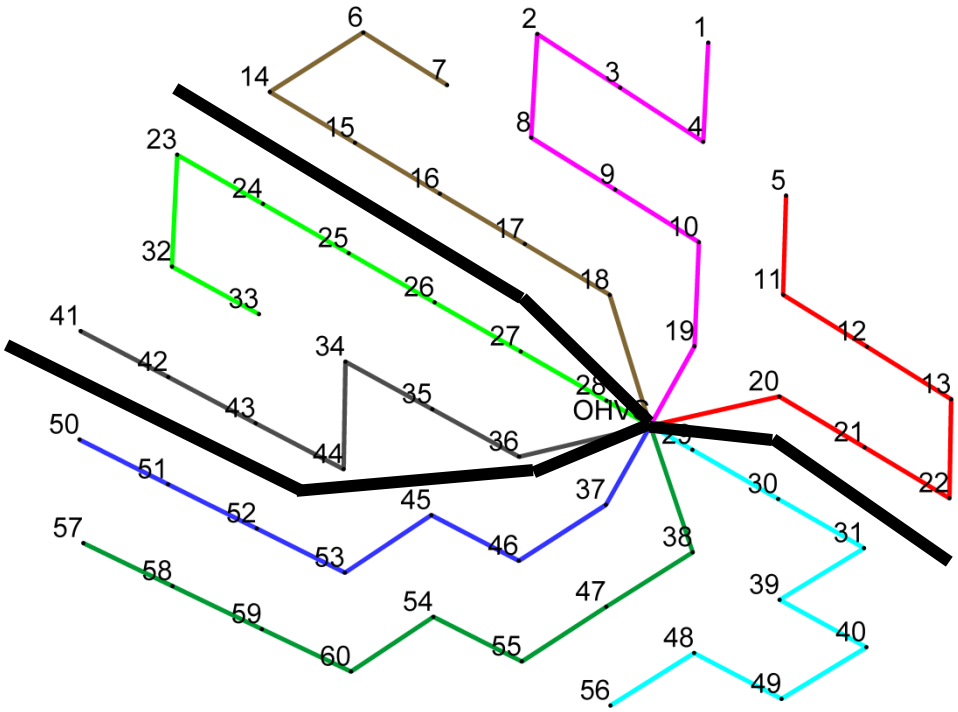


*Figure 4.4: Division of PAWP area in three parts*

*Table 4.2: Comparison of solutions for the flat bed after division of the PAWP area*

| ***Solution number*** | ***Total cable length [m]*** | ***Number of iterations*** | ***Difference with original cable length*** | ***Figure number*** |
|---|---|---|---|---|
| Original | $3.3487*10^4$ | | | Figure 2.2 |
| 2 parts | $3.3636*10^4$ | 5709 | 0.44 % | Figure D.7 |
| 3 parts | $3.3471*10^4$ | 1537 | -0.23 % | Figure 4.4 |
| 4 parts | $3.3536*10^4$ | 115 | 0.15 % | Figure D.9 |

Both Figure 4.4 and Table 4.2 show promising results. Especially the division in four parts shows a large decrease in number of iterations, which is a factor 250. Final layouts can still be seen as acceptable since difference in total length with the original layout is very small. However, division of the wind farm makes cable trajectories more restricted to a certain area. A smart area choice will definitely help to improve computational times and still provide an acceptable solution.

## 4.2 Wind farm layout under a static seabed

In the second optimization step, a static seabed is introduced. During this step, the seabed at one point in time is used. For the PAWP, two surveys are available. Since the 2013 survey is taken during wind farm operation, the filtered 2003 survey is chosen (Figure 2.2).

Route weights are based on cable lengths placed one meter under the seabed. For this step a filtered survey is used to satisfy the maximum cable-bending radius constrain. However, cable weights prove to be only a little bit longer for the static seabed compared to the flat seabed. For example, the connection between turbine 23 and 32 (Figure 2.2), crosses two sand waves but is only 0.28 meter longer. To show differences in outcomes, the layouts found during the flat bed optimization are calculated for the static seabed. Results are presented in table 4.3.

*Table 4.3: Comparison of solutions under a static bed with flat bed solutions*

| Solution number | Total cable length under filtered seabed [m] | Difference in total cable length with flat bed optimization |
|---|---|---|
| Original | $3.3487*10^4$ | $7.1*10^{-4}$ % |
| 1 | $3.3679*10^4$ | $8.0*10^{-4}$ % |
| 2 | $3.3776*10^4$ | $7.6*10^{-4}$ % |
| 3 | $3.3581*10^4$ | $7.2*10^{-4}$ % |
| 4 | $3.3468*10^4$ | $8.9*10^{-4}$ % |
| 5 | $3.3667*10^4$ | $7.7*10^{-4}$ % |
| 2 parts | $3.3637*10^4$ | $7.5*10^{-4}$ % |
| 3 parts | $3.347*10^4$ | $7.6*10^{-4}$ % |
| 4 parts | $3.3536*10^4$ | $8.5*10^{-4}$ % |

Results for the static bed optimization do not differ much from the flat bed optimization. Therefore, it is assumed that this optimization step provides layouts comparable to previous layouts found.

## 4.3 Optimized cable positions under a dynamic seabed

During the last step, the cable parts are optimized under a dynamic seabed. Since layouts found do not show a significant improvement over the original layout, the latter is chosen for further optimization. This section consists of determination of cost function parameters and vertical and horizontal optimization.

### 4.3.1 Cost function

To perform the vertical and horizontal optimization, the input for the cost function needs to be quantified. The parameters are defined in two ways. Common known values are determined based on literature and the ones left are defined based on expert review and comparable cases. Table 4.4 gives an overview of the parameters in the cost function, their corresponding values and their source. Except for the number of turbines, all parameters are worked out below. The number of turbines affected is determined based on the chosen connection to be optimized.

*Table 4.4: Values for parameters in cost function*

| ***Parameter*** | ***Value*** | ***Source*** |
|---|---|---|
| *Capital expenditures* | | |
| *Cable costs per meter* | *€300* | *Expert review* |
| *Excavation costs [-1 meter]* | *€125.000 [300 $m^{-1}$]* | *Expert review* |
| *Repair costs* | *€2.000.000 - €3.000.000* | *Expert review* |
| *Operational expenditures* | | |
| *Survey entire wind farm* | *€100.000 [$y^{-1}$]* | *Expert review* |
| *Powerloss* | | |
| *Average downtime* | *2-6 months* | *Expert review* |
| *Maximum turbine capacity* | *2.0 MW* | *(Amaliawindpark)* |
| *Capacity factor* | *0.41* | *(Andrew, 2014; EWEA, 2014)* |
| *Revenues per kWh* | *€0.15* | *Expert review* |

For optimization purposes, the upper limits of all parameters are used. Figure 4.5 shows the cost function for a cable with a length of 300 meter and burial depths varying from 0 to 3.0 meter for a static seabed. The number of wind turbines affected is chosen to be eight. However, as seabed dynamics are taken into account during this optimization step, costs will vary.

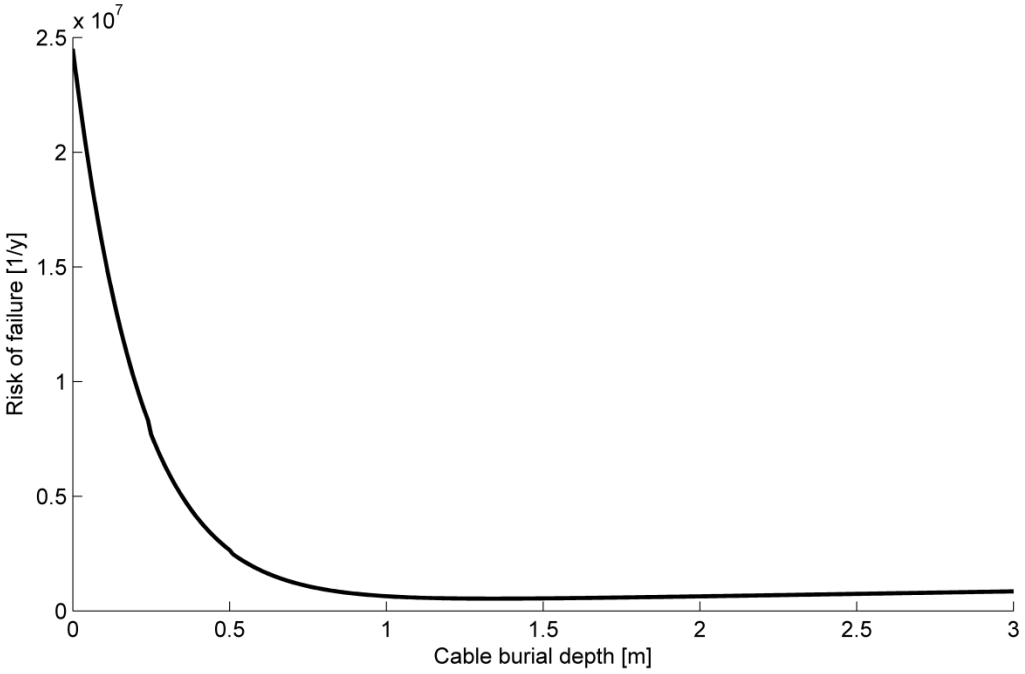


*Figure 4.5: Cost function for a 300 meter cable for burial depths between 0 and 3.0 meter*

### 4.3.2 Optimized cable position in the vertical plane

The dynamic bed optimization is started with finding an optimal position in the vertical plane, with no variation in the horizontal plane. All connections present in the PAWP cable layout are optimized separately. The seabed evolution is taken over the period 2003-2013 (Figure 2.3).

The vertical optimization is executed as described in paragraph 3.3.2. The optimal route found is then compared with the costs of a cable placed at a fixed initial burial depth. For comparison, three cases with a fixed burial depth are identified, at 1.0 meter, 1.5 meter and 2.0 meter. In addition, for the optimal route found two cases are present. In the first case, the initial burial depth cannot exceed the minimum required coverage, the second case has no limits in terms of burial depth.

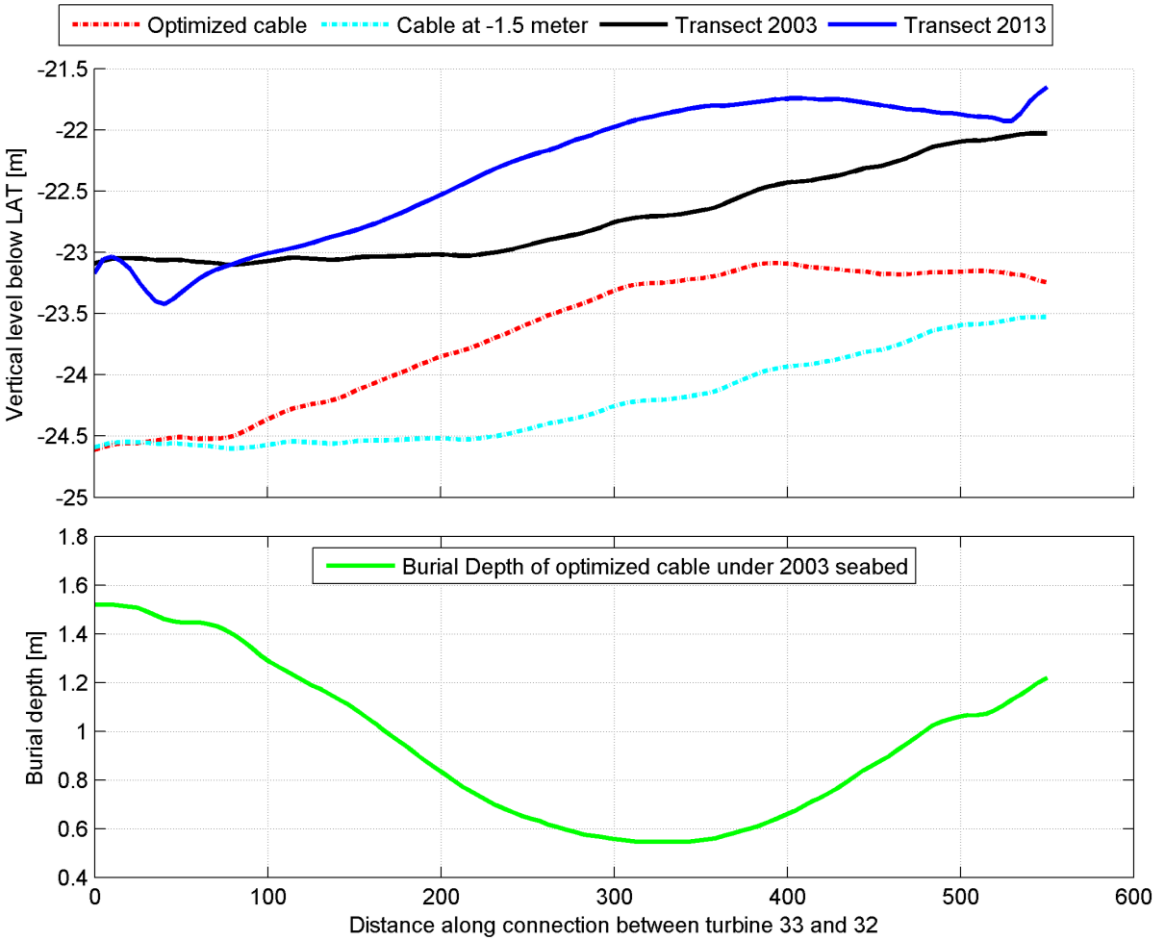


*Figure 4.6: Optimized position of power cable in connection between turbine 33 and 32*

Figure 4.6 shows the optimized position in the vertical plane of the power cable connection between turbine 33 and 32. In the figure, 5 lines are visible. The black and red lines represent respectively the 2003 and 2013 survey. The blue and red dotted lines represent respectively the cable with an initial burial depth of 1.0 meter under the 2003 survey and the optimized cable. The green line represents the burial depth of the power cable under the 2003 survey.

Figure 4.6 also shows that for a rising seabed, the optimal initial burial depth can be below 1.0 meter. Total cost savings for this configuration are €44.870 on a total original costs of €653.770. This is a cost saving of about eight percent. In addition, the risk is lowered by 15.6% percent. To indicate the difference with a subsiding seabed, Figure 4.7 shows the optimized cable connection between turbine 18 and the OHVS.

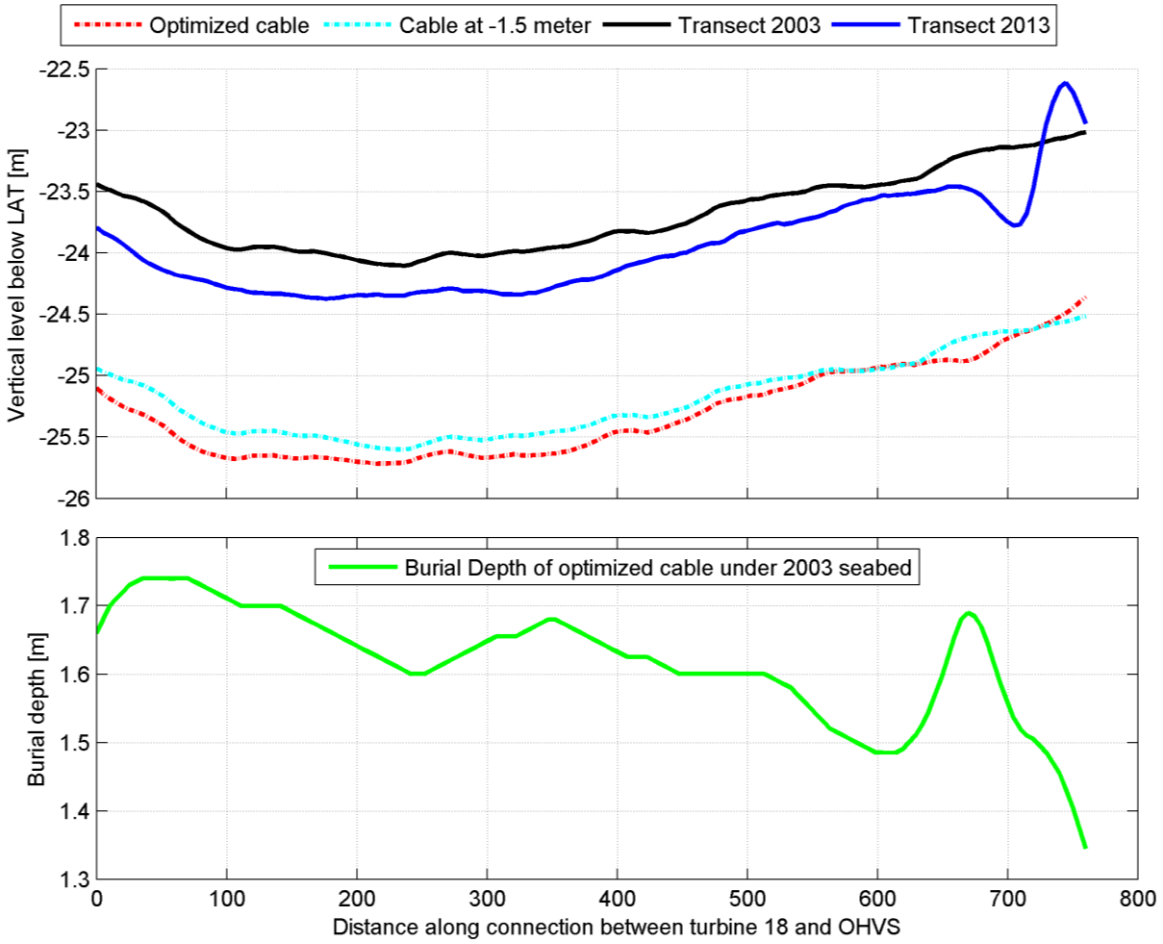


*Figure 4.7: Optimized position of power cable in connection between turbine 18 and OHVS*

The new cable position lies between 1.5 and 2.0 meter under the 2003 bed level (Figure 4.7). Total cost savings for this configuration are €70.430 compared to a total original costs of €1.706.700. The risks are reduced by 38.4% compared to a fixed initial burial depth of 1.0 meter . Based on both figures it can be stated that the position in the vertical plane very much depends on the seabed evolution. A subsiding seabed causes that the initial burial depth needs to be increased while a rising seabed causes the burial depth to decrease. Results for all cases are shown in Table 4.5.

*Table 4.5: Comparison of costs for the vertical optimization*

| Case | Total costs | Difference in costs with respect to case 1 | Difference in risk compared with case 1 |
|---|---|---|---|
| Straight fixed 1.0 m | € 56.272.000 | | |
| Straight fixed 1.5m | € 45.850.000 | -18.5% | - 35.6% |
| Straight fixed 2.0m | € 50.363.000 | - 10.5% | - 25.7% |
| Variable burial depth 1.0 - 3.0 m | € 44.670.000 | - 20.6% | - 38.4% |
| Variable burial depth 0 - 3.0 m | € 44.669.000 | - 20.6% | - 38.6% |

Results show that especially the cases with variable burial depth reduces the power cable costs. However, a fixed initial burial depth of 1.5 meter gives outcomes that do not deviate very much from the best solutions.

### 4.3.3 Optimized cable position in the horizontal plane

The second part of the dynamic bed optimization is to find the most optimal route in the horizontal plane. During this step, the initial burial depth is fixed, so there is no variation present in the vertical plane. All connections present in the PAWP cable layout are optimized separately. The seabed evolution is taken over the period 2003-2013 (Figure 2.3).

The horizontal optimization is executed as described in paragraph 3.3.3. For the horizontal optimization, fixed initial burial depths of 1.0, 1.5 and 2.0 meter are assessed. Results are compared with straight cables between turbines at the same fixed burial depth. Figure 4.8 shows the optimal route in the horizontal plane between turbine 33 and 32 for a fixed initial burial depth of 1.5 meter over the period 2003-2013. The figure contains the contour lines of the bedforms present in 2003. In the top right, the location of this connection in the wind farm is indicated. The figure displays the 2003 survey, which is given in Figure 2.2.

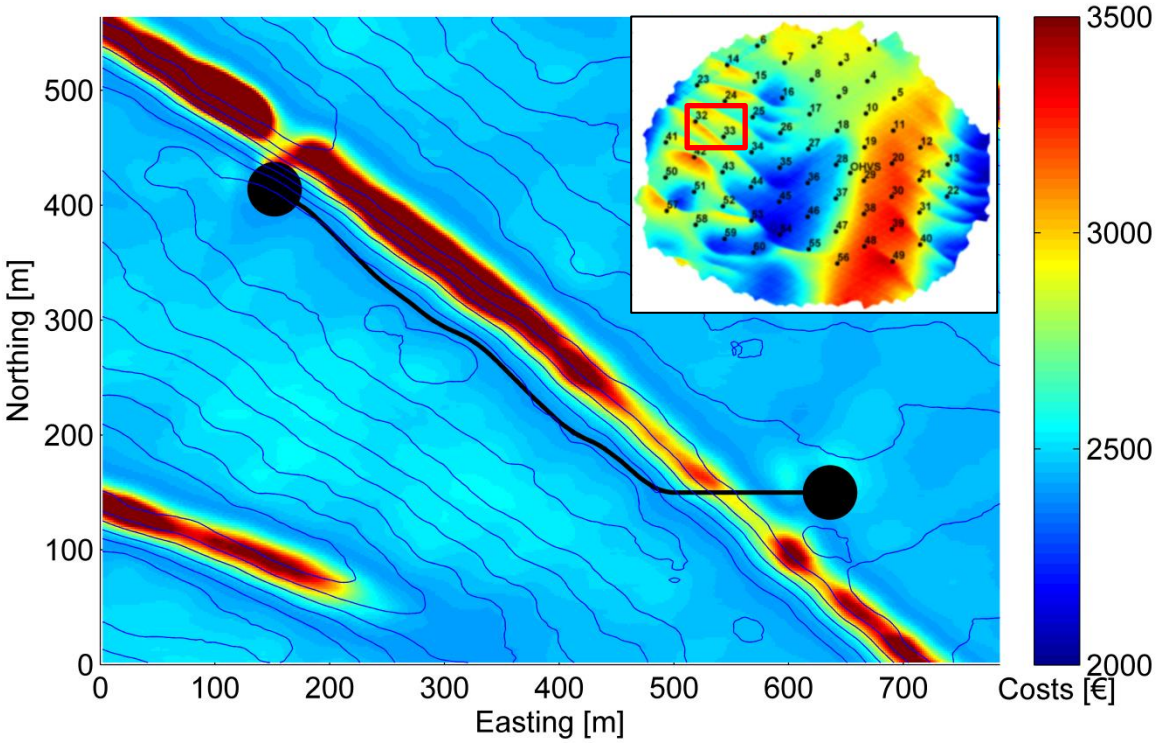


*Figure 4.8: Optimized route in the horizontal plane between turbine 33 and 32 for a fixed burial depth of 1.5 meter with contour lines (blue) showing the bedforms in the 2003 survey and location in the PAWP 2003 survey (Figure 2.2) (top right figure)*

The grid around turbine 33 and 32 is based on costs per cell (Figure 4.8). These costs are defined by applying the cost function on each cell based on the final coverage. The final coverage can be found by subtracting bed level change from the initial fixed burial depth. Total costs savings for this configuration are €12.440 on a total costs of €678.410 for the straight connection. The average risk of failure is also reduced by 11,1%. However as the cable does not follow the straight line between two turbines, cable length increases.

For comparison, Figure 4.9 and Figure 4.10 represent the same connection on the same scale, but now optimized with a fixed burial depth of respectively 1.0 and 2.0 meter. Table 4.6 compares the total costs, total length and average risk per case.

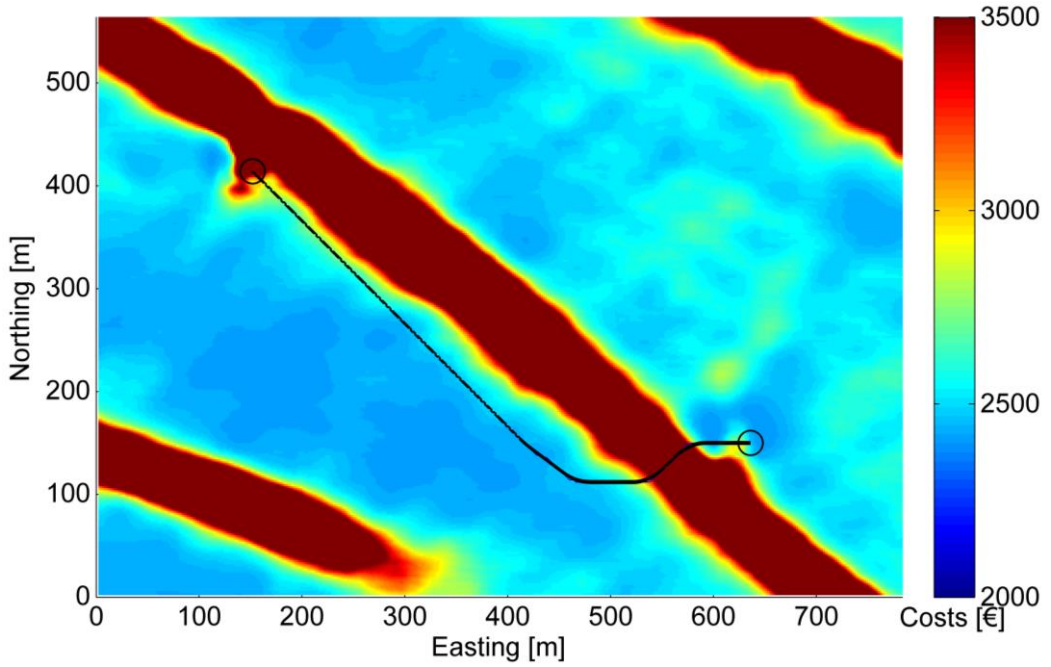


*Figure 4.9: Optimized route in the horizontal plane between turbine 33 and 32 for a fixed burial depth of 1.0 meter*

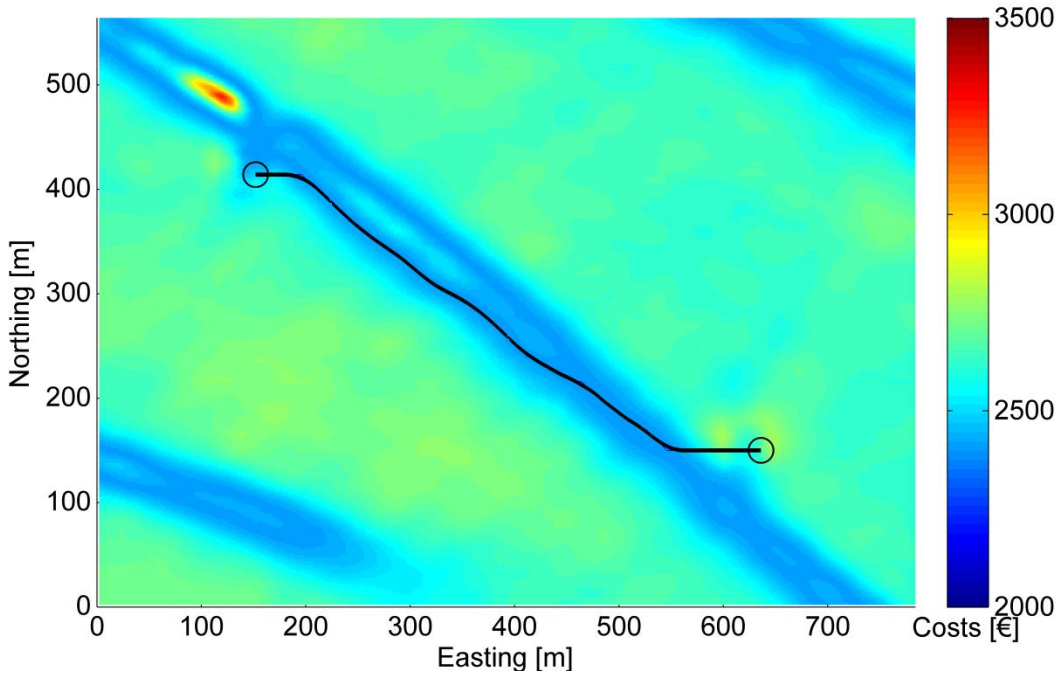


*Figure 4.10: Optimized route in the horizontal plane between turbine 33 and 32 for a fixed burial depth of 2.0 meter*

*Table 4.6: Comparison of costs for connection between turbine 33 and 32*

| Case | Costs | Length [m] | Risk [$y^{-1}$] |
|---|---|---|---|
| Straight fixed 1.0 m | € 653.770 | 549.9 | 0.0731 |
| Horizontal fixed 1.0 m | € 773.050 | 617.1 | 0.0957 |
| Straight fixed 1.5 m | € 678.410 | 549.9 | 0.0736 |
| Horizontal fixed 1.5 m | € 665.970 | 578.1 | 0.0654 |
| Straight fixed 2.0 m | € 749.320 | 549.9 | 0.0871 |
| Horizontal fixed 2.0 m | € 679.190 | 570.8 | 0.0641 |

Table 4.6 shows that a cost reduction can be made with a fixed burial depth of 1.5 and 2.0 meter. The figures representing the different cases also show that the optimization with a larger burial depth follows sand wave crests more.

The optimized connection between turbine 33 and 32 is mainly located in a rising area. To indicate the difference with a subsiding seabed, Figure 4.11 shows the optimized connection between turbine 18 and the OHVS.

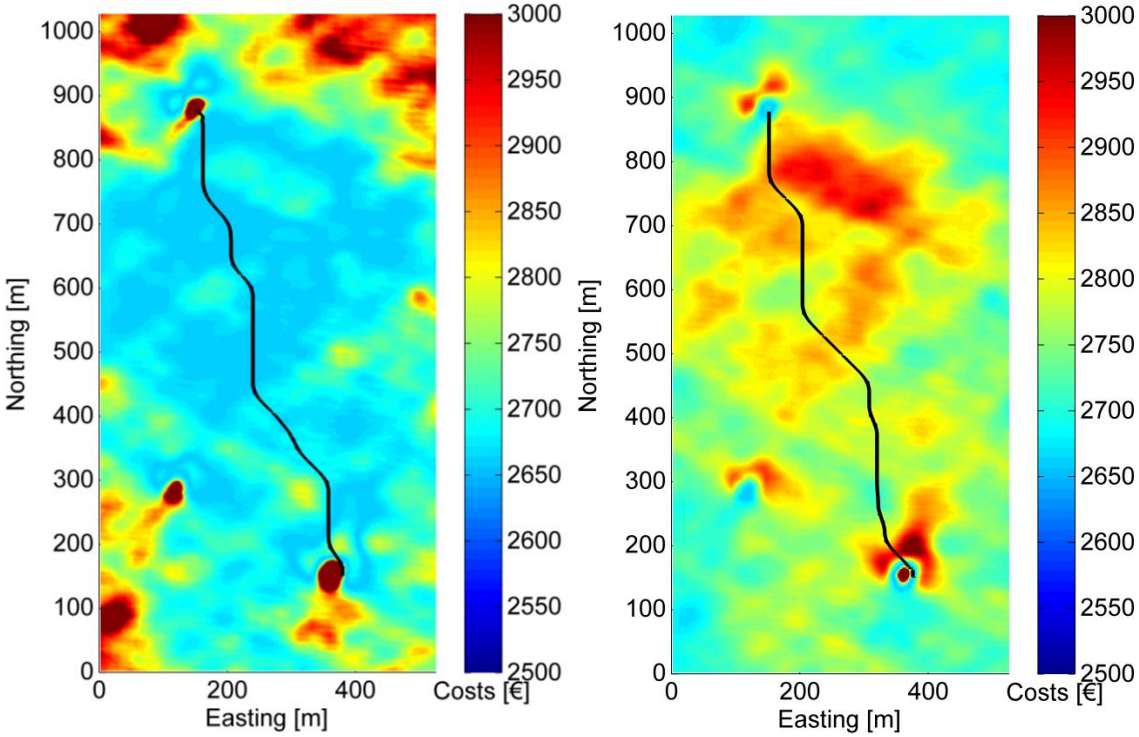


*Figure 4.11: Optimized route in the horizontal plane between turbine 18 and the OHVS with a fixed burial depth of 1.5 ,meter (left) and 1.0 meter (right)*

The configuration found costs €7000 more than the straight connection. The cause of difference is the approach of the vertical and horizontal optimization. The horizontal optimization tries to find a route from cell to cell, from which the length is always longer than the straight connection length. Second, minimum risks are found when coverage is around 1.4 meter, giving only small variations in total risks.

To indicate differences, Figure 4.11 (r) shows the same connection optimized with a fixed burial depth of 1.0 meter. The results of optimizing this connection are stated in Table 4.7. Here also the case with a fixed 2.0-meter burial depth is included.

*Table 4.7: Comparison of costs for connection between turbine 18 and OHVS*

| Case | Costs | Length [m] | Risk [$y^{-1}$] |
|---|---|---|---|
| Straight fixed 1.0 m | € 1.706.700 | 759.9 | 0.1715 |
| Horizontal fixed 1.0 m | € 998.300 | 803.8 | 0.0628 |
| Straight fixed 1.5 m | € 1.018.500 | 759.9 | 0.0652 |
| Horizontal fixed 1.5 m | € 1.072.400 | 805.7 | 0.0687 |
| Straight fixed 2.0 m | € 1.070.300 | 759.9 | 0.0682 |
| Horizontal fixed 2.0 m | € 1.198.000 | 806.0 | 0.0824 |

Table 4.7 shows a cost reduction for horizontal optimization with a fixed burial depth of 1.0 meter. It can be assumed that for subsiding areas the horizontal optimization only has a cost reduction when using a low fixed burial depth.

Table 4.8 shows total results for all 6 cases, comparing the total costs of the horizontal optimization with a straight cable at the same fixed burial depth.

*Table 4.8: Comparison of costs for the horizontal optimization*

| Case | Total costs | Difference in costs compared with straight cable case | Difference in risk compared with straight cable case |
|---|---|---|---|
| Straight fixed 1.0 m | € 56.272.000 | | |
| Horizontal fixed 1.0 m | € 49.470.000 | - 12.8% | - 26.6% |
| Straight fixed 1.5 m | € 45.850.000 | | |
| Horizontal fixed 1.5 m | € 47.470.000 | + 3.5% | - 0.31% |
| Straight fixed 2.0 m | € 50.363.000 | | |
| Horizontal fixed 2.0 m | €47.664.000 | + 3.6 % | + 0.13% |

Results presented in table 4.8 show that for a fixed burial depth of 1.0, the horizontal optimization reduces the total costs. For a burial depth of 1.5 and 2.0 meter however, the total horizontal optimization costs are higher. This is, as discussed earlier, caused by a different approach, having a longer and therefore more expensive cable. It can however be stated that horizontal optimization diverts the cable route around subsiding areas. Individual results for connection 33 & 32 and 18 & OHVS, showed that cost savings with the horizontal optimization depend on bed level change and fixed burial depth. Therefore, it is assumed that combining the horizontal and vertical optimization will even further decrease total costs. However, the change in risk can be neglected for the 1.5 and 2.0 meter burial depth cases.

## 4.4 Summary

Results show that with the greedy algorithm, the population size can be decreased with a factor 10 to 20. As an exact solution is not achievable due to the enormous amount of possible solutions, the found cable layout is regarded as a near optimal outcome. The second improvement in computational time is achieved by a division of the problem. Smaller problems decrease the amount of possible solutions and calculation time. However, the solutions are restricted due to the divided areas.

Table 4.1 and table 4.2 show that outcomes are comparable to the original layout. Differences in results are caused by small variations in turbine spacing. The optimization under the flat and static seabed gave similar results as route weights prove to be almost the same. Resulting layouts from the optimization were very close to the original layout in terms of total weight. Therefore, the original layout is chosen to be optimized under a dynamic seabed.

Effects of the horizontal and vertical optimization are visible in table 4.5 and table 4.8. What first comes forward is that both optimizations show good improvement over the original route. This is, assuming the parameters defined in table 4.4 a big benefit and therefore valuable to take into account prior to wind farm construction.

# 5 Sensitivity analysis

This chapter will describe the sensitivity of the cost function and sand wave dynamics in the results of the dynamic bed optimization. The chapter will start with a general description of the sensitivity analysis. Second, sensitivity of cost function parameters is analyzed. The chapter is concluded with parameter sensitivity based on predicted surveys.

## 5.1 General description

Results for the vertical and horizontal optimization are based on two surveys and a fixed cost function parameter input. Since all wind farms differ from each other, the influence of adjusting some parameters is to be investigated. To assess sensitivities in the cost function, a few parameters are chosen to be changed. Decreasing and increasing values with 50% gives a better overview of the influence on total costs. In this chapter, the following parameters, with their original values between brackets, are changed:

- Costs of repair (3 million €)
- Revenues per kWh (€ 0.15)
- Cable costs per meter (€ 300)
- Internal and external risks

The choice of the parameters is based on the cost function (Paragraph 3.3.1). Since the function roughly exists of four parts (risks, power loss, costs of repair and initial construction costs) one parameter from each part is taken. For the horizontal optimization only the case with a fixed burial depth of 1.5 meter is considered, it is also assumed that all other parameters stay the same when one is being analyzed.

## 5.2 Sensitivity of cost function parameters

To compare the sensitivity of the parameters, they are assessed for three connections. Since it also assumed that a variety in bed dynamics will show differences in parameter sensitivity, three connections are chosen. The connection choice is based on the area it crosses. Figure 5.1 shows the locations of the connections on the difference in bed level between 2003 and 2013. One connection is parallel to sand wave crests (33-32), one goes through multiple sand waves (13-22) and the last crosses a subsiding area (18-OHVS).

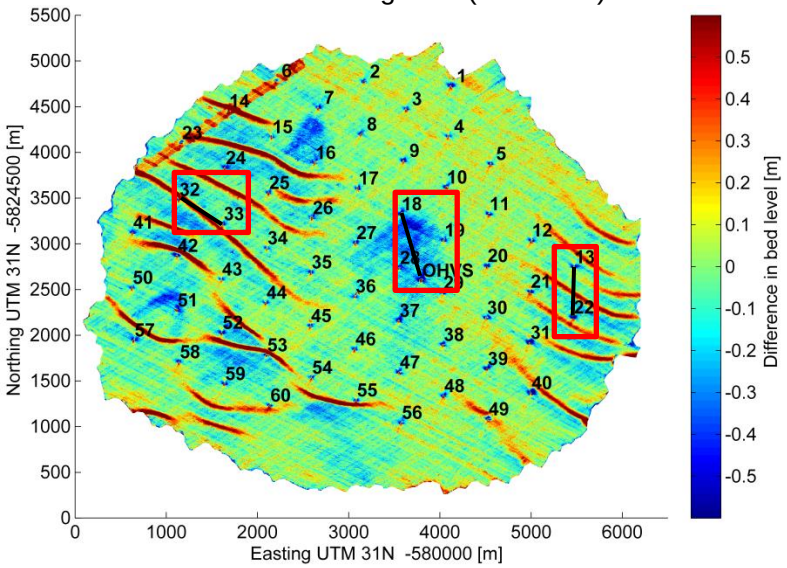


*Figure 5.1: Connections chosen for sensitivity analysis seen on the difference in bed level between 2003 and 2013*

For all connections, costs, using the original parameter values, are calculated. The comparison consists of the differences in percentage between the original costs and the costs found after adjusting one parameter. Results for the three connections are presented in Table 5.1 Table 5.2 Table 5.3.

*Table 5.1: Results of sensitivity analysis for connection between turbine 13 and 22*

| Parameter | Case | 2013 Horizontal optimization | 2013 Vertical optimization |
|---|---|---|---|
| Length [m] | | 551.1 | 549.0 |
| Original costs | | € 797.140 | € 763.330 |
| Cost of repair | - 50% | -12.7% | -13.6% |
| | +50% | +12.2% | +10.8% |
| Revenues per kWh | - 50% | -11.5% | -12.2% |
| | +50% | +10.8% | +9.8% |
| Cable costs per meter | - 50% | -10.8% | -12.1% |
| | +50% | +10.1% | +9.8% |
| Risks | - 50% | -23.9% | -29.9% |
| | +50% | +23.3% | +18.7% |

*Table 5.2: Results of sensitivity analysis for connection between turbine 18 and OHVS*

| Parameter | Case | 2013 Horizontal optimization | 2013 Vertical optimization |
|---|---|---|---|
| Length [m] | | 802.7 | 759.9 |
| Original costs | | € 1.086.800 | € 1.002.400 |
| Cost of repair | - 50% | -10.8% | -10.2% |
| | +50% | +8.1% | +8.5% |
| Revenues per kWh | - 50% | -13.2% | -13.1% |
| | +50% | +10.6% | +10.4% |
| Cable costs per meter | - 50% | -13.2% | -12.9% |
| | +50% | +10.0% | +10.2% |
| Risks | - 50% | -22.7% | -26.3% |
| | +50% | +20.0% | +17.3% |

*Table 5.3: Results of sensitivity analysis for connection between turbine 33 and 32*

| Parameter | Case | 2013 Horizontal optimization | 2013 Vertical optimization |
|---|---|---|---|
| Length [m] | | 582.6 | 549.9 |
| Original costs | | € 665.970 | € 610.890 |
| Cost of repair | - 50% | -13.8% | -17.9% |
| | +50% | +14.8% | +13.2% |
| Revenues per kWh | - 50% | -2.2% | -2.8% |
| | +50% | +3.1% | +2.7% |
| Cable costs per meter | - 50% | -13.7% | -15.7% |
| | +50% | +13.8% | +11.9% |
| Risks | - 50% | -16.8% | -21.8% |
| | +50% | +17.3% | +15.2% |

Results show that the largest influence in the cost function is caused by the costs of repair and the risks. From the results three main conclusions can be drawn. First, is that the magnitude of parameters are an indication of influence on results. Second, the number of turbines affected has a great influence on parameter sensitivity. For the connection between turbine 18 and OHVS, seven turbines are affected compared to one for the connection

between turbine 33 and 32. Comparing Table 5.2 and Table 5.3 shows that a higher number of turbines affected increases the influence of power loss (revenues per kWh) and decreases influence of costs of repair. Last, Table 5.1 shows that the influence of risks becomes larger for a connection crossing a (partly) subsiding area. The connection between turbine 33 and 32 is mainly located in a rising area. Results for the vertical and horizontal optimization are comparable for the parameters and show some more difference for the risks.

Since initial cable costs form the largest part in the cost function, it was assumed that for a connection with a significant longer cable length, the influence of initial cable costs will rise. The connection between turbine 18 and OHVS is about 35% longer than the two other connections; however, the influence of cable costs is about the same. It can be concluded that the influence of the area crossed by the connection is more important than the influence of a change in cable length.

## 5.3 Sensitivity of survey prediction on cost function parameters

The goal of the route optimization tool is to predict the optimum cable burial depth over the wind farm lifetime. Chapter 4 only discussed results regarding the ten year span between the surveys of 2003 and 2013. Therefore, the first step is to extend the 2013 survey towards 2028. Since migration speeds also influence results, this is done using the minimum, mean and maximum migration speed presented in Table 2.3.

For this extension some assumptions are made, first is that only sand waves migrate, second is that the present migration speed remains constant over time, third is that shape and dimensions of sand waves do not change and finally it is assumed that the vertical movement in the rest of the wind farm area remains constant.

Since it is assumed that only sand waves migrate, they are separated from the other bedforms. The sand wave field can be subtracted from the filtered survey by the same technique used in excluding ripples and megaripples. For the filtering, each cell of a survey is averaged by its surrounding cells. As size for the averaging square the maximum sand wave length is chosen. This will average a sand wave field to a plane going through the sand waves, giving a survey with only sand banks visible. Subtracting the new survey from the original survey provides the sand wave field. Figure 5.2 represents the sand wave field taken from the 2003 survey.

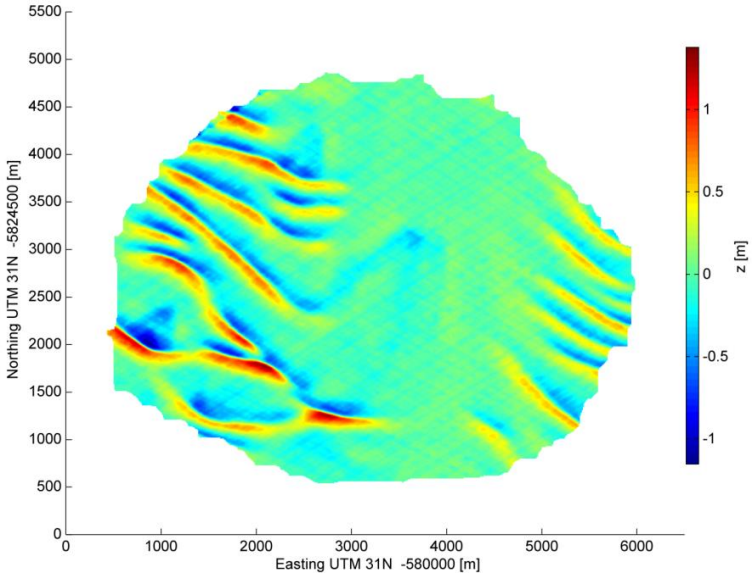


*Figure 5.2: Sand wave field in the 2003 survey*

The survey is extended by moving the sand wave field with the main migration direction and a fixed migration speed. In addition, the vertical movement of the sandbank survey is extended towards 2028. The predicted 2028 survey based on a maximum migration speed is shown in. Comparing this figure with Figure 2.3 shows that all sand waves move in Northern/north-eastern direction. Note the difference in scale between the two figures.

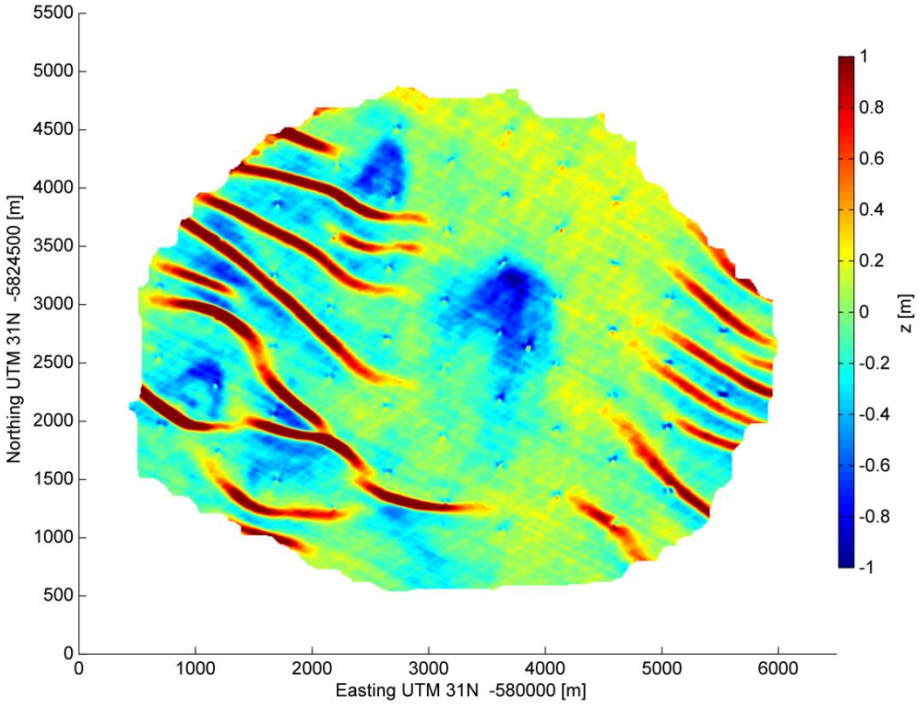


*Figure 5.3: Evolution of PAWP bathymetry over the period 2003-2028, predicted with maximum migration speed*

To show the influence of the migration speed on predicting the survey, the sensitivity analysis is executed for the minimum, mean and maximum migration speed (Table 2.3). Differences in migration speed are elaborated in Figure 5.4. This figure shows the filtered western sand wave field transect (Figure 3.5) for the 2003, 2013 and the three 2028 surveys.

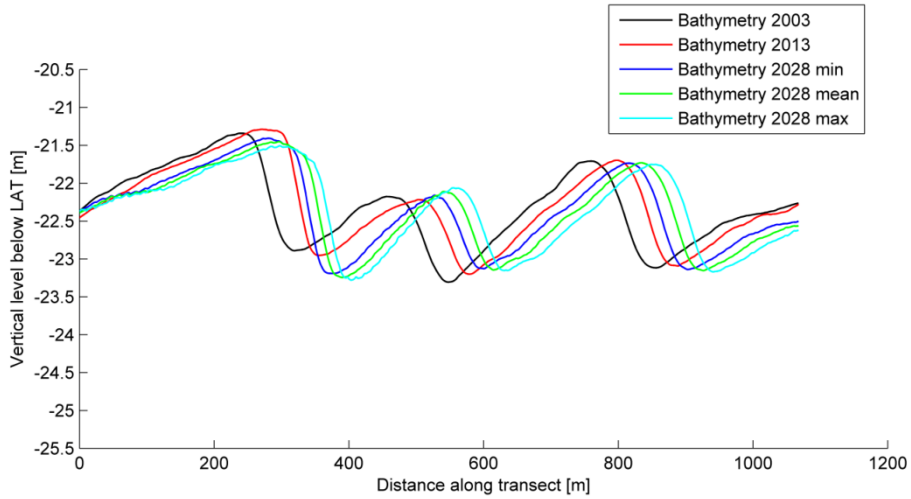


*Figure 5.4: Comparison of the filtered 2003, 2013 and the three predicted 2028 surveys for the transect in the western sand wave field*

Figure 5.4 shows a transect in the main sand wave migration direction. From the figure it can be concluded that this direction is valid, as a clear migration in x-direction is visible. However,

a small deviation in y-direction is visible. This is caused by taking only one migration speed for predicting surveys. However, only the rough influence of survey prediction on parameter sensitivity is assessed. Therefore it is not necessary to predict an exact 2028 survey.

To show the influence of the predicted morphological evolution, the sensitivity analysis is repeated. However, now the sensitivity of the parameters is assessed over a longer period (25 years) and for the three predicted 2028 surveys. The results for connection 33-32 are described in Table 5.4, Table 5.5 and Table 5.6. Results for connection 13-22 and 18-OHVS are presented in Appendix E.

*Table 5.4: Parameter sensitivity for connection 33-32 from 2028 survey predicted with minimum migration speed*

| Parameter | Case | 2028_min Horizontal optimization | 2028_min Vertical optimization |
|---|---|---|---|
| Length [m] | | | 549.9 |
| Original costs | | € 677.760 | € 604.090 |
| Cost of repair | - 50% | -14.7% | -18.1% |
| | +50% | +14.7% | +13.3% |
| Revenues per kWh | - 50% | -2.6% | -2.8% |
| | +50% | +2.7% | +2.7% |
| Cable costs per meter | - 50% | -14.4% | -15.9% |
| | +50% | +13.3% | +12.0% |
| Risks | - 50% | -17.4% | -22.1% |
| | +50% | +17.2% | +15.3% |

*Table 5.5: Parameter sensitivity for connection 33-32 from 2028 survey predicted with mean migration speed*

| Parameter | Case | 2028_min Horizontal optimization | 2028_min Vertical optimization |
|---|---|---|---|
| Length [m] | | 586.7 | 549.9 |
| Original costs | | € 694.650 | € 598.290 |
| Cost of repair | - 50% | -15.2% | -18.3% |
| | +50% | +15.0% | +13.4% |
| Revenues per kWh | - 50% | -2.7% | -2.9% |
| | +50% | +2.7% | +2.7% |
| Cable costs per meter | - 50% | -14.5% | -16.0% |
| | +50% | +13.2% | +12.1% |
| Risks | - 50% | -18.1% | -22.3% |
| | +50% | +17.7% | +15.4% |

*Table 5.6: Parameter sensitivity for connection 33-32 from 2028 survey predicted with maximum migration speed*

| Parameter | Case | 2028_min Horizontal optimization | 2028_min Vertical optimization |
|---|---|---|---|
| Length [m] | | 590.0 | 549.9 |
| Original costs | | € 706.290 | € 597.460 |
| Cost of repair | - 50% | -15.7% | -18.3% |
| | +50% | +15.4% | +13.4% |
| Revenues per kWh | - 50% | -2.8% | -2.9% |
| | +50% | +2.8% | +2.7% |
| Cable costs per meter | - 50% | -14.3% | -16.1% |
| | +50% | +13.0% | +12.2% |
| Risks | - 50% | -18.5% | -22.4% |
| | +50% | +18.2% | +15.5% |

By comparing the parameter sensitivity of the predicted surveys with the 2013 survey, it can be seen that for the vertical optimization, parameter sensitivity is not influenced by much. Even in the case with maximum migration speed, parameter sensitivity is only changed by 0 – 0.6%.

Effects of survey prediction on parameter sensitivity found with the horizontal optimization are larger. For the connection between turbines 33 and 32, the influence of all parameters will increase with a higher migration speed. Since this connection runs parallel to sand wave crests, it is assumed that the sand will move away from the connection. Comparing Figure 5.5 (r) with Figure 5.5 (l), shows that the effect of sand wave movement is extended and that the optimal cable position is now located under the sand wave crest present in 2003. The results for the two other connections show that parameter sensitivity is mainly influenced when the crossed area contains dynamic bedforms. Survey prediction for connection 18-OHVS, crossing a subsiding area showed almost no alteration in parameter sensitivity.

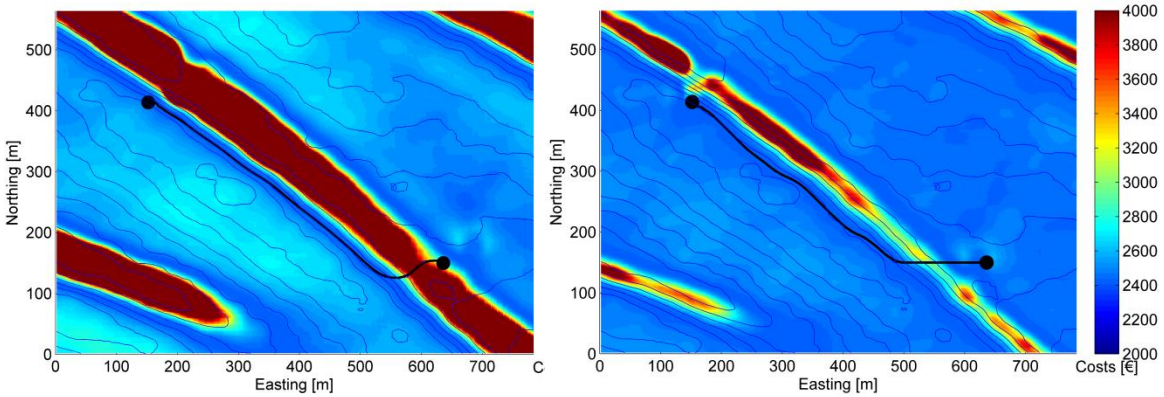


*Figure 5.5: Optimized route in the horizontal plane between turbine 33 and 32 for a fixed burial depth of 1.5 meter over the period 2003-2028, predicted with the maximum migration speed, (l) and over the period 2003-2013 (r) with contour lines (blue) showing bedforms in the 2003 survey*

## 5.4 Summary

Results of this research were all based on fixed cost function parameters. To assess the influence of changes in these parameters on outcomes, a rough sensitivity analysis is conducted. A parameter from all four cost function parts is decreased and increased with 50%. Results show that results are mainly influenced by parameter magnitude, number of turbines affected and area crossed by a connection between two turbines. Results for vertical and horizontal optimization were comparable except for influence of risks.

Since the research objective is to optimize cable layout over the wind farm design lifetime, a parameter analysis is executed based on survey prediction. By extending the 2013 survey towards 2028 with three different fixed sand wave migration speeds, the influence of morphological evolution can be found. Results show no big differences in sensitivity during the vertical optimization. For the horizontal optimization however, some results were visible in cases in which connections interfered with sand wave fields.

# 6 Applicability of the tool

Results from chapter 4 show that for the Prinses Amaliawindpark some big improvements in cable layout can be reached. Previous research only focused on the connections between turbines based on a flat seabed. With the optimization under a dynamic seabed, some cost reductions can be achieved before and during wind farm operation. This chapter discusses the general applicability of the tool, possible innovations and contribution towards renewable energy targets. With this chapter the research questions belonging to the tool evaluation are answered.

## 6.1 General applicability of the route optimization tool

The route optimization tool is developed based on the PAWP case study. This case study is chosen because of good quality and quantity of available data. Because this wind farm is operational, the tool outcomes can only be compared and not applied. The PAWP results only showed possible improvements in the dynamic bed optimization. Since, the outcomes are heavily dependent on the input and dynamic behaviour of the seabed, the tool needs to be applied onto a second case study.

For conceptual offshore wind farms, the tool can achieve an actual cost reduction compared to present methods. One big difference with a case study is that for new wind farms only one survey is available. To use the tool for this new wind farm, the morphological development needs to be predicted. Only the larger bedforms, possibly influencing the power cables, are taken into account. To predict the morphological evolution, a survey is needed including the main migration direction and the migration speed. The influence of the migration speed is discussed in chapter 5, based on this; a range of migration speeds is given to predict possible future bathymetries.

Given the sensitivity analysis it is shown that the influence of risk of failure is larger for connections crossing subsiding areas and with a higher number of turbines affected. Since all strings start at the OHVS, it is recommended to locate the station on a static place on the seabed. This will decrease risk and, because the number of turbines affected is high around the OHVS, has a great influence on reduction of total cable costs.

However, even without a seabed extension, the optimization can be executed. The analysis of the seabed gives information about the sand wave and sand bank evolution. Considering, migration of the sand waves, the area in front of the sand wave crest can be assumed a preferable area for cable construction.

A second limitation is that prior to construction, wind turbine locations are not fixed. Only when the locations are known, the cable layout under a flat or static seabed can be determined. When the turbine placement is comparable to the PAWP, the genetic algorithm can provide similar results having only small variations in cable layout. Next, the possible layouts have to be checked for crossing large bedforms. Routes going through one or more sand waves are not preferable. The final, near optimal, layout is presented after expert review on the found layouts.

To generalize applicability, the tool should include an option for case specific characteristics and parameters. First, the population size, maximum cable capacity and the number of iterations can be determined for every simulation or case. In addition, a selection can be made if and in what form the greedy algorithm is used. The second option is the possibility to

optimize a part of the wind farm, reducing the computational time. The tool includes an option to draw a closed polygon in the wind farm and select all turbines inside this area (Figure 6.1). The OHVS is automatically to the selection when not included.

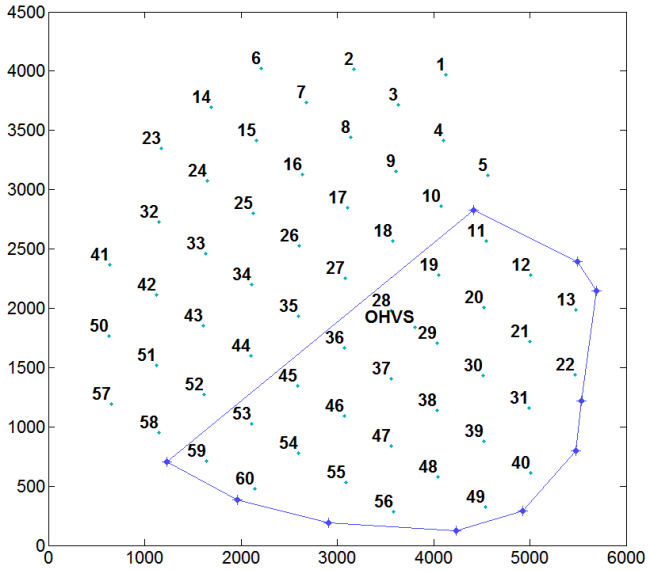


*Figure 6.1: Drawn polygon in wind farm to decrease size of the layout problem*

The next step in the tool is the optimization in the vertical and horizontal plane. As default, the tool uses the parameters defined for the PAWP optimization. However, case specific input overwrites these values. The second option is that the user can define the time over which the optimization takes place. In most cases, the cables are optimized over the design lifetime. However, it can occur that a sand wave migrates completely over a certain point in this time. This makes it possible that even if cable coverage is increased over the entire design lifetime, the cable can become exposed halfway through.

## 6.2 Possible innovations in material and routines

Power cable restrictions and layout options influence the route optimization outcome. Most important restrictions are the maximum number of turbines per string, cable bending radius and not branching strings. The restrictions present in this research all apply on the PAWP. Therefore, it is important to map the different preconditions for the selected offshore wind farm.

The restrictions cause limitations for the further cable layout improvement. For instance, a maximum of eight turbines can be connected to one string. More capacitated strings make it easier to find a next turbine for the route. More strings, taking into account that cables cannot cross, causes the freedom of the strings to find a path to decrease. Especially turbines close to the OHVS are limited and more strings causes larger first connections. In addition, as more turbines are connected, the power loss for the first connection in a string increases.
Branching of the power cables would even further increase the layout pattern. Branching would lower the cost function for certain routes. Figure 6.2 shows a non-branched and a branched layout. The costs of failure for the cable between turbine 1 and 2 are lower in the branched layout. Due to the branched layout, only three turbines are affected by cable failure instead of six in the non-branched layout. However, as the optimization is concentrated on non-branching strings, this would involve an adjustment in the genetic algorithm.

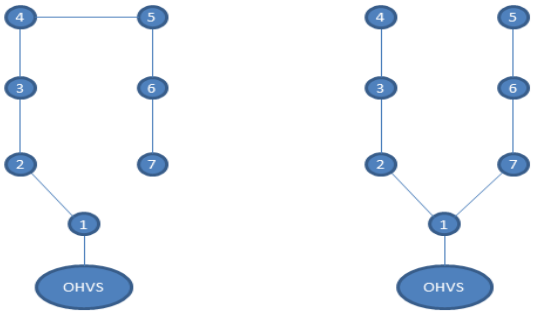


*Figure 6.2: Non-branched string compared to a branched string*

The last big restriction in this research is the maximum cable-bending radius. For the optimization under a dynamic field, the cable position is of great importance. This position depends on the minimization of the cost function and the cable-bending radius. For results presented in this research, the influence of the cable-bending radius is not of big importance. Since bedforms are quite long compared to cable trajectories, the cable position can deviate somewhat from the most optimal position. This deviation does not influence the total costs of that cable part very much.

## 6.3 Contribution towards renewable energy targets

The Far and Large Offshore Wind (FLOW) aims at a cost reduction for wind at sea by innovations through collaboration. To achieve this goal, the FLOW project has set four main targets:

- Increase reliability of offshore wind farms;
- Accelerate development;
- Lower risks;
- Make a significant contribution to lower offshore wind energy costs by 20%.

The power cable optimization helps to improve three of the four FLOW targets. The official project description regarding the power cables is as follows:

> *"To lower the costs of offshore wind farms, costs resulting from power cable installation and inspection, repair and maintenance (IRM) need also be reduced. In current projects, cable management and installation is a regular contributor to cost overruns and schedule delays.*
>
> *Though 5 to 10% of the projects costs can be assigned to power cable installation, this activity accounts for 70 to 80% of the insurance costs of a project. This project aims to lower these costs and risks by means of a life cycle approach. Optimized cable installation can reduce the LCOE of offshore wind by 0.65% – 0.9%" FLOW (2014).*

The description states that this project aims to increase reliability, decrease risks and contribute to cost lowering. Results of this research show that these three targets are improved with the power cable optimization. Only the acceleration of the development is not achieved with this research. The contributions of this research to the three FLOW targets are discussed in this section.

### 6.3.1 Increase reliability of offshore wind farms

The wind farm power cable layout is discussed by Bauer and Lysgaard (2013) and Jenkins et al. (2013). These studies however, do not take bedforms and seabed evolution into account and only try to find an optimal layout under a flat seabed. The case study of the PAWP

showed that bedforms influence the cable coverage and the associated cable costs. With a subsiding seabed, it cannot be guaranteed that power cables stay buried over the lifetime of the wind farm. This causes the reliability of power cable functioning to decrease.

In this research, the initial power cable position is assessed in the vertical and horizontal plane. The new position is determined based upon the cost function and bed level change over the wind farm design lifetime. To meet the demand of minimum cable coverage, the initial and final coverage should always be more than 1.0 meter. For the vertical optimization, the cable is initially buried deeper at places with a subsiding seabed. The results for the horizontal optimization show that the cable follows a path with seabed rise or the lowest possible subsidence.

Optimization under a dynamic seabed increases the reliability for the power cables. With the optimization tool, the power cables are designed to have at least 1.0-meter coverage over the design lifetime of the wind farm.

### 6.3.2 Lowering of risks

The risk of cable failure is the highest uncertainty for wind farm power cables. Increasing the reliability, as discussed in previous paragraph, also lowers the risk of cable failure. Figure 3.6 shows the combined internal and external risk as a function of cable coverage. The figure indicates that the total risk increases drastically when cable coverage drops below 1.0 meter. Therefore, by always guaranteeing minimum cable coverage, the total risk of cable failure is lowered. Since the initial position depends on the cost function, the most optimal configuration will be close to the lowest possible risk.

### 6.3.3 Contribution to cost lowering

The FLOW project target is to lower the costs for offshore wind farms. The main goal is to make a significant contribution to cost lowering of offshore wind energy by 20%. The vertical and horizontal optimization respectively show costs compared to the original situation. However, for the horizontal optimization this depends very much on the fixed burial depth. Here, CAPEX, OPEX and costs of cable failure are taken into account. Cable installation and management contributes greatly to cost overruns and schedule delays. Lowering the risks and the costs of power cables, leads towards a lowering in project costs and insurance costs.

## 6.4 Summary

Since the route optimization tool is developed based upon the PAWP case study, some adjustments need to be executed before the tool is general applicable. The possibility to incorporate site-specific input makes the tool less specified onto one case.

The optimization is limited to the constraints defined in advance. Expanding these constraints gives more opportunities for the system to optimize. During this research, three constraints prove to influence the results: the maximum number of turbines per string, branching of strings and cable bending radius. It is assumed that especially innovation in the first two constraints provide significant improvements in the cable layout.

The main aim of the route optimization tool is the contribution towards renewable energy. It is shown that power cable optimization of the power cables under a dynamic seabed gave improvements in total costs. Especially project insurance costs can be decreased by optimizing the power cable position. With the cable position based upon the change in bed level, it can be guaranteed that the power cables always have a minimum coverage over the wind farm design lifetime.

# 7 Discussion

The results of this study are influenced by choices and assumptions made. These were made to exclude arbitrariness, make the outcomes be of significance for the case study and delineate the research. This chapter discusses the choices and assumptions made.

To develop the route optimization tool a case study is needed. In this research, the Prinses Amaliawindpark is chosen as a case study. This wind farm has three surveys available. However only the 2003 and 2013 survey are used. The size and quality of the 2006 survey prove to decrease reliability. Small uncertainties in bed levels of the other two surveys do not influence results very much and can be neglected.

Using only two surveys has an uncertainty in sand wave migration speed. This sensitivity is assessed by taking the 2006 survey in consideration, giving large uncertainties in migration speed. This however, cannot be assumed correct because of the lower 2006 survey quality.

To meet the maximum bending radius constrain, ripples and megaripples are filtered out of the surveys. Filtering is executed by averaging a cell in the survey with its surrounding cells. This gives an uncertainty in bed levels. However, figures show that bed levels in the filtered survey follows the troughs of the ripples and megaripples. Therefore, it is assumed that the effect of filtering is limited.

The number of possible cable layouts for the PAWP is enormous. Since not every possible solution can be assessed, the found layouts are stated as near optimal. Results show that layouts somewhat differ in visual representation, but are very comparable in terms of total weight. The layout similarities make it plausible that assumptions for the number of iterations and population size are correct. However, decreasing both assumptions has a large effect on outcomes. The second component influencing outcomes are the initial solutions. Having a complete random population increases number of iterations and cause uncertainties in outcomes. Adding the greedy algorithm helps to get more directed solutions and lowers the uncertainties in outcomes.

Dividing the wind farm area decreases the number of possible solutions exponentially, since less turbines have to be connected per area. The division made restricts cable trajectories to a certain area. Taking a random division influences cable layout, however a smart choice shows almost no difference with a non-divided area.

The dynamic bed optimization forms the most important step in this research. The optimal positions in the vertical and horizontal plane are based on a cost function. For this function, many assumptions are made. First, the costs are determined at the end of the wind farm design lifetime and not over the entire period. Second almost all parameters, external and internal risks are defined based on expert review. Results found during this research are based on these assumptions.

However, the effects of the horizontal and vertical optimization can be recognized. Only the magnitude of cost reduction depends very much on cost function parameters. Finally, cable coverage should never go under 1.0 meter. However, justification for this requirement is lacking. To show the effect, a case in the vertical optimization is included, which can exceed the minimum burial depth (Figure 4.6).

Results for the horizontal optimization very much depend on burial depth and bed level change. Since the horizontal optimization has a fixed burial depth, this can even cause an increase in costs. The uncertainties in outcome differences of the vertical and horizontal optimization are caused by their specific approach. The optimal path in the horizontal plane is found by moving from cell to cell and minimizing the total route costs. Since the path only crosses a cell from corner to corner, the total length is always longer than a straight line, increasing total costs.

Since results are based on two surveys and fixed parameters, the sensitivity is assessed. The sensitivity analysis executed in this research focuses mainly on the rough sensitivity of the parameters. This gives a better overview what will happen with the results if a single parameter is adjusted. However, uncertainties present in the parameter ranges are not taken into account. Also, survey prediction is based on a fixed migration speed. To assess the sensitivity over time, survey prediction needs to be executed based on migration speed per sand wave.

Finally, assumptions are made regarding the general applicability of the tool. Since all case specific input can be defined and outcomes heavily depend on this input, it can be stated that this uncertainty is limited. The tool is originally developed for an existing wind farm. To make it applicable to new offshore wind farms a single survey needs to be extended with the aid of migration direction and speeds. Since both can change over time it is important to take a range in both parameters and analyse all possible cases.

# 8 Conclusions and recommendations

The focus of this research was to develop a Matlab based tool that optimizes the route layout in an offshore wind farm over the expected morphological behaviour in the design lifetime of an offshore wind farm. To develop the tool, the Prinses Amaliawindpark is used as a case study. This chapter summarizes the research findings. Recommendations are given based on the discussion in chapter 6 and the answers based on the research questions.

## 8.1 Conclusions

**What are the site-specific conditions of the PAWP and how can these be combined in a route optimization tool?**

The PAWP case study provided two comparable bathymetrical surveys of very good quality, the first taken prior to the wind farm construction and the second one with the park in operation. In addition, the wind farm includes two sand wave fields and a sand bank. Bedforms are important, as previous research did not consider bed evolution.

**How can the cable route layout be optimized based on a wind farm with a flat and static seabed?**

The first step in minimizing the layout costs is to find a cable layout under a flat and static seabed. The genetic algorithm is selected to find a layout in which cables cannot cross and branch based on a maximum number of turbines connected to a string. The greedy algorithm forms the initial population used for the genetic algorithm. With the aid of mutual distances between wind turbines and both algorithms, a near optimal layout is found.

**How can the cable routes be optimized in the vertical and horizontal plane based on cable limitations and what are the implications for the route optimization?**

The near optimal layout is used in the dynamic bed optimization. Every connection is optimized in vertical and horizontal direction. Cable position in both planes are found by minimizing the capital and operational expenditures and costs of failure.

**How can the route weight be identified based on risks and cable and excavation costs?**

The execution of the genetic algorithm showed results comparable to the original PAWP layout. Together with the use of the greedy algorithm, problem subdivision in smaller parts proves to decrease computational time drastically. As near optimal solutions are very close to the original layout, the latter is chosen for the optimization under a dynamic seabed.

**What are the cost savings of the route optimization tool compared to the existing layout throughout the entire life span of the wind farm?**

Every cable part between two turbines is optimized in vertical and horizontal direction. The results show large improvements compared to the original cable position. Especially the vertical optimization provided cost savings for all connections. Cost savings for the horizontal optimization very much depend on the fixed burial depth and bed level change.

**What is the sensitivity of parameters in the cost function and the survey prediction?**

The influence of the parameters depends on their magnitude, amount of turbines affected and the area that is crossed. With more turbines affected, the influence of power loss raises and the influence of costs of repair lowers. Also, the sensitivity of risk increases when a connection crosses a subsiding area. The effect of survey prediction is minimal for the vertical optimization. Parameter sensitivity for the horizontal optimization of predicted surveys changed. However effects are only visible in connections interfering with sand waves.

**Can the route optimization tool be developed for general use?**
To general applicability of the route optimization tool is ensured, as all case specific information can be loaded into the tool user friendly. Since the vertical optimization provides decreased costs for all connections, it can be stated that this method is generally applicable.

**Can innovations in materials and routines lead towards an even higher cost reduction?**
The results show that constraints influence the study outcomes. The option to branch the power cable strings in the wind farm is of great interest for the layout problem. Branching reduces the amount of turbines affected. This leads to a reduction in costs of failure of the connection. With this, the initial burial depth decreases and together forms a cheaper option.

**What are the contributions towards renewable energy targets?**
The main aim of the route optimization tool is to provide a contribution towards renewable energy targets described in the FLOW program. The tool guarantees minimal cable coverage throughout the wind farm design lifetime. The guarantee causes a lowering of risk of failure, an increase in reliability, a decrease in project costs and a decrease in insurance costs. The tool also showed that OHVS construction on a static place will decrease risks and cost

## 8.2 Recommendations

The route optimization tool developed in this research shows promising results. Further research based on this study should start with the development of a more specified optimization algorithm. The genetic algorithm, which is used, provides good results, but still takes a lot of computational time. The algorithm is also only specified to non-branching power cable strings. Second, the amount of strings is minimized based on the maximum capacity. The new optimization algorithm can be specified on the algorithm used in this research, but needs to incorporate the greedy algorithm and cable branching.

The tool is developed based upon two surveys over a given period. The tool purpose is to optimize cable route design over the wind farm design lifetime. To make the tool applicable to new offshore wind farms a second survey needs to be created. With the use of migration speeds and direction a few predictions can be made.

With the bathymetry prediction, the tool can be applied to wind farms still in the planning phase. A second extension is to optimize the turbine locations in the designated wind farm area. This influences whether or not the power cables are subject to large morphological changes in the seabed. With the optimized locations, subsiding areas can be avoided and in line with the previous, the risks will be lower.

Parameters in the cost function are mostly case-specific and based on expert review. Due to ranges of some parameters, the results are alive to changes. To assess the influence an extended sensitivity analysis needs to be conducted. Present analysis focuses mainly on the rough influence of parameters. Extended analysis should cover the ranges of certain parameters as well as uncertainties in predicted surveys.

In this research, the vertical and horizontal optimization are executed separately. Combining the two options can provide an even further improvement in the costs of the cable routes. Executing the vertical optimization on each grid cell gives optimal burial depths and costs for the entire grid. Executing the horizontal optimization with this grid will provide the optimal position in both vertical and horizontal plane.

# 9 References

Amaliawindpark, P. Feiten en cijfers. from http://projecten.eneco.nl/prinses-amaliawindpark/projectgegevens/feiten-en-cijfers/

Andrew. (2014). Capacity factors at Danish offshore wind farms. Retrieved October 14, 2014, from http://energynumbers.info/capacity-factors-at-danish-offshore-wind-farms

Bauer, J., & Lysgaard, J. (2013). The offshore wind farm array cable layout problem - A planar open vehicle routing problem. *Journal of the Operational Research Society*.

Besio, G., Blondeaux, P., Brocchini, M., & Vittori, G. (2004). On the modelling of sand wave migration. *Journal of Geophysical Research, 109*(4), 1-13.

Bijker, R. (2013). Mogelijke morfologische effecten van het Prinses Amaliawindpark.

Bijker, R., Wilkens, J., & Hulscher, S. J. M. H. (1998). *Sandwaves: Where and why.* Paper presented at the Proceedings of the International Offshore and Polar Engineering Conference.

Borsje, B. W., Roos, P. C., Kranenburg, W. M., & Hulscher, S. J. M. H. (2013). Modeling tidal sand wave formation in a numerical shallow water model: The role of tubulence formulation. *Continental Shelf Research, 60*, 17-27.

Caldeira, T. C. M. (2009). Optimization of the Multi-Depot Vehicle Routing Problem: an Application to Logistics and Transport of Biomass for Electricity Production.

Dijkstra, E. W. (1959). A Note on two problems in connexion with graphs. *Numerische Mathematik, 1*, 269-271.

EWEA. (2014). Wind energy statistics and targets. Retrieved October 14, 2014, from http://www.ewea.org/uploads/pics/EWEA_Wind_energy_factsheet.png

FLOW. (2014). FLOW program. Retrieved May 14, 2014, from http://flow-offshore.nl/

Holmstrøm, O. (2007). Survey of reliability of large offshore wind farms.

Hulscher, S. J. M. H., & van den Brink, M. (2001). Comparison between predicted and observed sand waves and sand banks in the North Sea. *Journal of Geophyiscal Research, 106*(5), 9327-9338.

Huntley, D. A., Huthance, J. M., Collins, B., Liu, C.-L., Nicholls, R. J., & Hewitson, C. (1993). Hydrodynamics and sediment dynamics of North Sea sand waves and sand banks. *Philosophical Transactions: Physical Sciences and Engineering, 343*(1669), 461-474.

Jenkins, A. M., Scutariu, M., & Smith, K. S. (2013). *Offshore wind farm inter-array cable layout.* Paper presented at the PowerTech (POWERTECH), 2013 IEEE Grenoble.

Kumar, S. M., & Panneerselvam, R. (2012). A Survey on the Vehicle Routing Problem and its Variants. *Intelligent Information Management, 4*, 66-74.

McCave, N. (1971). Sand Waves in the North Sea off the coast of Holland. *Marine Geology, 10*(3), 199-225.

Morelissen, R., Hulscher, S. J. H. M., Knaapen, M. A. F., Németh, A. A., & Bijker, R. (2003). Mathematical modelling of sand wave migration and the interaction with pipelines. *Coastal Engineering, 48*(3), 197-209.

Németh, A. A. (2003). *Modelling offshore sand waves.* (Doctoral dissertation), University of Twente.

Németh, A. A., Hulscher, S. J. M. H., & Vriend, d., H.J. (2002). Modelling sand wave migration in shallow shelf seas. *Continental Shelf Research, 22*(18-19), 2795-2806.

Pemmaraju, S., & Skiena, S. (2003). *Computational Discrete Mathematics: Combinatorics and Graph Theory with Mathematica*. New York: Cambridge University Press

Petersen, J. K., & Malm, T. (2006). Offshore windmill farms: Threats to or possibilities for the marine environment. *A Journal of the Human Environment, 35*(2).

Raaijmakers, T., Luger, D., Lottum, H. v., Diafera, G., Vermaas, T., Scheel, F., & Hasselaar, R. (2014). Assessment of cable burial depth, associated risks and mitigation measures for Prinses Amaliawindpark.

Roetert, T. J. (2014). Offshore wind farm power cable rote optmization: Literature review.

Schillings, C., Wanderer, T., Cameron, L., van der Wal, J. T., Jacquemin, J., & Veum, K. (2012). A decision support system for assessing offshore wind energy potential in the North Sea. *Energy Policy, 49*, 541-551.

Sirnevas, S., & Musial, W. (2014). Assessment of Offshore Wind System Design, Safety, and Operation Standards.

Staub, C., & Bijker, R. (1990). *Dynamic numerical models for sand waves and pipeline self-burial.* Paper presented at the Coastal Engineering Proceedings.

Sterlini, F., Hulscher, S. J. M. H., & Hanes, D. M. (2009). Simulating and understanding sand wave variation: A case study of the Golden Gate sand waves. *Journal of Geophysical Research, 114*(F2), 1-15.

# A Analysis of bathymetry

The bathymetrical surveys and their comparison are presented in this appendix.

## A.1 Bathymetrical surveys

For the Prinses Amaliawindpark three bathymetrical surveys are available. The surveys are executed in 2003 (Fugro), 2006 (inhouse) and 2013 (Deep). For all surveys, the bathymetry is plotted on the same scale together with wind turbine locations. The wind farm cable layout is visible in Figure 2.2. In the 2013 bathymetrical survey, the exact locations are not plotted. Due to seabed evolution, scour holes exist around the wind turbines. These holes give the exact turbine locations and show an important morphological evolution.

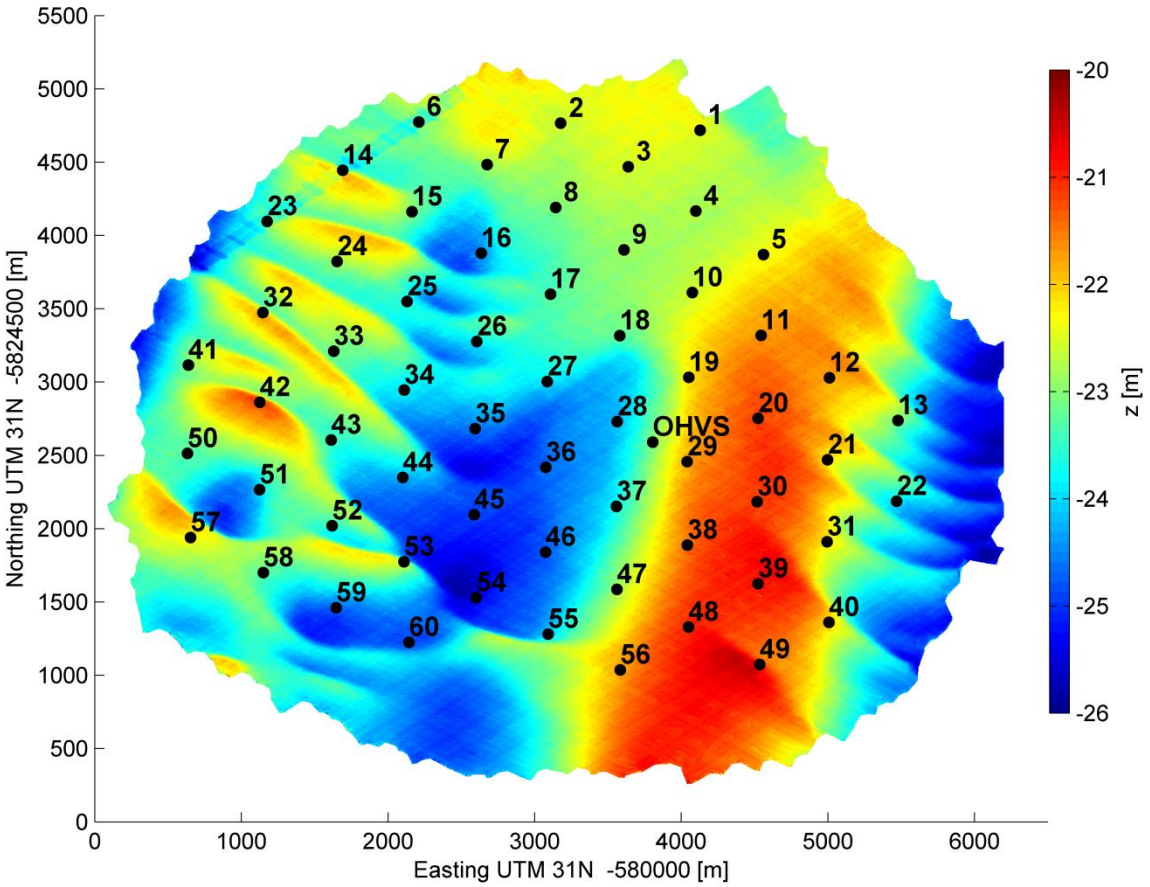


*Figure A.1: 2003 bathymetrical survey with wind turbine locations*

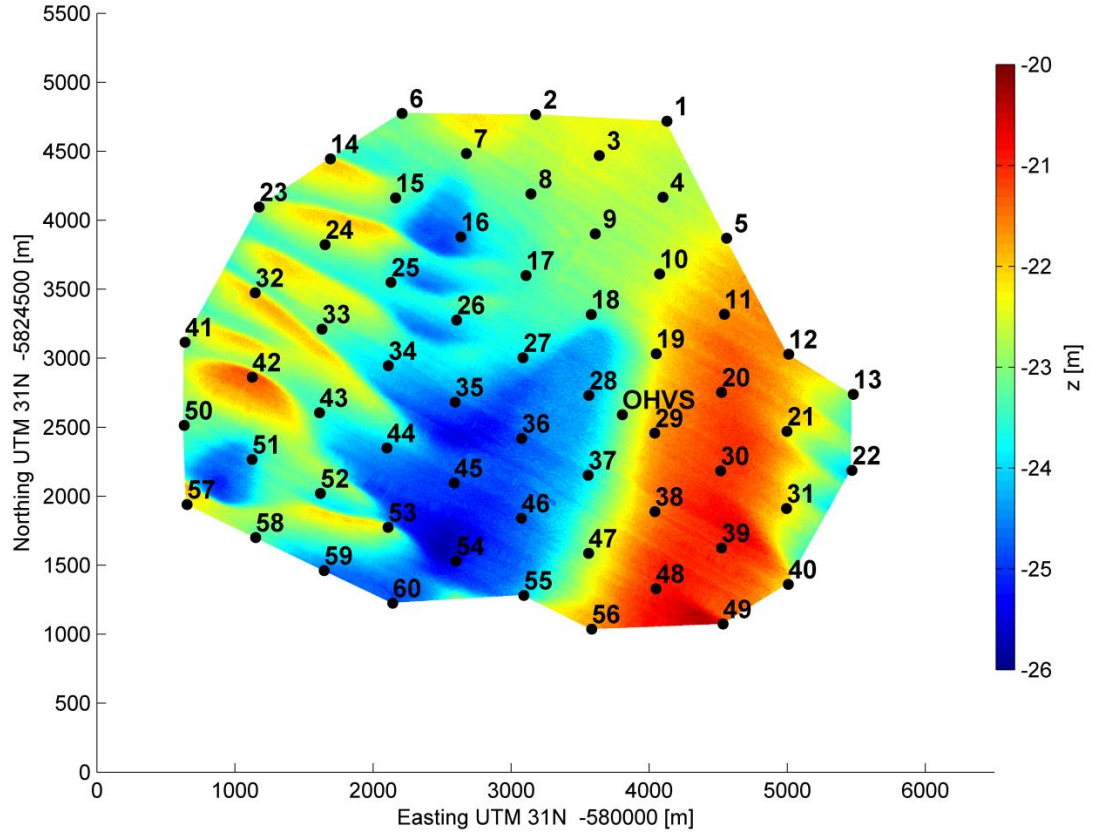


*Figure A.2: 2006 bathymetrical survey with wind turbine locations*

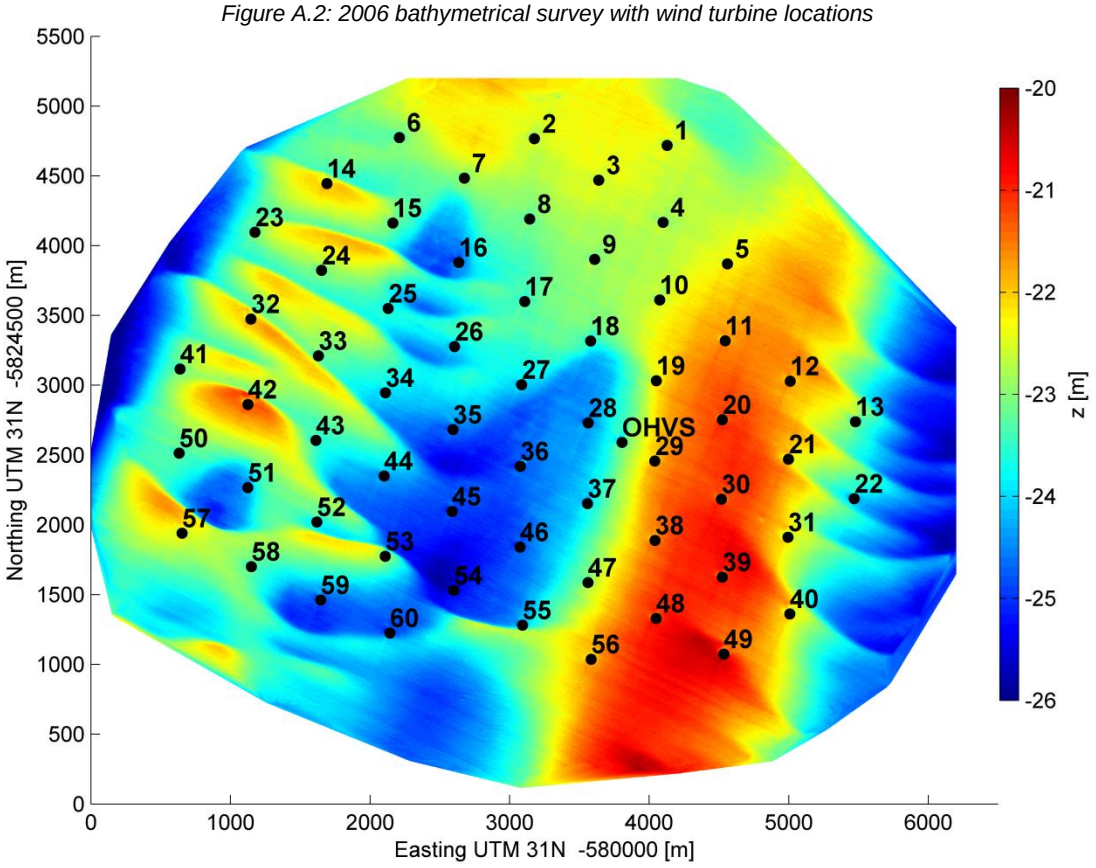


*Figure A.3: 2013 bathymetrical survey with wind turbine locations*

## A.2 Differences between bathymetrical surveys

The three bathymetrical surveys presented in appendix A.1 are compared in this section. The difference plots show the evolution of the seabed over time.

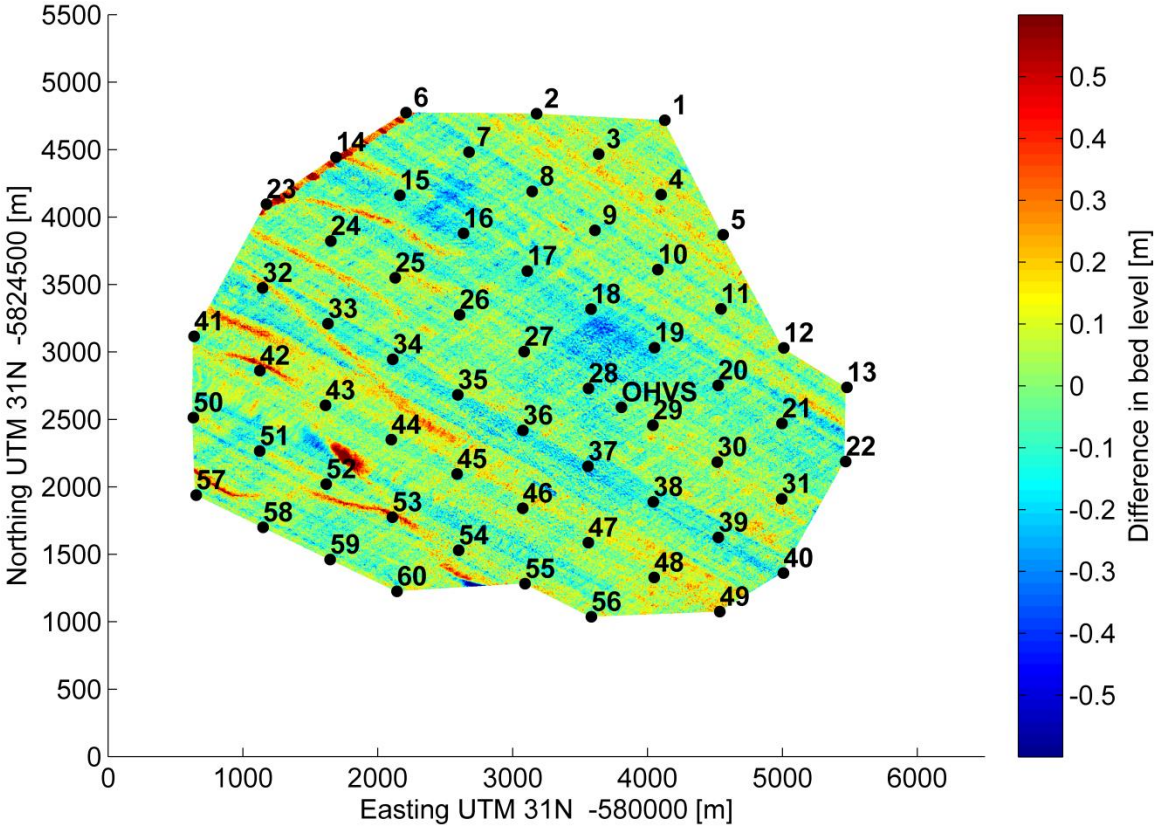


*Figure A.4: Difference between bathymetry 2003 and 2006*

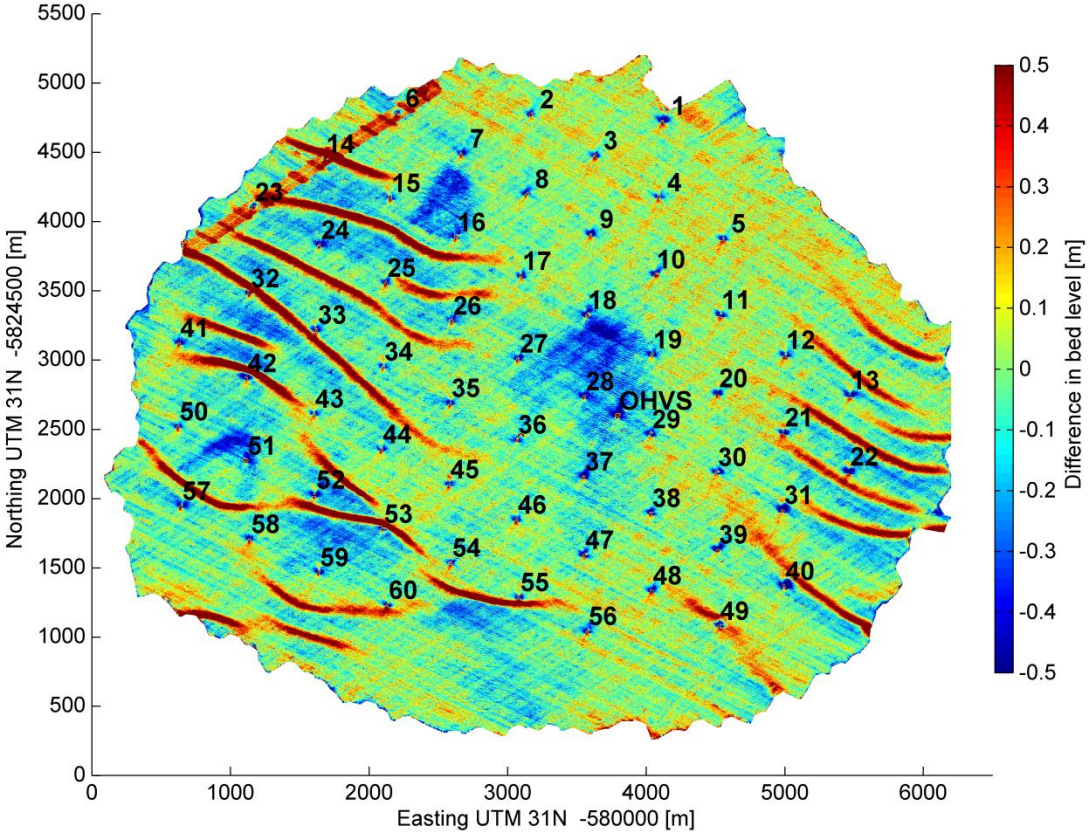


*Figure A.5: Difference between bathymetry 2003 and 2013*

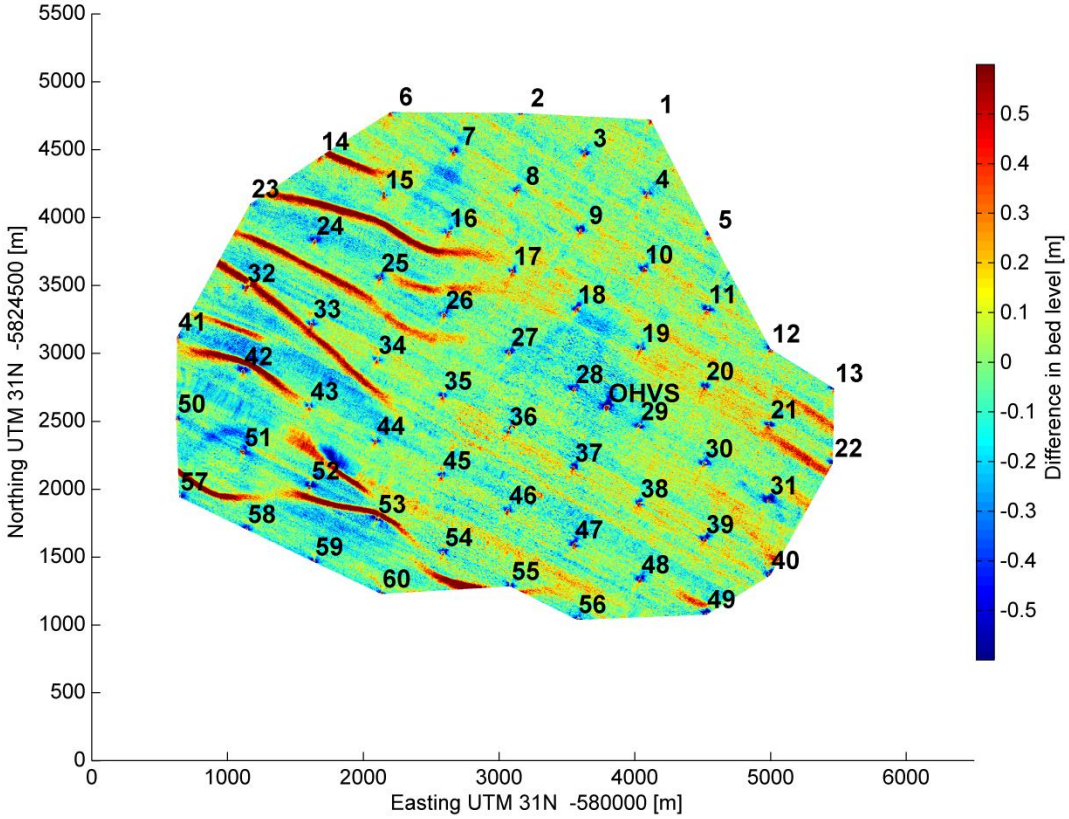


*Figure A.6: Difference between bathymetry 2006 and 2013*

# B Optimization algorithms

The different optimization algorithms available to solve the combinatorial optimization problem are presented in this appendix. In addition, Dijkstra's algorithm, used in the horizontal optimization, is described.

## B.1 Genetic Algorithms

The genetic algorithm is based on the principles of Darwin's evolution theory. The genetic algorithm applies the principles of evolution and adaption to the environment that are present in every species to optimization problems. The application of the evolution principles finally leads to survival of the fittest (Caldeira, 2009). Where the tabu search also looks for the best or fittest solution, there is one major difference. The genetic algorithm uses a population of solutions instead of one single solution. The advantages of a population are that many possibilities are evaluated at once and that there is more exchange of information between the solutions.

The biggest challenge in the genetic algorithms is the way in which the selected solutions are treated. A general solution for the genetic algorithm is to select a certain set of the total population. From the selected set, the best solution or the fittest is chosen. For the length of the set some different adjustment are done to the best solution. The solutions can be swapping of points, changing of the routes or alter the length of the strings. The new solutions are then put back in the population and the algorithm starts over.

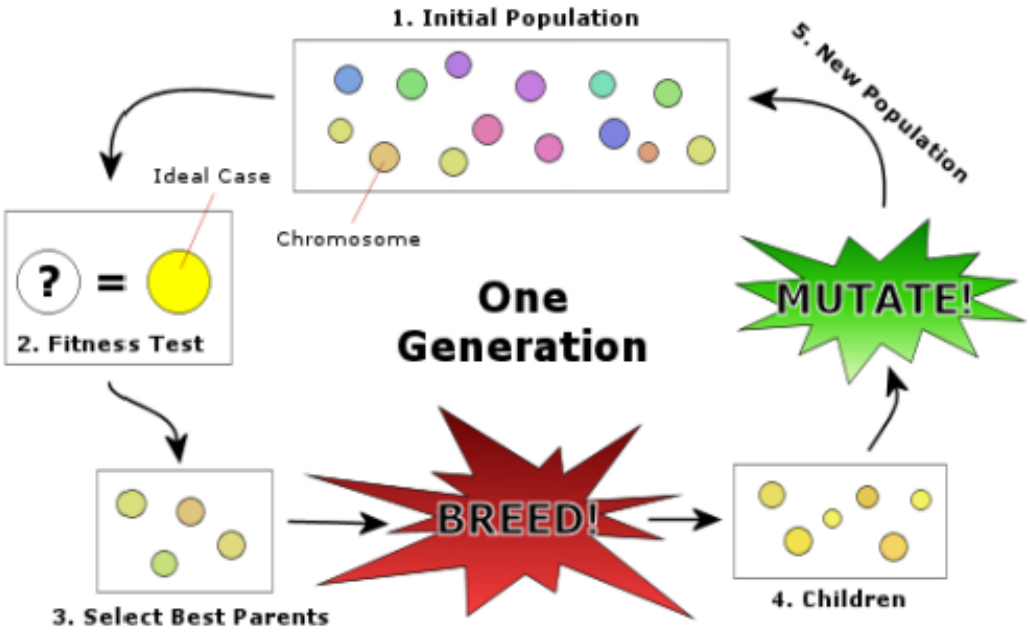


*Figure B.1: General description of genetic algorithm based on evolution (Caldeira, 2009)*

The genetic algorithm clearly describes the process of natural selection in a population. The best species reproduce and that circle goes on and on until no further improvement is found. The genetic algorithm is best described with the natural selection visible in Figure B.2.

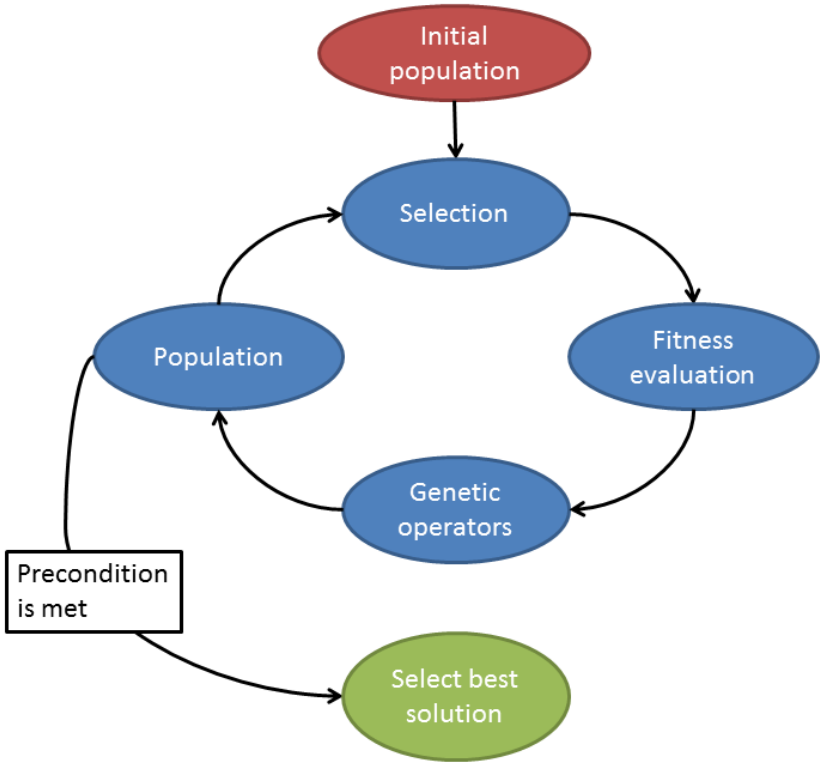


*Figure B.2: Genetic algorithm used in route optimization tool*

### B.1.1 Initial population

In the first step, an initial population is constructed. The population consists of individual solutions to the problem. The population size is dependent on the number of wind turbines. This step consists of two parts. First, all initial solutions are created by putting the wind turbine numbers in a random order. The next step is the determination of string lengths. For example, a wind farm with 10 turbines has an initial population. One random initial solution can be defined as:

$$[4\ 5\ 3\ 7\ 6\ 9\ 10\ 1\ 2\ 8]$$

Assuming that the maximum string capacity is four and minimizing the number of strings, the solution exists of three strings. Each string has a length of maximal four and the strings together add up towards ten. In this example, the string lengths are chosen randomly. An possible string configuration can be:

$$String\ 1: [4\ 5\ 3\ 7]$$
$$String\ 2: [6\ 9\ 10]$$
$$String\ 3: [1\ 2\ 8]$$

All ten turbines from the example are put in a string not exceeding its maximum (Figure B.3). All strings follow their prescribed route starting at the OHVS.

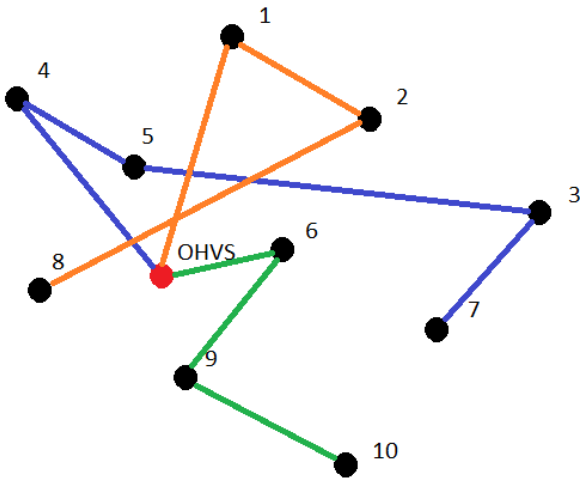


*Figure B.3: Random initial solution*

### B.1.2 Selection, fitness evaluation and genetic operators

In the second step, a set of eight consecutive solutions is taken from the population. The total weight of all solutions is analysed in the third step. The solution with the lowest total weight is chosen as best solution from the set. The fourth step consists of selecting two random places in the vector and the execution of eight operations on the selected best solution.

1. Flip vector between the two random places in the vector
2. Swap turbines placed at the two random places
3. Slide the turbine in the first place next to the second place in the vector
4. Choose different random string lengths
5. Combine option 1 and 4
6. Combine option 2 and 4
7. Combine option 3 and 4
8. Do nothing

The eight operators can be described by means of the previous wind farm example. Place 3 and place 6 are chosen as random places in the vector. In the example, vertical lines denote string breaks and highlighted parts show adjustments done during the specific step.

1. Flip: [4 5 3 7| 6 9 10| 1 2 8] → [4 5 9 6| 7 3 10| 1 2 8]
2. Swap: [4 5 3 7| 6 9 10| 1 2 8] → [4 5 9 7| 6 3 10| 1 2 8]
3. Slide: [4 5 3 7| 6 9 10| 1 2 8] → [4 5 7 6| 9 3 10| 1 2 8]
4. Different breaks: [4 5 3 7| 6 9 10| 1 2 8] → [4 5 3| 7 6 9| 10 1 2 8]

Case five to eight represent a combination of the first four cases and are therefore not shown in this example.

### B.1.3 Population and selection of best solution

The set of eight modified solutions are placed back in the population and form together with other sets the new population. The process iterates until a set condition is met. This condition can be the number of iterations, no significant improvement and when a certain computational time is reached. When the stop condition is met, the solution with lowest total weight is chosen. Since not all possibilities are analysed, it is called a near optimal solution.

### B.1.4 Limitations

The aim of the genetic algorithm is to find the most optimal solution for the cable layout problem. However, as the initial population is chosen randomly, there is some arbitrariness present. This can be solved by increasing the population size. However, since the genetic algorithm analyses the whole population during every iteration, the computational time increases.

## B.2 Greedy algorithm

The greedy algorithm always chooses the best local solution possible. In the layout problem, the greedy algorithm builds strings by choosing the nearest turbine to connect, not exceeding maximum capacity. The operation of the greedy algorithm can be seen in Figure B.4a. Starting with the substation (black dot); the route is created by constantly connecting the nearest turbine. Figure B.4b shows a more optimal route in terms of length. However, the solution shown, especially for larger configurations, costs more computational time.

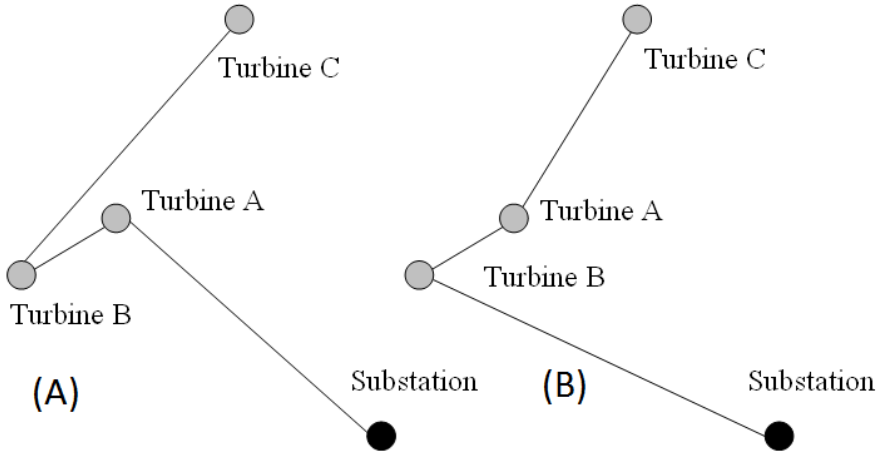


*Figure B.4: (A) Greedy algorithm and (B) optimal route (Jenkins et al., 2013)*

The amount of strings is minimized based on the maximum cable capacity. It is assumed that a lower number of strings gives a more optimal solution. Adding more strings causes difficulties since all strings start at the OHVS and the turbines near are limited. With the number of strings known, the length of each individual string can be determined. The length of each string indicates the amount of wind turbines connected. String lengths are determined randomly varying from one to the maximum capacity. This is done until all strings do not exceed maximum capacity and together add up to the number of turbines. Finally, strings are described as empty vectors with predefined lengths.

To still have some variations in the initial population a few trial solutions are created. Together with random string lengths, all possibilities have some more variations:

- String per string solution
- Turn by turn solution
- Random selection of turns
- String per string and turn by turn combined
- String per string and random selection

In the first variation, the strings are built after each other. When a string is filled with turbines, the next string is built. This continues until all strings are filled and all turbines are connected. For the second variation, the strings take turns to build. All the strings first connect the

nearest node, then connect the second and so forth. For the third variation, the string to connect the next nearest node is chosen randomly. The fourth variation is a combination of the first two. Here, the first two turbines are chosen turn by turn, the rest is chosen string per string. The last variation is the same as the fourth, but now the last turbines are chosen randomly. Figure B.5 presents an example trial solution for the PAWP created with the greedy algorithm.

Selecting the nearest turbine causes the last available turbines to be spread around the wind farm. This gives enormous connection lengths, as all turbines need to be connected. However, as the greedy algorithm only creates trial solutions, this is accepted.

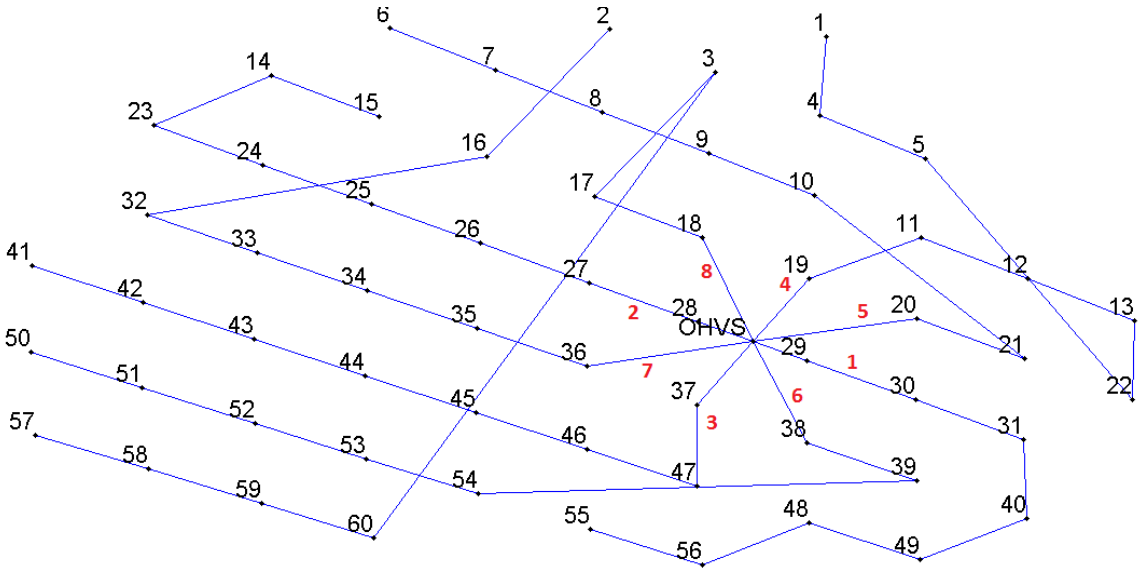


*Figure B.5: Trial solution for the PAWP produced by the greedy algorithm*

## B.3 Ant colony optimization

The third meta-heuristic is the ant colony optimization. The principle behind the algorithm is that a colony of ants always find the shortest route between the nest and food source, despite the fact that each individual ant is blind (Caldeira, 2009).

Each ant starts and sets out to find the food source leaving a pheromone trial. When the ant is presented alternative paths, one is chosen randomly. In the total population, all ants choose a random path. The ants choosing the shortest path walk it more frequently in a given amount of time. This increases the pheromone concentration on the path. As ants will tend to follow a path with a higher concentration of pheromones, eventually all ants converge to the shortest path (Caldeira, 2009). The ant colony principle is visible in Figure B.6.

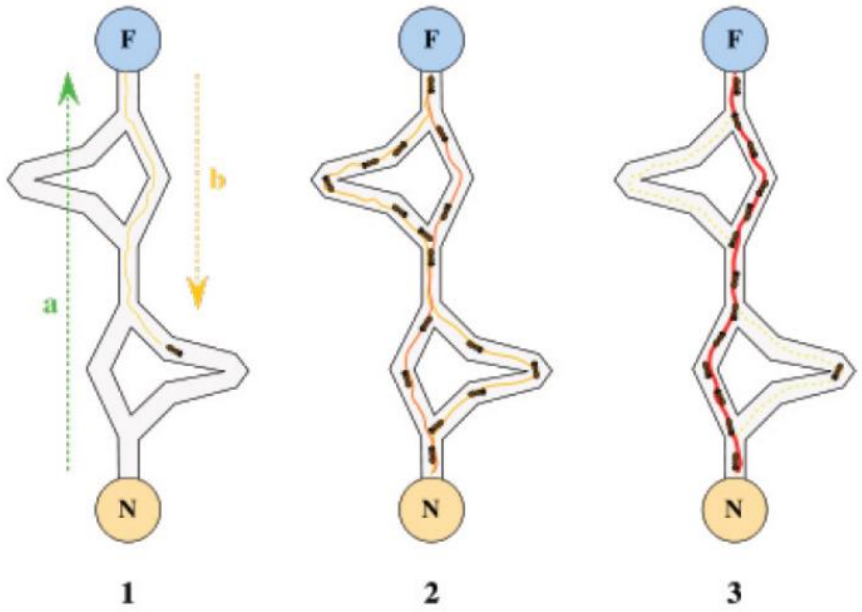


*Figure B.6: Ant colony optimization (Caldeira, 2009)*

The probability that an ant moves from turbine *i* to turbine *j* is given by:

$$P_{i,j} = \frac{\tau_{i,j}^{\alpha} * \eta_{i,j}^{\alpha}}{\sum \tau_{i,j}^{\beta} * \eta_{i,j}^{\beta}}$$

$\tau$ is a matrix of the pheromone and $\eta$ is the desirability matrix. $\alpha$ and $\beta$ are parameters that control the influence of each (Caldeira, 2009) The choice of the path increases the corresponding value in the pheromone matrix by a factor relative to its importance. When the ant colony iterations end, the matrix suffers evaporation, reducing the pheromone matrix by a fixed percentage. This causes the ants to forget bad choices made in the past. Better solutions eventually drop better results in the pheromone matrix. After a given number of iterations, the ant colony shows the shortest path.

The ant colony optimization can be applied to the open vehicle routing problem with some adjustments. For the total solution, only the starting point and number of strings are known. The different paths, which the ants can take, are formed by the connections between turbines.

## B.4 Dijkstra's algorithm

Dijkstra's algorithm is first discussed in Dijkstra (1959). The algorithm searches for the shortest path for a graph with non-negative edges. The algorithm uses two distinct arrays to record the structure of the shortest path in the graph G (Pemmaraju & Skiena, 2003).

- The distance array: For point i on the graph, dist (i) maintains the length of the shortest path known between the starting point s and i. For example dist (s) should be zero as the route is still at is starting point. The distances towards each point not included in the route are denoted as dist (i) = ∞
- The parent array: For each point i on the graph, parent (i) maintains the predecessor of i on the shortest path from s to i

Dijkstra's algorithm goes through n-1 iterations. N stands for the number of points on the graph, as the distance to the starting point is zero; there is no shortest path to the first point. The efficiency of the algorithm depends on the following observation:

S is the set of points for which the shortest path is already found. So the distance array includes the correct distance towards all points i $\in$S. It is also assumed that all routes outgoing from S are relaxed. Then, among all points not in S, point i with the smallest distance towards s has its distance value set correctly (Dijkstra, 1959).

During each iteration, the points not in S are scanned for point i with the smallest distance. From this point, all routes (i,j) to other points are analysed and adjusted if the distance to point i plus the weight (i,j) is smaller than the shortest path to point j.

When the distance array contains the shortest distances from point s to every other point on the graph, it can be said that for any edge (i,j) with weight w(i,j), dist (j) $\leq$ dist(i) + w(i,j). This statement says that for all routes (i,j) with a specific weight, the distance to point j is smaller than or equal to the distance to point i plus the route weight. When the inequality in the statement holds, another route towards point j is shorter. The routes (i,j) for which the inequality holds are denoted as relaxed. At the termination of the algorithm, all routes are relaxed and the distance array contains the correct shortest-path distances.

# C External risks

The external risks defined in Raaijmakers et al. (2014) are presented in this appendix. The tables only show the risks for the infield power cables, as the export cable is not in the focus of this study. The risks are divided in two parts, the penetrating & dropped objects and the dragged objects visible in table c.3 and table c.4. For the determination of the risks the frequency and probability is of importance. Table C.1 and table c.2 show the subjective scales used in the determination of the estimated risk.

## C.1 Recurrence period and damage probability

*Table C.1: Recurrence scale for potential damage events (Raaijmakers et al., 2014)*

| **Subjective frequency/ recurrence scale for potential damage events** | | |
|---|---|---|
| (ELF) | Extremely low | - once per 1000 years or less |
| (VLF) | Very low | - once per 100 years (once during lifetime or less) |
| (LF) | Low | - once per 10 years |
| (MF) | Medium | - Once per year |
| (HF) | High | - 10 events per year |
| (VHF) | Very high | - 100 events per year |
| (EHF) | Extremely high | - 1000 events per year |

*Table C.2: Probability scale for actual damage (Raaijmakers et al., 2014)*

| **Subjective frequency/ recurrence scale for potential damage events** | | |
|---|---|---|
| (ELP) | Extremely low | $-10^{-6}$ |
| (VLP) | Very low | $-10^{-5}$ |
| (LP) | Low | $-10^{-4}$ |
| (MP) | Medium | $-10^{-3}$ |
| (HP) | High | $-10^{-2}$ |
| (VHP) | Very high | $-10^{-1}$ |
| (EHP) | Extremely high | -1 |

## C.2 Risk of penetrating objects

*Table C.3: External risks due to penetrating objects (Raaijmakers et al., 2014)*

| | Object list | Likely type of event | Estimated penetration in seabed | Event frequency | Probability that event results in damage | Estimated risk of damage cable/year |
|---|---|---|---|---|---|---|
| 1a | Spudcans or spudpiles | Marine ops for wind turbine construction. Positioning error / Procedures not followed./ Insufficient cover | 1.0 – 2.0 m | VLF | ELP | $10^{-8}$ |
| 1b | | Marine ops for wind turbine maintenance Positioning error / Procedures not followed ./ Insufficient cover | 1.0 - 2.0 m | MF | ELP | $10^{-6}$ |
| 2a | Anchors | Planned mooring Positioning error / Procedures not followed | < 0.5 m | ELF | VLP | $10^{-8}$ |
| 2b | | Emergency mooring Mechanical failure / Positioning error / No-anchor zone ignored / Procedures not followed. / Insufficient cover | < 0.5 m | VLF | VLP | $10^{-7}$ |
| 2c | | Accidental anchor drop Mechanical failure / Anchor not secured / Insufficient cover | < 0.5 m | ELF | VLP | $10^{-8}$ |
| 3a | High elevation dropped materials dropped blades, turbine parts, gearboxes, steel parts | Wind turbine construction Mechanical failure / human error | 0.5 – 2.0 m | VLF | HP | $10^{-4}$ |
| 3b | | Wind turbine maintenance Mechanical failure / human error | 0.5 – 2.0 m | LF | HP | $10^{-3}$ |
| 4a | At or below water level dropped materials erosion protection mattresses, erosion protection rockfill | Protective cover or erosion protection installation Uncontrolled placement / Excessive dumping / Too large stone size | < 0.25 m | LF | MP | $10^{-4}$ |
| 5a | Construction tools | Turbine construction Mechanical failure / human error | < 0.25 m | VLF | LP | $10^{-6}$ |
| 5b | | Turbine maintenance Mechanical failure / human error | < 0.25 m | LF | LP | $10^{-5}$ |
| 6 | Lost freight | Passing cargo vessels / Mechanical failure / human error / storm loading / bad lashing | 0.5 – 1.0 m | ELF | LP | $10^{-7}$ |
| 7 | Ships or parts of ships | Heavy storm, passing vessels in distress Mechanical failure / human error / storm loading | 1.0 – 5.0 m | ELF | LP | $10^{-7}$ |

## C.3 Risk of dragged objects

*Table C.4: External risks due to dragged objects (Raaijmakers et al., 2014)*

| | Object list | Likely type of event | Estimated penetration in seabed | Event frequency | Probability that event results in damage | Estimated risk of damage cable/year |
|---|---|---|---|---|---|---|
| 1a | Anchors | Planned mooring<br>Anchor is slowly dragged through seabed, crosses cable while penetrated beyond burial depth / Positioning error / Procedures not followed. | 2.0 m<br>(drag < 20m | ELF | MP | $10^{-6}$ |
| 1b | | Emergency mooring<br>Anchor is dragged over cable at intermediate speed and penetrates beyond burial depth / Mechanical failure / Positioning error / Procedures not followed / Insufficient burial depth | 1.0 m<br>(drag < 200m) | VLF | MP | $10^{-5}$ |
| 1c | | Accidental anchor drag<br>Anchor is dragged over seabed at normal sailing speed. / Mechanical failure / Anchor unsecured / Cable not or hardly buried | 0.25 m<br>(drag > 200m) | ELF | LP | $10^{-7}$ |
| 2a | Anchor chain | Planned mooring<br>Anchor is slowly dragged through seabed, crosses cable while penetrated beyond burial depth | 1.0 m | ELF | HP | $10^{-6}$ |
| 2b | | Emergency mooring<br>Anchor is dragged over cable at intermediate speed and penetrates beyond burial depth, hardly any chain penetration | 0.25 m | VLF | LP | $10^{-6}$ |
| 2c | | Accidental anchor drag<br>Anchor is dragged over seabed at normal sailing speed / No chain penetration | 0.25 m | ELF | LP | $10^{-7}$ |
| 3 | Fishing gear | Fishing activity over cable position. Violation of no-fishing zone / Insufficient burial depth | 0.25 – 0.5 m | HF | VLP | $10^{-4}$ |
| 4 | Dredging gear | Cutter or Hopper dredger head cuts across cable. Trencher deviates from planned route, proceeds too close to existing cables | 0.5 – 2.5 m | ELF | VHP | $10^{-3}$ |
| 5 | Trenching ploughs and jetting devices | Trencher hits cable. Trencher deviates from planned route, proceeds too close to existing cables where crossing is planned. | 1.0 – 3.0 m | ELF | VHP | $10^{-3}$ |

# D Wind farm cable layouts

The wind farm cable layouts determined during the flat and static bed optimization are presented in this appendix. In total nine layouts are shown, the original layout, the five layouts found with the algorithms and the three layouts found with the subdivision.

## D.1 Near optimal solutions with total wind farm

This paragraph presents the wind farm layout found with the greedy and genetic algorithm. The optimization is based on the entire wind farm.

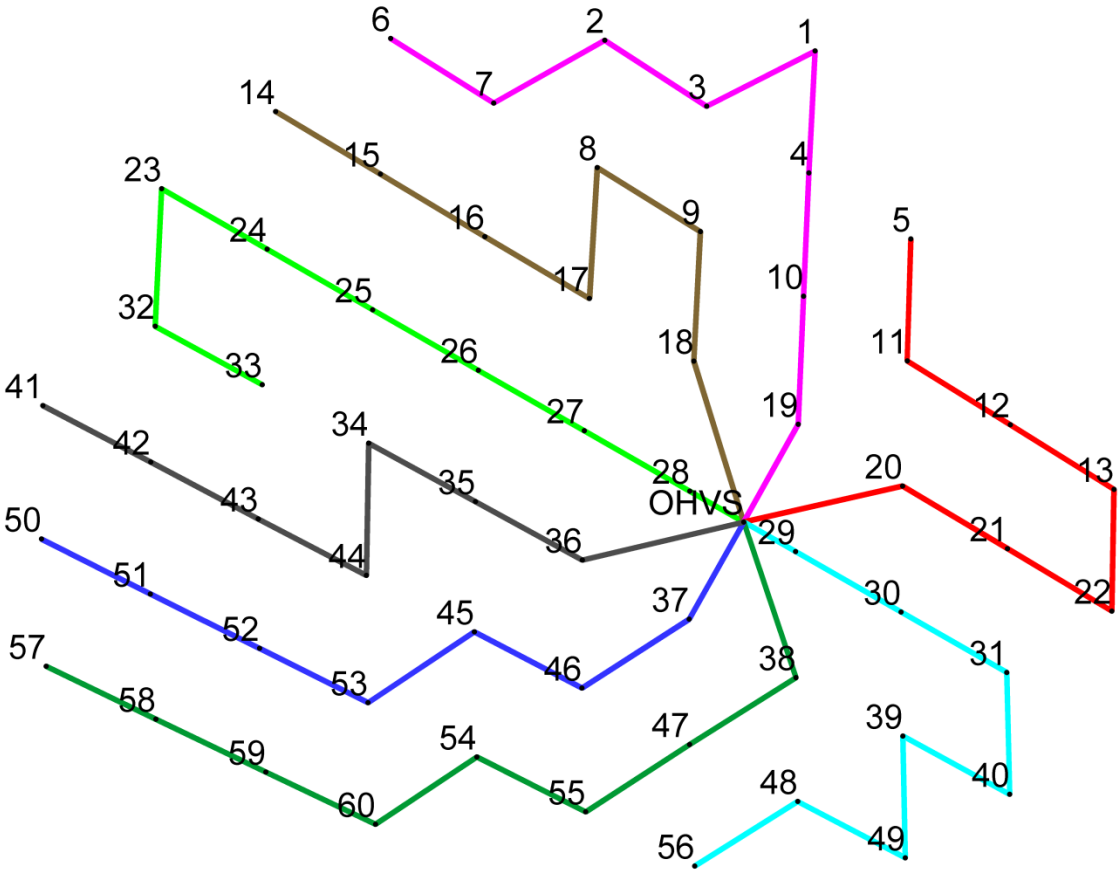


*Figure D.1: Original layout of the Prinses Amaliawindpark*

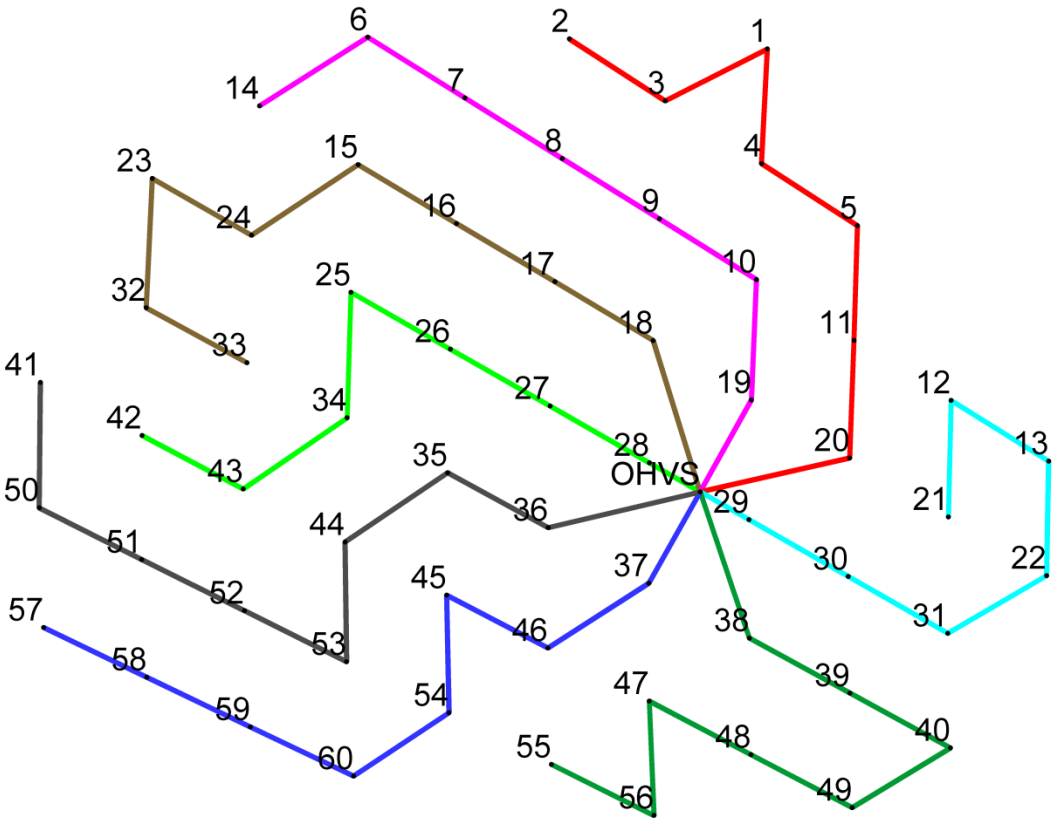


*Figure D.2: Found near optimal route 1 under a static seabed*

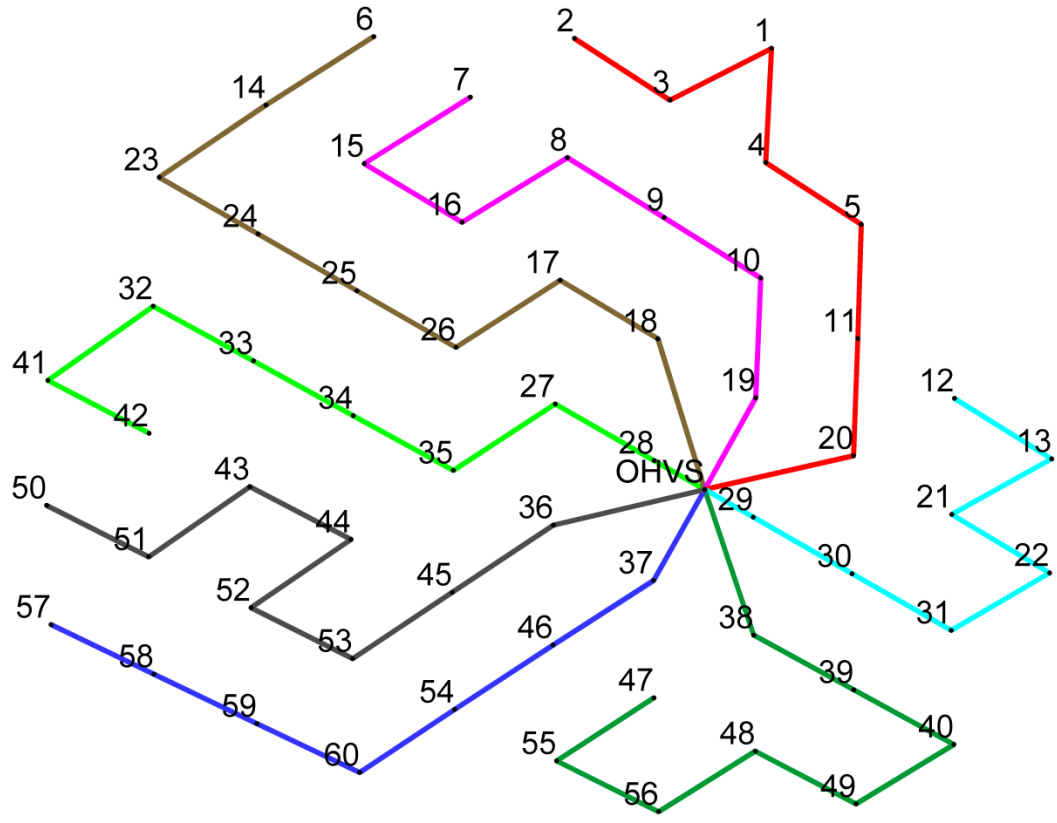


*Figure D.3: Found near optimal route 2 under a static seabed*

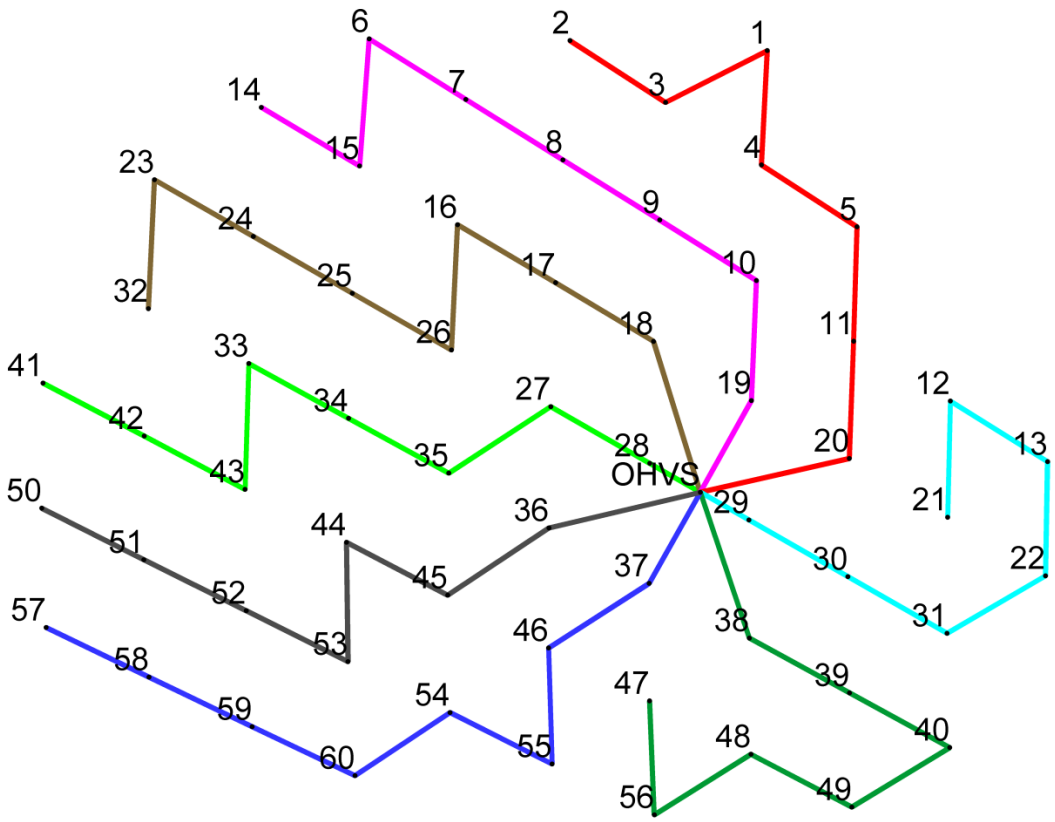


*Figure D.4: Found near optimal route 3 under a static seabed*

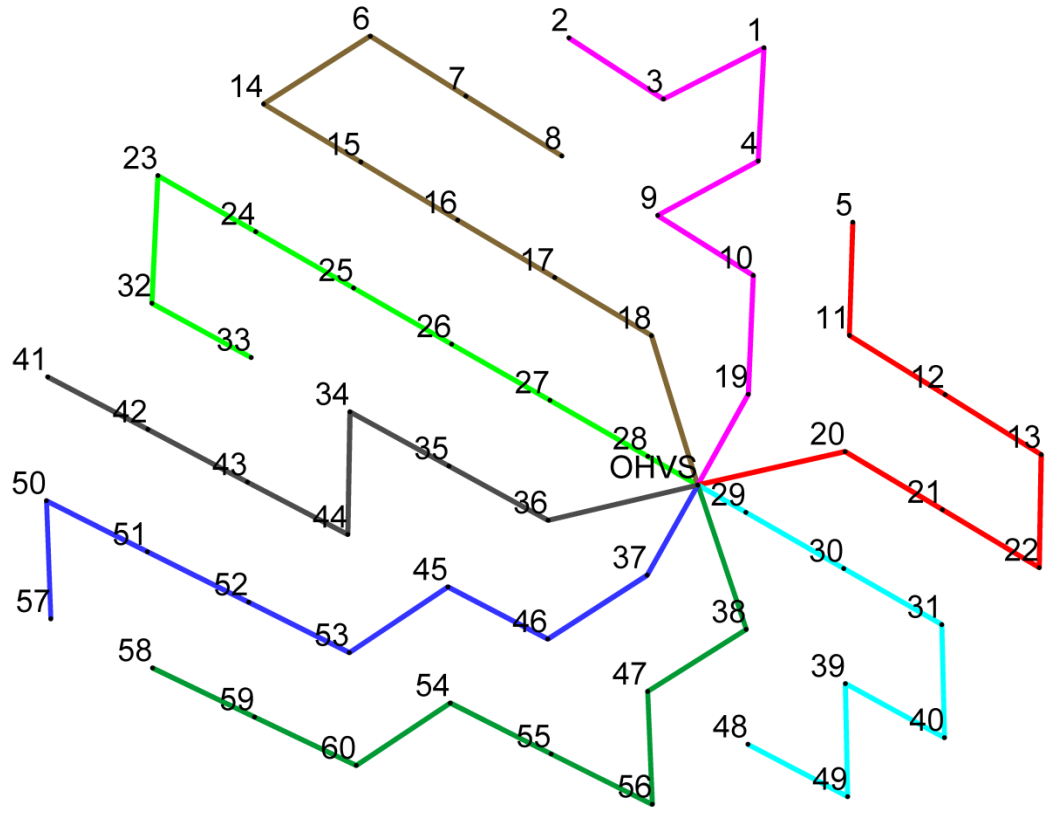


*Figure D.5: Found near optimal route 4 under a static seabed*

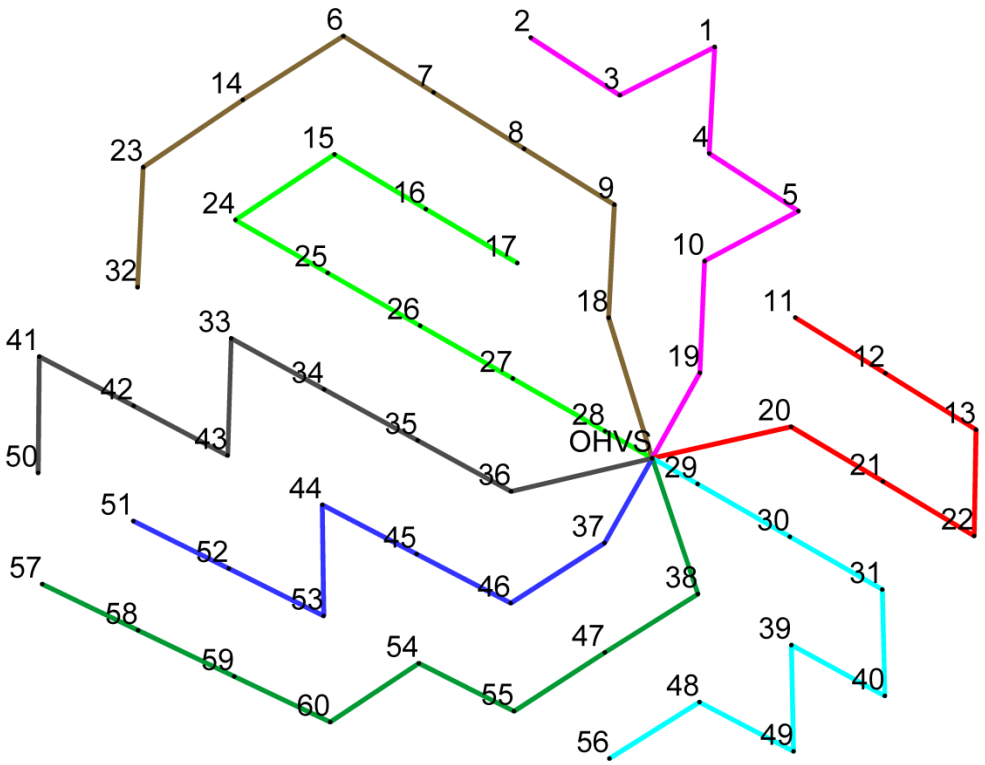


*Figure D.6: Found near optimal route 5 under a static seabed*

## D.2 Near optimal solutions with subdivision

This paragraph presents the wind farm layout found with the greedy and genetic algorithm. The optimization is based on the subdivision of the wind farm in two, three and four parts.

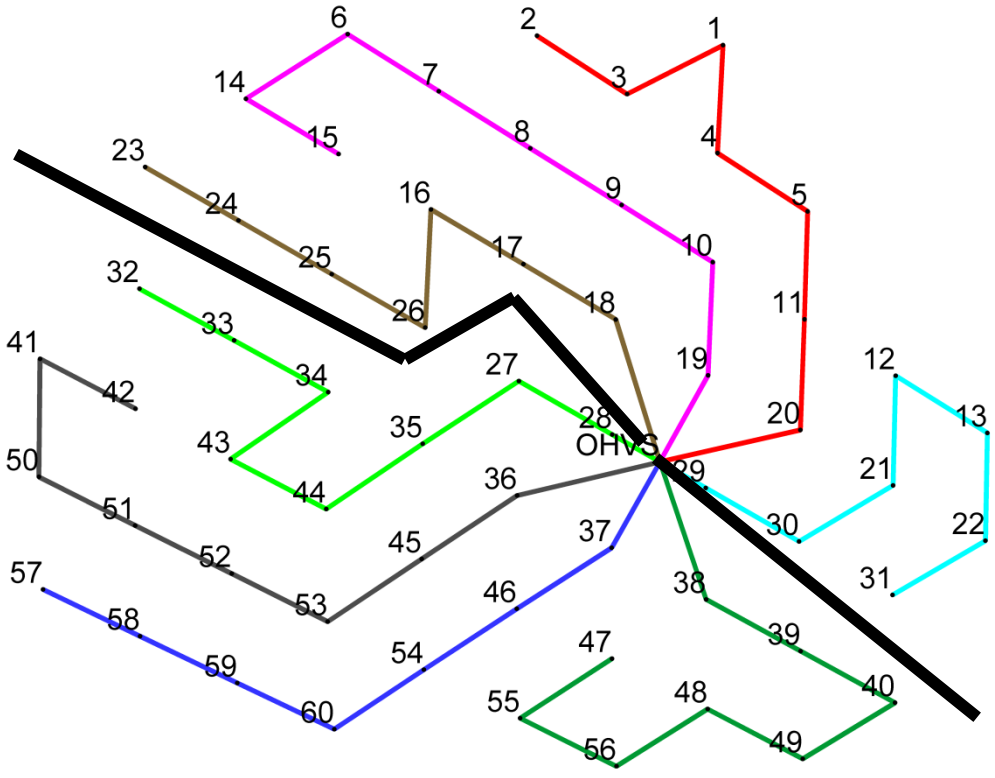


*Figure D.7: Found near optimal route under a static seabed with a 2-part division*

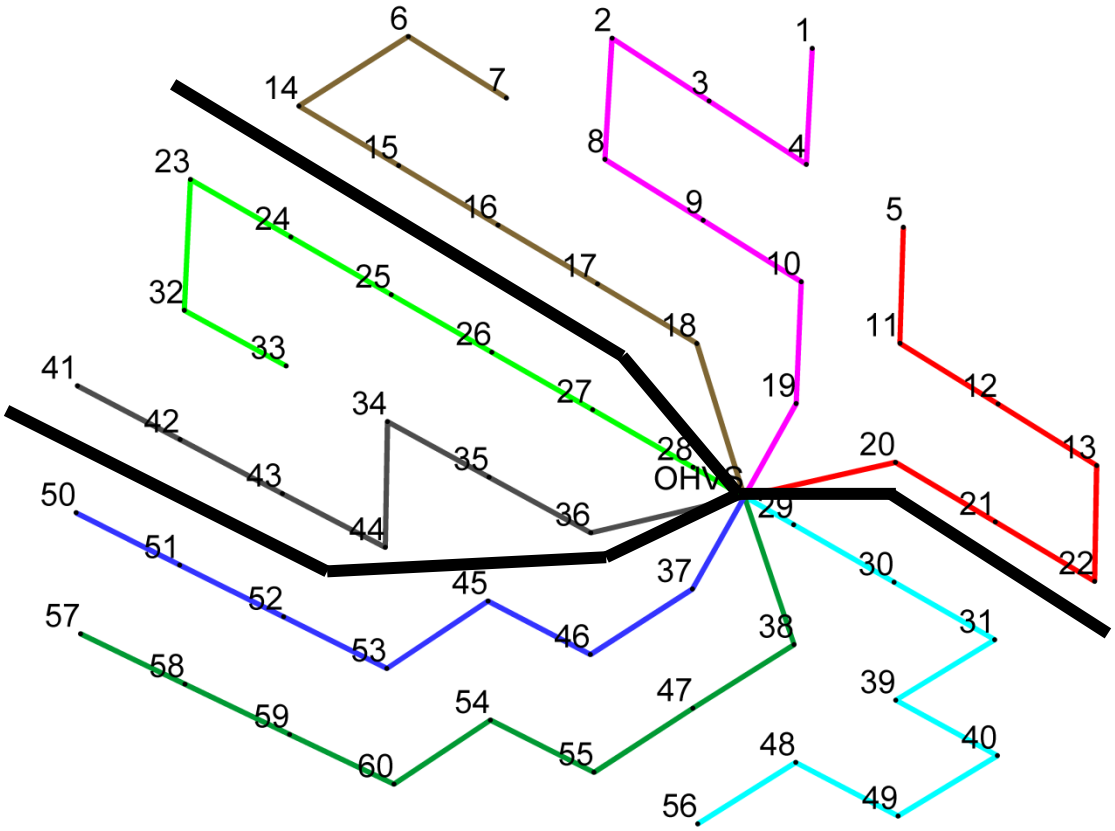


*Figure D.8: Found near optimal route under a static seabed with a 3-part division*

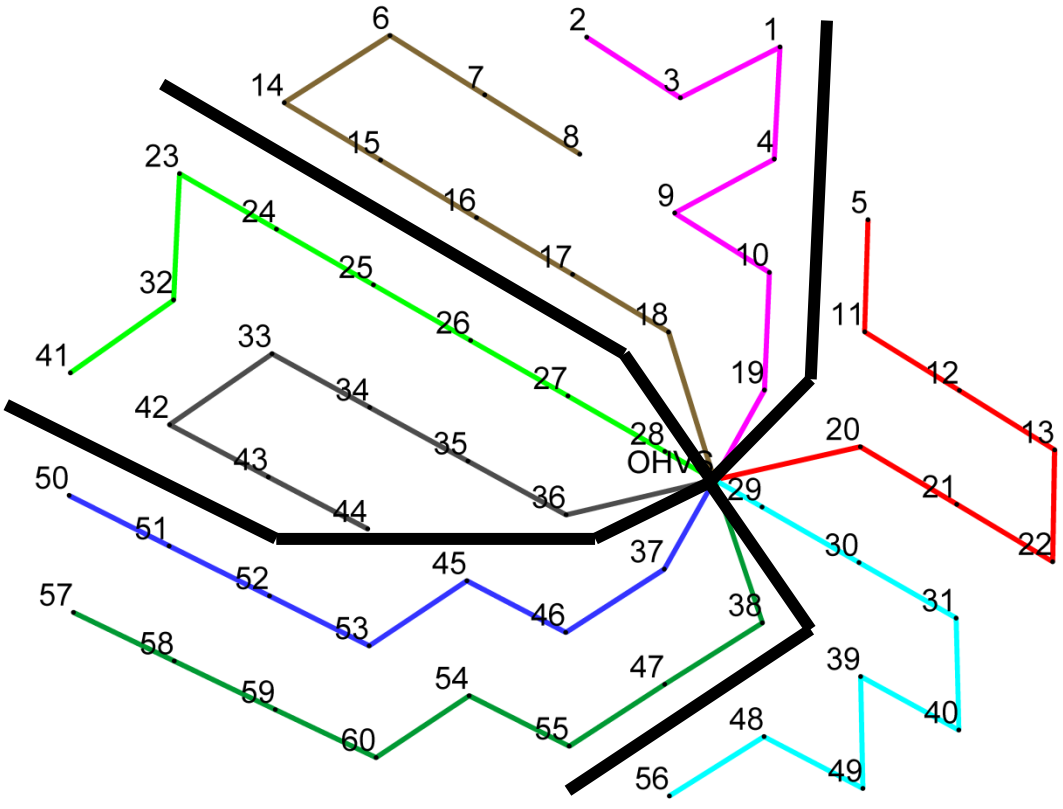


*Figure D.9: Found near optimal route under a static seabed with a 4-part division*

# E Sensitivity analysis results

This appendix will provide results of the parameter sensitivity conducted for the three predicted surveys for three connections (Figure 5.1).

## E.1 Sensitivity analysis for the predicted 2028 survey using minimum migration speed

*Table E.1: Parameter sensitivity for connection 13-22 from 2028 survey predicted with minimum migration speed*

| Parameter | Case | 2028_min Horizontal optimization | 2028_min Vertical optimization |
|---|---|---|---|
| Length [m] | | 551.1 | 549.0 |
| Original costs | | € 809.710 | € 766.090 |
| Cost of repair | - 50% | -12.7% | -13.7% |
| | +50% | +12.4% | +10.8% |
| Revenues per kWh | - 50% | -11.4% | -12.2% |
| | +50% | +11.2% | +9.8% |
| Cable costs per meter | - 50% | -10.7% | -12.1% |
| | +50% | +10.3% | +9.7% |
| Risks | - 50% | -24.2% | -29.8% |
| | +50% | +23.8% | +18.7% |

*Table E.2: Parameter sensitivity for connection 18-OHVS from 2028 survey predicted with minimum migration speed*

| Parameter | Case | 2028_min Horizontal optimization | 2028_min Vertical optimization |
|---|---|---|---|
| Length [m] | | 800.1 | 759.9 |
| Original costs | | € 1.031.800 | € 977.600 |
| Cost of repair | - 50% | -9.1% | -10.5% |
| | +50% | +9.1% | +8.7% |
| Revenues per kWh | - 50% | -11.5% | -13.5% |
| | +50% | +11.5% | +10.6% |
| Cable costs per meter | - 50% | -12.6% | -13.2% |
| | +50% | +12.0% | +10.5% |
| Risks | - 50% | -20.6% | -27.2% |
| | +50% | +20.6% | +17.6% |

*Table E.3: : Parameter sensitivity for connection 33-32 from 2028 survey predicted with maximum migration speed*

| Parameter | Case | 2028_min Horizontal optimization | 2028_min Vertical optimization |
|---|---|---|---|
| Length [m] | | 581.9 | 549.9 |
| Original costs | | € 677.760 | € 604.090 |
| Cost of repair | - 50% | -14.7% | -18.1% |
| | +50% | +14.7% | +13.3% |
| Revenues per kWh | - 50% | -2.6% | -2.8% |
| | +50% | +2.7% | +2.7% |
| Cable costs per meter | - 50% | -14.4% | -15.9% |
| | +50% | +13.3% | +12.0% |
| Risks | - 50% | -17.4% | -22.1% |
| | +50% | +17.2% | +15.3% |

## E.2 Sensitivity analysis for the predicted 2028 survey using mean migration speed

*Table E.4: Parameter sensitivity for connection 13-22 from 2028 survey predicted with minimum migration speed*

| Parameter | Case | 2028_min Horizontal optimization | 2028_mean Vertical optimization |
|---|---|---|---|
| Length [m] | | 551.1 | 549.0 |
| Original costs | | € 819.500 | € 766.850 |
| Cost of repair | - 50% | -12.9% | -13.7% |
| | +50% | +12.8% | +10.8% |
| Revenues per kWh | - 50% | -11.6% | -12.2% |
| | +50% | +11.5% | +9.8% |
| Cable costs per meter | - 50% | -10.4% | -12.1% |
| | +50% | +10.1% | +9.7% |
| Risks | - 50% | -24.5% | -29.7% |
| | +50% | +24.3% | +18.6% |

*Table E.5: Parameter sensitivity for connection 13-22 from 2028 survey predicted with minimum migration speed*

| Parameter | Case | 2028_min Horizontal optimization | 2028_min Vertical optimization |
|---|---|---|---|
| Length [m] | | 806.2 | 759.9 |
| Original costs | | € 1.030.500 | € 978.860 |
| Cost of repair | - 50% | -9.0% | -10.4% |
| | +50% | +9.0% | +8.6% |
| Revenues per kWh | - 50% | -11.3% | -13.5% |
| | +50% | +11.3% | +10.6% |
| Cable costs per meter | - 50% | -12.4% | -13.2% |
| | +50% | +12.0% | +10.4% |
| Risks | - 50% | -20.3% | -27.1% |
| | +50% | +20.3% | +17.6% |

*Table E.6: Parameter sensitivity for connection 13-22 from 2028 survey predicted with minimum migration speed*

| Parameter | Case | 2028_min Horizontal optimization | 2028_min Vertical optimization |
|---|---|---|---|
| Length [m] | | 586.7 | 549.9 |
| Original costs | | € 694.650 | € 598.290 |
| Cost of repair | - 50% | -15.2% | -18.3% |
| | +50% | +15.0% | +13.4% |
| Revenues per kWh | - 50% | -2.7% | -2.9% |
| | +50% | +2.7% | +2.7% |
| Cable costs per meter | - 50% | -14.5% | -16.0% |
| | +50% | +13.2% | +12.1% |
| Risks | - 50% | -18.1% | -22.3% |
| | +50% | +17.7% | +15.4% |

## E.3 Sensitivity analysis for the predicted 2028 survey using maximum migration speed

*Table E.7: Parameter sensitivity for connection 13-22 from 2028 survey predicted with minimum migration speed*

| Parameter | Case | 2028_min Horizontal optimization | 2028_min Vertical optimization |
|---|---|---|---|
| Length [m] | | 552.9 | 549.0 |
| Original costs | | € 822.580 | € 766.200 |
| Cost of repair | - 50% | -12.8% | -13.7% |
| | +50% | +12.9% | +10.8% |
| Revenues per kWh | - 50% | -11.5% | -12.2% |
| | +50% | +11.6% | +9.8% |
| Cable costs per meter | - 50% | -10.3% | -12.1% |
| | +50% | +10.3% | +9.7% |
| Risks | - 50% | -24.5% | -29.8% |
| | +50% | +24.5% | +18.7% |

*Table E.8: Parameter sensitivity for connection 13-22 from 2028 survey predicted with minimum migration speed*

| Parameter | Case | 2028_min Horizontal optimization | 2028_min Vertical optimization |
|---|---|---|---|
| Length [m] | | 801.5 | 759.9 |
| Original costs | | € 1.026.200 | € 978.410 |
| Cost of repair | - 50% | -9.0% | -10.4% |
| | +50% | +9.0% | +8.6% |
| Revenues per kWh | - 50% | -11.4% | -13.5% |
| | +50% | +11.4% | +10.6% |
| Cable costs per meter | - 50% | -12.6% | -13.2% |
| | +50% | +12.0% | +10.4% |
| Risks | - 50% | -20.4% | -27.2% |
| | +50% | +20.4% | +17.6% |

*Table E.9: Parameter sensitivity for connection 13-22 from 2028 survey predicted with minimum migration speed*

| Parameter | Case | 2028_min Horizontal optimization | 2028_min Vertical optimization |
|---|---|---|---|
| Length [m] | | 590.0 | 549.9 |
| Original costs | | € 706.290 | € 597.460 |
| Cost of repair | - 50% | -15.7% | -18.3% |
| | +50% | +15.4% | +13.4% |
| Revenues per kWh | - 50% | -2.8% | -2.9% |
| | +50% | +2.8% | +2.7% |
| Cable costs per meter | - 50% | -14.3% | -16.1% |
| | +50% | +13.0% | +12.2% |
| Risks | - 50% | -18.5% | -22.4% |
| | +50% | +18.2% | +15.5% |

# F Route optimization tool manual

This appendix will give the manual for using the route optimization tool developed in this research. In this appendix, all options are discussed step by step following this research. Figure F.1 shows the possibilities incorporated in the route optimization tool. The tool roughly consists of three parts: Input, calculations and visualizations. All three parts are explained in the next sections. Figure F.1 shows the route optimization tool used during this research.

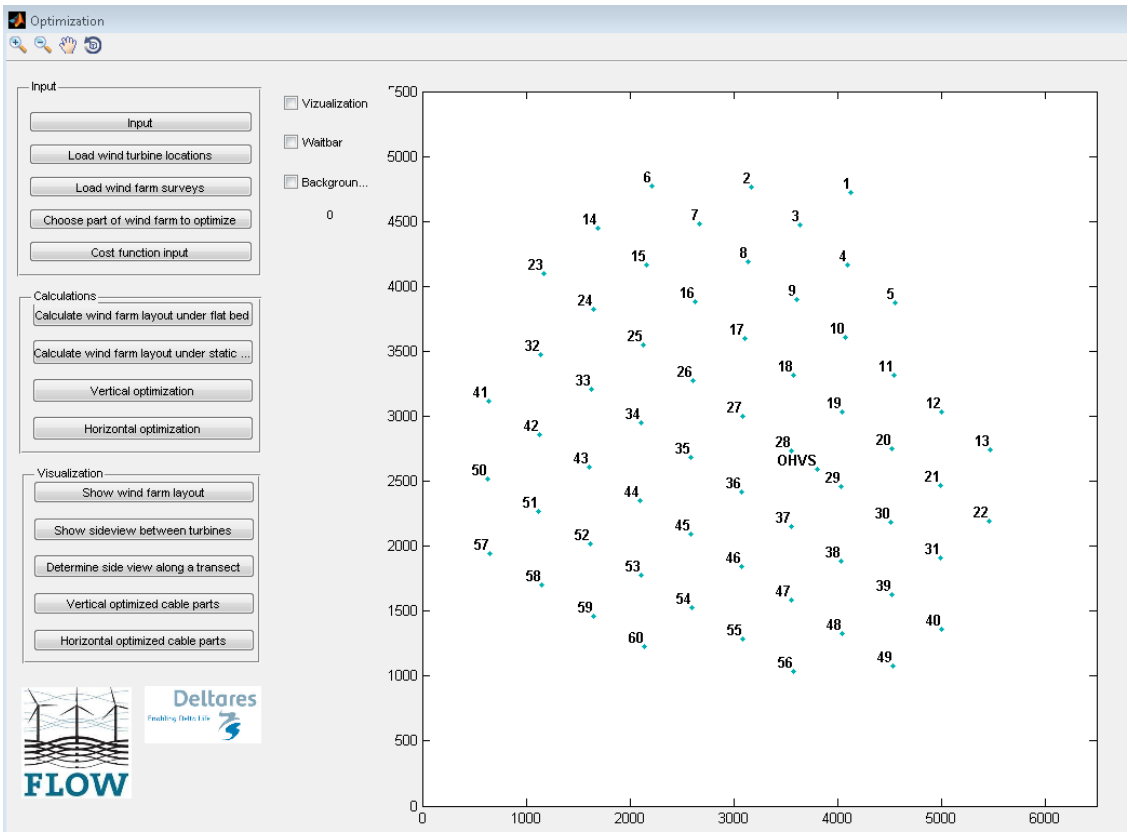


*Figure F.1: Route optimization tool developed during this research*

## F.1 Wind farm input

Input for the route optimization tool makes the tool general applicable. For each wind farm case input will differ en thereby outcomes. The input options included in the route optimization tool are shown in Figure F.2.

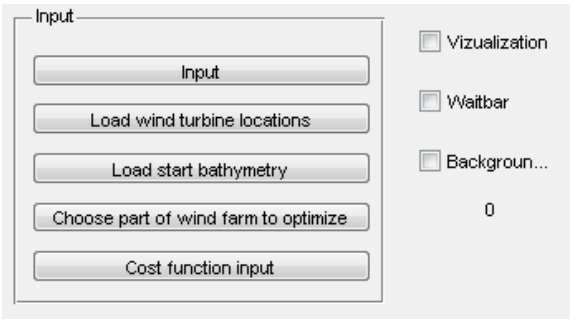


*Figure F.2: Possible options for route optimization tool input*

From the five input options, the first three need to be determined when starting a new optimization. The last two, choose parts of wind farm to optimize and cost function input can be determined for specific cases but are not necessary for calculations. Below all input options are described:

### F.1.1 Input

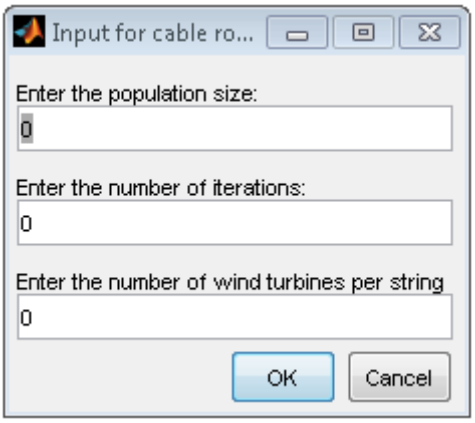


*Figure F.3: Input for genetic algorithm*

Figure F.3 shows the input needed for the genetic algorithm, which determines the wind farm layout under a flat and static seabed. The population size indicates the number of initial solution used during optimization, the number of iterations is used as stopping criterion for the genetic algorithm. The last option is the number of wind turbines per string or string capacity. During optimization, the number of strings is minimized based on string capacity. Default values assigned to the input are based on the PAWP case study, which includes 60 wind turbines. Population size is 1000, number of iterations is 40.000 and string capacity is eight.

### F.1.2 Load wind turbine locations

This option loads the wind turbine and OHVS locations. Locations should include x and y coordinates. It is important to use the same coordinate system for both turbine locations and bathymetrical surveys. This option includes transformation of longitude and latitude coordinates to kilometres.

### F.1.3 Load wind farm surveys

For calculations, the wind farm seabed is needed. Here, two options are included, first is the choice of having two surveys as input, the second is that the end survey will be predicted. For both options, three files need to be loaded, a grid with x-coordinates, y-coordinates and z-coordinates. All three need to be the same size. These files are then combined to a triscattered data interpolant, which is used to determine transects. For the first option, also an end survey can be chosen. This option is often applied to existing wind farms with a time span of multiple years between two surveys. For new wind farms, mostly only one survey is available, to optimize cables under a dynamic bed, the end survey needs to be predicted. To predict a new survey, migration speeds and direction need to determined in advance. Applying this and the years between the start survey and the predicted survey, a new end survey can be constructed. Since smaller bedforms, ripples and megaripples, are unwanted, they are filtered out during this step.

### F.1.4 Choose part of wind farm to optimize

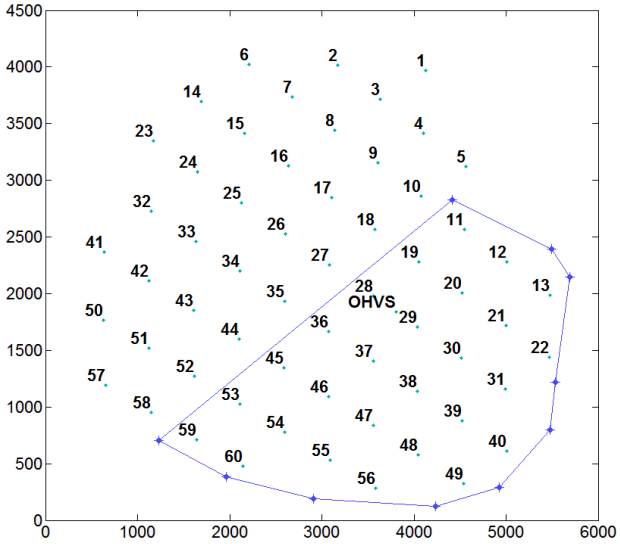


*Figure F.4: Selection of part of wind farm, for optimization*

Figure F.4 shows the PAWP turbine layout together with a selected area. With this option, a part of the wind farm area can be selected for further optimization. The use of this option is to lower the amount of iterations needed. The selected area will then be stored as wind turbines, which are included in the layout optimization. Since an OHVS always needs to be selected, it is added to the selection, when it is not selected.

### F.1.5 Checkboxes

The checkbox visualization is used to show the genetic algorithm finding an optimal layout. To visualize time needed during the calculations under a flat and static seabed, the waitbar box can be checked. The checkbox for background plot is used to include the seabed survey as background when showing the wind farm area. Here, always the start survey is chosen. Below, number is shown, this number indicates the amount of turbines selected for optimization.

## F.2 Calculations

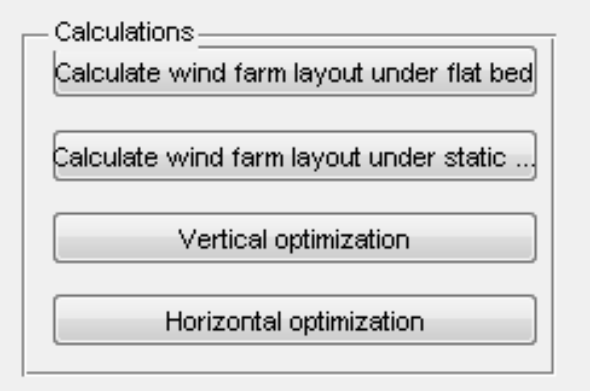


*Figure F.5: Calculation options for route optimization tool*

Figure F.4 shows the four calculation steps included in the route optimization tool. The first two options will determine wind farm layout under a flat and static seabed based on genetic algorithm input given. The layout found with one of the two options is necessary for optimizing in the vertical and horizontal plane.

For the vertical and horizontal optimization, a fixed initial burial depth needs to be given. In addition, cost function parameters need to determined in advance and two surveys are needed. For the vertical optimization, this is used to show differences with straight cables. For the horizontal optimization it is used for both comparison and to determine a path in the horizontal plane. It is assumed that his path will follow a route in which initial burial depth plus bed level change minimizes the total risk in that area. Since calculation times are high for horizontal optimizations, an option is included to choose only a single connection to optimize. All results are stored in the Matlab workspace and can be recalled after calculations are executed.

## F.3 Visualizations

After calculations are executed, results can be visualized. Figure F.6 shows the options included in the route optimization tool.

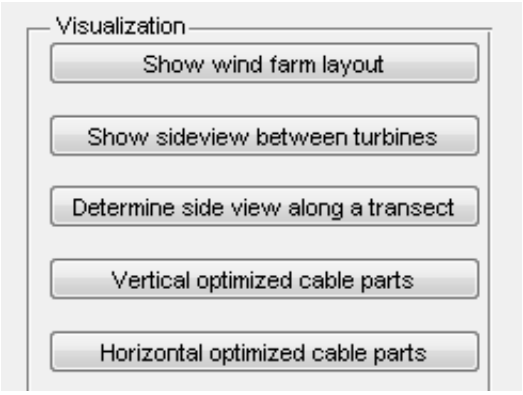


*Figure F.6: Visualization options for route optimization tool*

### F.3.1 Show wind farm layout

Layouts found during calculations under a flat and static seabed can be visualized with this option. When calculating multiple results, a choice can be made of which solution is to be shown. A visualization of the wind farm area can be seen in Figure F.7, showing the original PAWP layout.

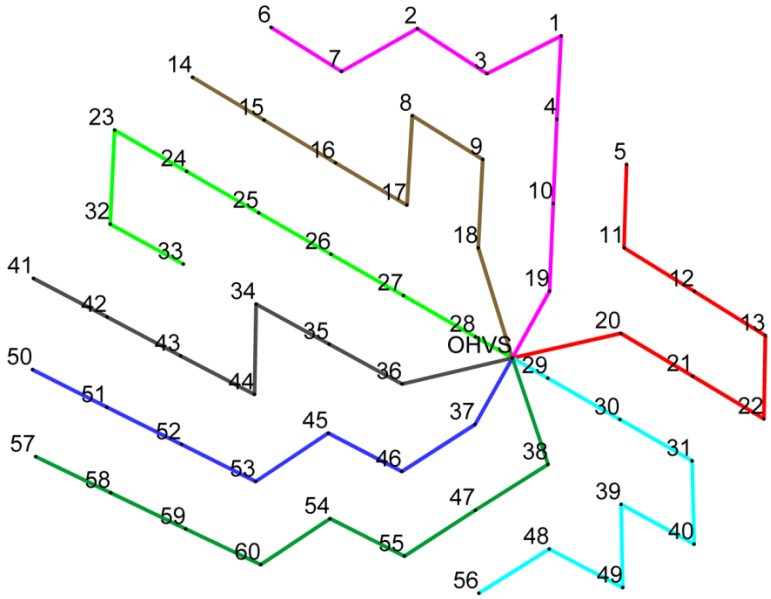

*Figure F.7: Possible wind farm layout visualization*

### F.3.2 Show side view between two turbines

One of the most clear ways to show the bed forms in the survey area is by showing a transect. Since power cables between two turbines are often straight in the horizontal plane, this visualization shows the bedforms needed to be followed by the power cables. The user can give input on which connection is to be shown. To show the morphological evolution the transects in both start and end survey are shown. For this step, only wind farm input is necessary and no calculations are needed.

### F.3.3 Determine side view along a transect

An extension to previous step is that the user can determine transect location. For this the user can select a number of points and show a combined transect along those points. Figure F.8 shows a transect in the PAWP wind farm created by selecting points in the survey.

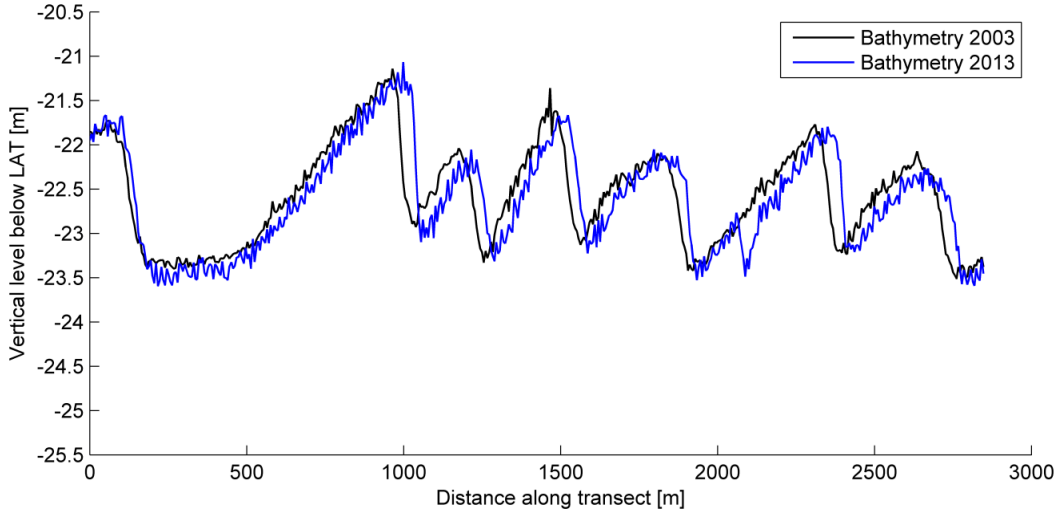


*Figure F.8: Side view along a transect determined by user input*

### F.3.4 Vertical optimized cable parts

This option will visualize cable parts optimized in the vertical plane. Figure F.9 shows a resulting visualization of a connection after optimizing in the vertical plane. Together with the figure the original and optimized costs, risks and lengths are presented for this connection.

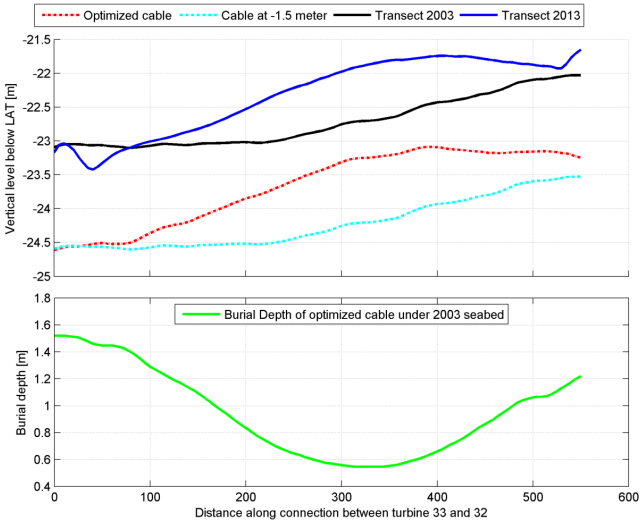


*Figure F.9: Visualization of vertical optimization*

### F.3.5 Horizontal optimized cable parts

With this option results from the horizontal optimization can be visualized. A user can select the connection to be shown, including the costs scale on which it is shown. In addition, contour lines of bedforms present in the start survey can be switched on or off. Figure F.10 presents a visualization of a connection after optimization in the horizontal plane.

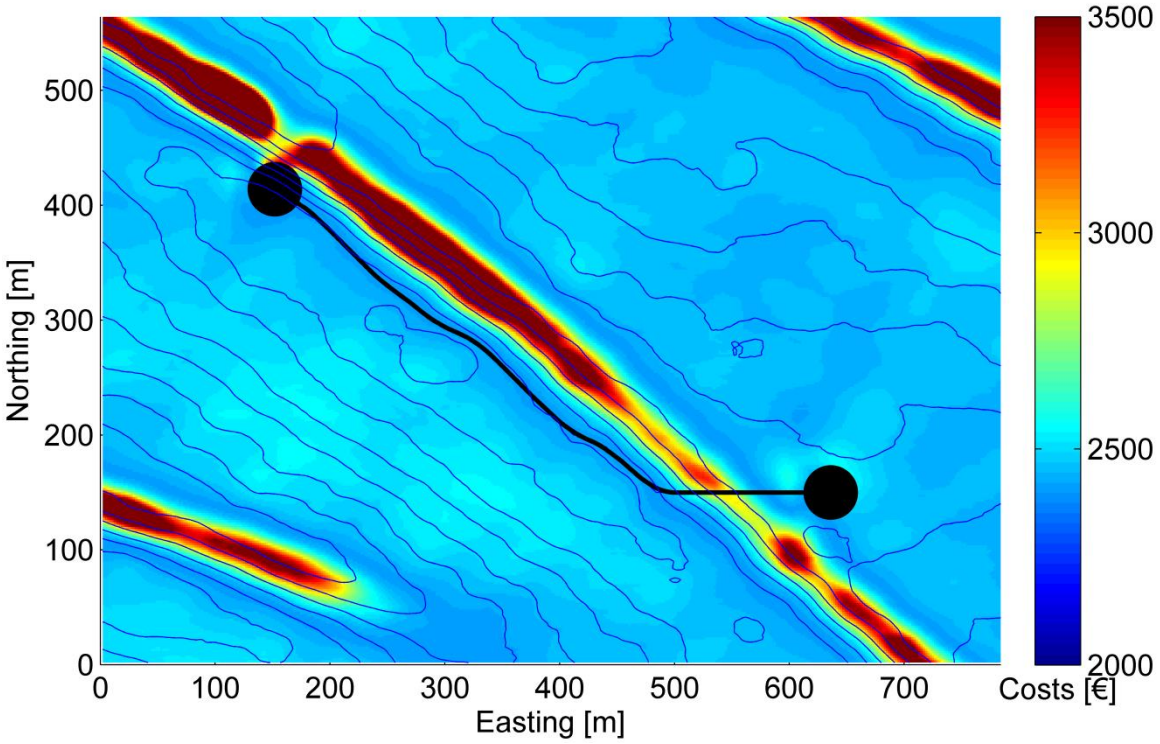


*Figure F.10: Visualization of horizontal optimization*